U.S. weighs a crackdown on risky pathogen studies p. 242

Timing of eating affects how calories are burned pp. 251 & 276

On the edge of ultraefficient networks p. 270

Science

$15
21 OCTOBER 2022
science.org
AAAS

COLOR PATTERNING

A ground plan for butterfly wings

pp. 249 & 304

EVOLUTION

Deep cis-regulatory homology of the butterfly wing pattern ground plan

Anyi Mazo-Vargas[1,2]*, Anna M. Langmüller[3], Alexis Wilder[2], Karin R. L. van der Burg[1], James J. Lewis[1,4], Philipp W. Messer[3], Linlin Zhang[1,5], Arnaud Martin[2], Robert D. Reed[1]*

Butterfly wing patterns derive from a deeply conserved developmental ground plan yet are diverse and evolve rapidly. It is poorly understood how gene regulatory architectures can accommodate both deep homology and adaptive change. To address this, we characterized the cis-regulatory evolution of the color pattern gene *WntA* in nymphalid butterflies. Comparative assay for transposase-accessible chromatin using sequencing (ATAC-seq) and in vivo deletions spanning 46 cis-regulatory elements across five species revealed deep homology of ground plan–determining sequences, except in monarch butterflies. Furthermore, noncoding deletions displayed both positive and negative regulatory effects that were often broad in nature. Our results provide little support for models predicting rapid enhancer turnover and suggest that deeply ancestral, multifunctional noncoding elements can underlie rapidly evolving trait systems.

Trait evolution frequently occurs through sequence divergence in noncoding regions of the genome that control gene expression (*1*). Few case studies, however, have characterized the history of regulatory systems that underlie rapidly evolving traits (*2*). In this work, we performed comparative chromatin analyses and regulatory knockouts of the butterfly wing pattern gene *WntA* to investigate how trait homology is reflected in regulatory sequences of a highly diverse, continually adapting character system. *WntA* encodes a signaling ligand that induces major color pattern elements of the butterfly wing pattern ground plan (*3*–*6*), and *WntA* noncoding variation underlies color pattern adaptation in multiple unrelated butterfly species (*4*, *7*). Thus, allelic variation at the *WntA* locus underlies pattern variation at microevolutionary scales yet also explains macroevolutionary aspects of pattern divergence.

To characterize the cis-regulatory architecture of the *WntA* [i.e., identities and locations of regulating cis-regulatory elements (CREs)], we first used Hi-C to infer the topologically associating domain (TAD) of the *WntA* locus in developing wings. Inside individual TADs, CREs and genes preferentially interact with each other (*8*). In imaginal discs of *Junonia coenia*, when *WntA* is expressed (*5*), we identified a TAD that spans *WntA* and its two intergenic regions (Fig. 1, A and B). The strongest CRE-to-promoter interactions occurred just upstream of the *WntA* promoter and across its lengthy first intron. These data, coupled with sequence association studies (*7*, *9*), led us to focus our functional screens for *WntA* CREs on these regions.

We performed the assay for transposase-accessible chromatin using sequencing (ATAC-seq) to profile chromatin accessibility in heads, forewings, and hindwings from the last larval instar of five nymphalids (Fig. 1C and fig. S1). By comparing head and wing profiles, we identified regions showing wing-specific activity. We next asked to what extent individual wing-specific CREs are conserved or are lineage specific. By overlapping the most conserved sequences (Fig. 1C) with the differentially accessible chromatin regions, we observed that 69 to 88% of wing-specific CREs in the *WntA* TAD were in areas with strong sequence conservation between the nymphaline, satyrine, and heliconiine subfamilies. The exception was the monarch butterfly, *Danaus plexippus*, for which 70.6% of the ATAC-seq peaks were in danaine-specific regions (fig. S2). Whereas the nymphaline and heliconiine datasets highlighted both orthologous and novel CREs, most wing-specific CREs were conserved within and between these nymphalid subfamilies. By contrast, the sister group to the rest of the nymphalids, the Danainae clade showed a largely lineage-specific repertoire of CREs (figs. S1 and S2), consistent with the divergent mode of *WntA* expression previously reported in monarchs (*6*).

We functionally assessed regions containing candidate *WntA* CREs using a CRISPR-Cas9 shotgun mosaic deletion approach (*10*), where we injected multiple single-guide RNAs (sgRNAs) tiled across open chromatin regions (Fig. 2A, fig. S3, and tables S1 and S2). This approach results in pattern mutant clones derived from a spectrum of deletions of different lengths and positions around candidate CREs. To identify regions that potentially play a role in establishing the nymphalid ground plan, we targeted wing-specific CREs conserved between *J. coenia* and *Vanessa cardui*—two species with ancestral-like *WntA*-induced color patterns (*5*, *6*). We observed that most of our deletions generated mutant clones affecting similar or overlapping wing color pattern elements (fig. S3 and data S1) (*11*) and also affected basal, central, and distal pattern elements across both wings (Fig. 2B and fig. S3). This high prevalence of overlapping phenotypic effects is consistent with the Hi-C data, which reveal physical interactions across multiple CREs and the *WntA* promoter (Fig. 1A) and support a model where color patterns are determined by a spatially distributed array of physically interacting noncoding sequences.

This conserved *WntA* regulatory architecture prompted us to investigate the role of recently evolved sequences in pattern formation. To test this, we deleted a region centered on *CRE 24*, which appears to be specific to *V. cardui*. *CRE 24* is not found in congenerics *Vanessa tameamea* or *Vanessa atalanta* (which diverged ~10 to 15 million years ago) (*12*) (fig. S4) or any other currently sequenced butterfly. Deletion of this region caused the reduction and/or loss of basal, central, and marginal pattern elements (figs. S1 and S5), thus demonstrating how even recently evolved noncoding sequences can be integrated into cis-regulatory networks.

Color pattern homologies of *Heliconius* butterflies are a long-standing question (*13*, *14*). *WntA* specifies melanic patches in this genus that may be derived from the nymphalid ground plan (*3*, *6*). We thus investigated to what degree ancestral versus *Heliconius*-specific CREs determine these patterns. ATAC-seq and comparative sequence analysis showed a large number of *WntA* CREs with deep sequence conservation between heliconiines and nymphalines (Fig. 1C and fig. S1), including CREs required for ground plan patterning in *J. coenia* and *V. cardui*. We generated deletions centered on five of these deeply conserved CREs in *Heliconius himera* (figs. S3C and S4). Notably, deletions spanning all five CREs, including on opposite ends of the first intron, had similar broad effects on melanic *Heliconius* wing patterns (Fig. 2D) (*11*). Deletions spanning two additional heliconiine-specific CREs revealed similar, overlapping phenotypes (*11*). We conclude that *Heliconius WntA* shares a conserved cis-regulatory architecture with nymphaline butterflies and that the highly derived mimicry-related color patterns of *Heliconius* appear to share deep regulatory homology with the nymphalid ground plan.

It has been speculated that the color patterns of basal heliconiines, which typically show fragmented black, brown, and silver spots, may represent an intermediate state bridging the ancestral ground plan with the *Heliconius* pattern archetype (*13*, *14*). We tested this in the

[1]Department of Ecology and Evolutionary Biology, Cornell University, Ithaca, NY, USA. [2]Department of Biological Sciences, The George Washington University, Washington, DC, USA. [3]Department of Computational Biology, Cornell University, Ithaca, NY, USA. [4]Baker Institute for Animal Health, College of Veterinary Medicine, Cornell University, Ithaca, NY, USA. [5]CAS and Shandong Province Key Laboratory of Experimental Marine Biology, Center for Ocean Mega-Science, Institute of Oceanology, Chinese Academy of Sciences, Qingdao, China.
*Corresponding author. Email: anyimv@gwu.edu (A.M.-V.); robertreed@cornell.edu (R.D.R.)

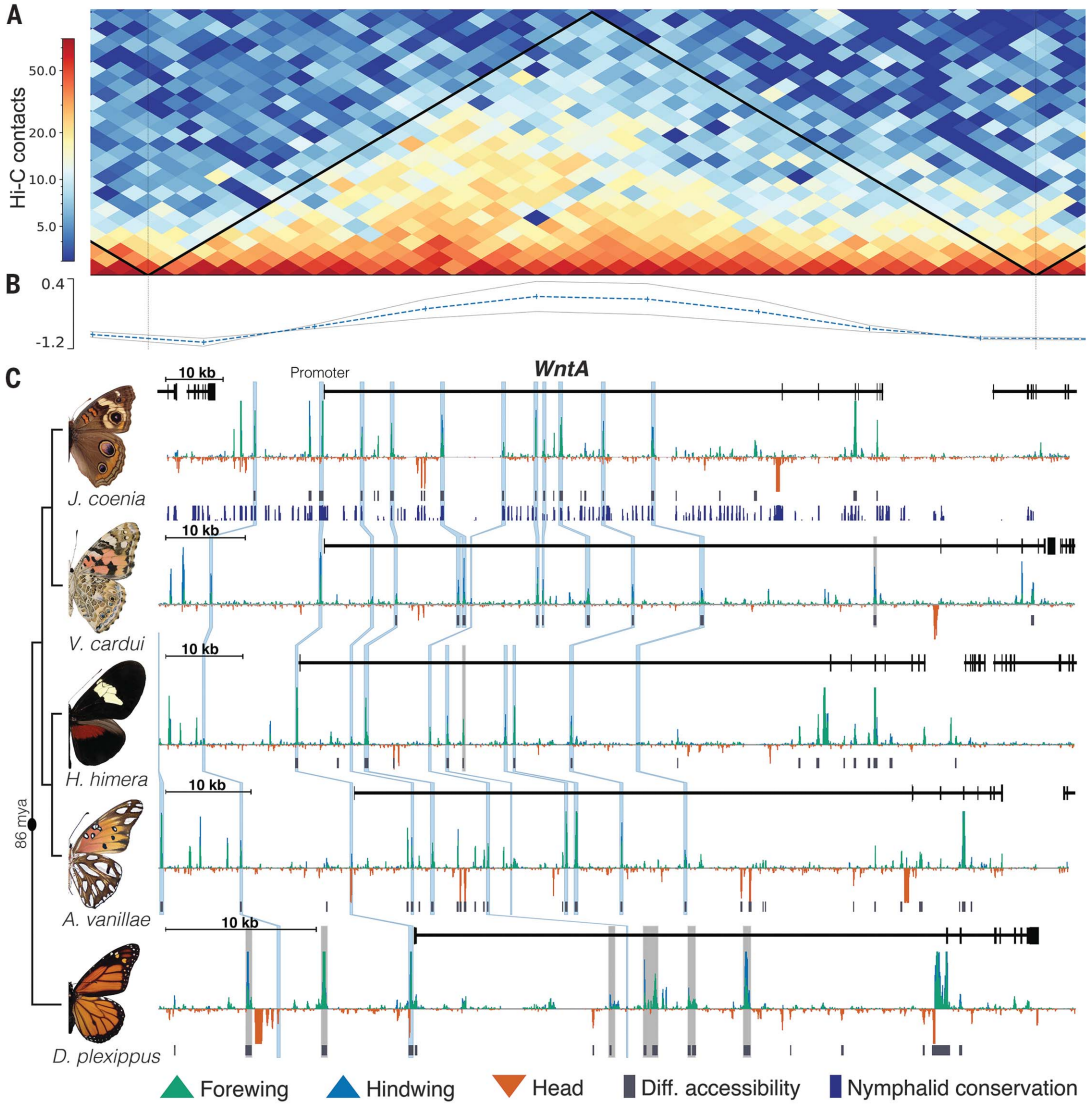

Fig. 1. Deeply conserved chromatin landscape of the *WntA* regulatory region. (**A**) Hi-C reveals abundant chromatin interactions across the upstream and first-intron regions of *WntA*. Color intensity corresponds to the contact frequency per bin. (**B**) TAD separation score. Black lines in (A) depict TAD boundaries as predicted by the TAD separation score. (**C**) Chromatin accessibility tracks (ATAC-seq) for each species sampled in this study, with phylogenetic relationships shown. Orthologous CREs assessed in this study are in blue shadows connecting different species, whereas lineage-specific elements are shown in gray; see figs. S1 and S4 for details. mya, million years ago; Diff., differential.

basal heliconiine *Agraulis vanillae* by producing deletions spanning the same regulatory regions tested in *H. himera* (Fig. 2D) and several additional heliconiine-specific CRE regions (fig. S4). Again, we found similar results—deletions of regulatory sequences across very different regions of the first intron had overlapping effects distributed across all *WntA*-induced color patterns (data S1) (*11*). This supports models that heliconiine color patterns evolved through simplification of the nymphalid ground plan and suggests that this process occurred partly through the tinkering of an ancestral cis-regulatory apparatus.

We next examined *D. plexippus*, the monarch butterfly—an exemplar of the nymphalid subfamily Danainae—to investigate how deeply the cis-regulatory architecture described above is conserved in nymphalids. In monarchs, *WntA* shows distinctive vein-associated expression patterns, and *WntA* knockouts cause the loss of these patterns (*6*). These patterns are highly derived and challenging to homologize with the nymphalid ground plan (*6*). Overall, the noncoding region of the monarch *WntA* locus shares relatively little sequence similarity with those of other nymphalids and shows a reduced number of ATAC-seq peaks (Fig. 1C), most of which are in danaine-specific genomic sequences (figs. S2 and S4). Although there are a few orthologous CREs, including the *WntA* promoter, most show no identifiable sequence similarity with other nymphalids, which suggests that they are independently derived or that their sequences are so divergent that orthology is difficult to ascertain (*15*, *16*). To test the wing patterning function of monarch CREs, we generated mosaic deletions centered on six danaine-specific CREs and one ancestrally conserved CRE. Again, we found that even distantly spaced regions had similar effects on *WntA*-induced color patterns (Fig. 2E and data S1). Thus, although many nymphalid wing patterns appear to derive from a deeply conserved regulatory architecture, there are also cases where divergent regulatory sequences underlie lineage-specific patterns.

Previous work has shown that *WntA* knockouts result in a highly specific loss of *WntA*-expressing color patterns (*3*, *6*). Our deletions that phenocopy *WntA* coding knockouts (Fig. 2) validate the enhancer-like function of these noncoding regions. However, we were surprised to observe expansions of *WntA*-expressing color patterns in several mosaic deletion experiments (data S1) (*11*). These expansions are phenocopied by heparin injections, which enhance *WntA* signaling during color pattern formation (*5*, *6*, *17*). Because deletion-induced color pattern expansion accurately replicates *WntA* gain-of-function effects, we speculate that some regulatory deletions had a positive impact on *WntA* transcription. These dual gain- and loss-of-function effects are well illustrated in *A. vanillae*, in which *WntA* is expressed in a subset of silver and black spots (Fig. 3A). When

heparin is injected, the *WntA*-expressing silver spots expand, whereas *WntA*-negative spots melanize or disappear. *WntA* coding knockouts present the opposite results—*WntA*-expressing silver spots disappear, whereas *WntA*-negative spots extend (*6*). Both expansion and reduction effects were observed in many deletion clones (Fig. 3B) across all species (fig. S6 and data S1). Our results show that *WntA* regulatory sequences encode both positive and negative regulatory instructions for color pattern formation.

The color pattern expansion and contraction phenotypes described above are present in mosaic individuals that bear deletion alleles

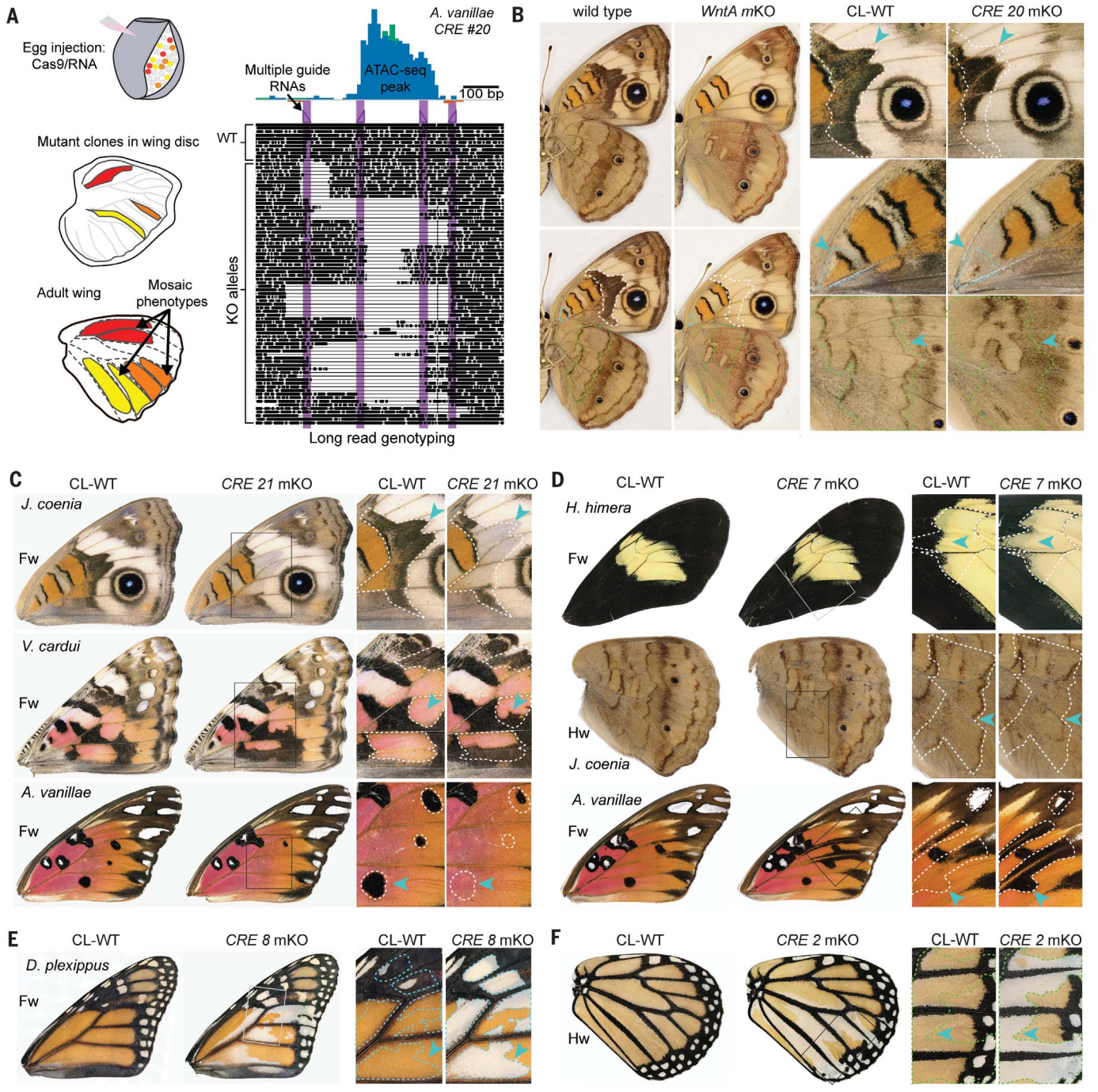

Fig. 2. In vivo mosaic deletions of *WntA* CREs reveal evolutionarily conserved wing pattern development functions. (**A**) Shotgun deletion generates butterflies that are mosaic for different deletion lengths. bp, base pair; WT, wild type. (**B**) A *J. coenia WntA* null mutant shows loss of *WntA*-expressing color pattern elements (left). This effect is phenocopied by the *CRE 20* mosaic knockout (mKO). (**C**) *CRE 21* ortholog mKOs across nymphaline (*J. coenia* and *V. cardui*) and heliconiine (*A. vanillae*) species illustrate deep evolutionary conservation of wing pattern ground plan CREs. (**D**) *CRE 7* ortholog mKOs across nymphaline (*V. cardui*) and heliconiine (*H. himera* and *A. vanillae*) species suggest that the highly divergent *Heliconius* wing patterns share a deep regulatory architecture with the nymphalid ground plan. (**E** and **F**) *D. plexippus* lineage-specific wing pattern CREs illustrated by *CRE 8* (E) and *CRE 2* (F) mKOs. CL-WT refers to contralateral wings with mostly or completely wild-type color patterns from the same individuals as the pictured mKO phenotypes. Cyan arrowheads point to asymmetric color patterns. Fw, forewing; Hw, hindwing.

of different lengths (Fig. 2A). The mosaic nature of the shotgun mutations, however, limits our ability to make precise mechanistic conclusions about the functions encoded within individual CREs. Therefore, to link specific color pattern effects to specific mutant alleles, we in-crossed *V. cardui* G_0 crispants to generate F_1's and then in-crossed further to get F_2 germline mutants bearing deletions in *CRE 23* (Fig. 3, E and F, and fig. S7). We confirmed heterozygous and compound inheritance of deletions within this single CRE (fig. S7), which caused different color pattern changes exemplified by specific gain-of-function effects in dorsal and ventral melanic subelements on the forewings (Fig. 3, E and F). This allelic series shows that small changes in a single CRE are enough to cause localized phenotypic

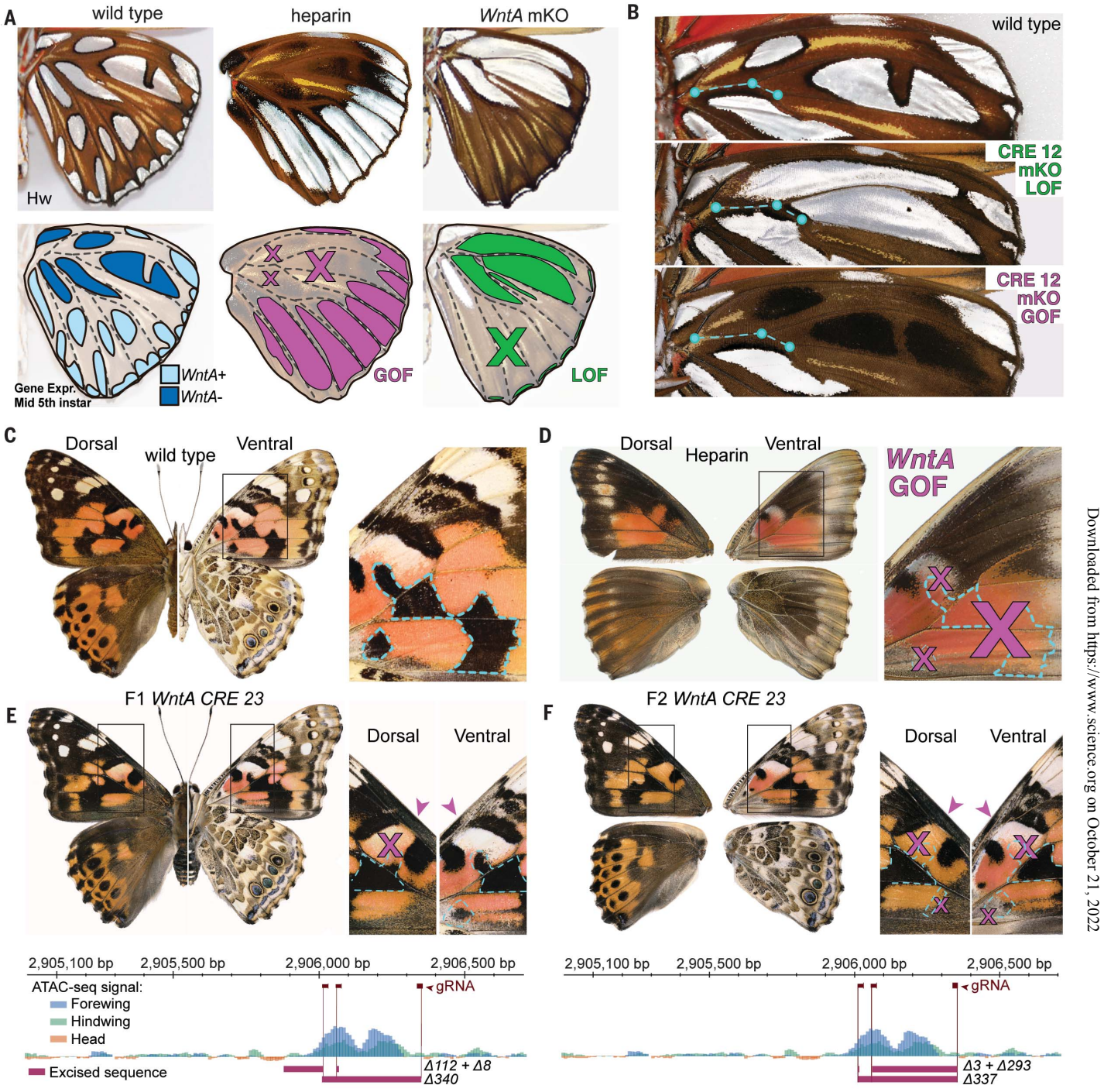

Fig. 3. Positive and negative regulatory activity is a characteristic of color pattern regulation. (**A**) Heparin injections [gain-of-function (GOF), magenta] and *WntA* knockouts [loss-of-function (LOF), green] in *A. vanillae* highlight the effects of experimental manipulations of the *WntA* signaling axis. Expr., expression. (**B**) Mosaic shotgun deletions of *WntA CRE 12* in *A. vanillae* variably result in expansion and contraction of the anterior hindwing silver spots, consistent with a *WntA* LOF and GOF, respectively. (**C**) Wild-type *V. cardui* butterfly with closeup of ventral middle forewing region. (**D**) Heparin injections in *V. cardui* illustrate the *WntA* GOF phenotype. (**E** and **F**) F_1 (E) and F_2 (F) *WntA CRE 23* deletion in *V. cardui*. Each individual represents a different combination of deletion alleles (fig. S7). Cyan dots and dashed annotations show wing landmarks. The "X" marks indicate an absence of pattern with respect to the wild-type phenotype. Arrowheads point to the extension of melanic pigmentation. gRNA, guide RNA.

changes (Fig. 3E) and illustrates the role of negative, silencer-like regulatory directives during patterning.

In testing the wing patterning functions of many orthologous and lineage-specific regulatory regions across five different butterfly species, we made several discoveries that reshape our understanding of the regulatory architecture of morphological evolution. First, in contrast to traditional models, most noncoding deletions that we studied acted globally across forewings and hindwings, often without restriction to any specific *WntA*-expressing color pattern elements. These broad effects suggest an unexpected regulatory fragility to wing patterning. Similar sensitivity to perturbation was also observed for the *Heliconius* color pattern gene *optix* (*10*) and may indicate that these loci require the assembly of clusters of CREs into transcriptional hubs to mediate gene expression, consistent with emerging superenhancer models (*18*–*20*). Second, many deeply conserved wing pattern CREs are shared between nymphalid butterflies. These conserved elements control homologous ground plan components as well as divergent color patterns in species that evolved derived modes of *WntA* expression. We propose that this deep conservation reflects an ancestral regulatory homology that underlies the nymphalid ground plan. Third, noncoding regions have the capacity to both promote and suppress *WntA* color patterns. Overall, the combination of deep conservation and dense functionality of *WntA* regulatory sequences suggests a mode of evolution marked less by the gain and loss of pattern-specific enhancers and more by nuanced modification of an array of deeply ancestral, multifunctional ground plan sequences.

REFERENCES AND NOTES

1. M. Rebeiz, M. Tsiantis, *Curr. Opin. Genet. Dev.* **45**, 115–123 (2017).
2. A. Monteiro, M. D. Gupta, *Curr. Top. Dev. Biol.* **119**, 205–226 (2016).
3. C. Concha *et al.*, *Curr. Biol.* **29**, 3996–4009.e4 (2019).
4. A. Martin *et al.*, *Proc. Natl. Acad. Sci. U.S.A.* **109**, 12632–12637 (2012).
5. A. Martin, R. D. Reed, *Dev. Biol.* **395**, 367–378 (2014).
6. A. Mazo-Vargas *et al.*, *Proc. Natl. Acad. Sci. U.S.A.* **114**, 10701–10706 (2017).
7. J. R. Gallant *et al.*, *Nat. Commun.* **5**, 4817–4827 (2014).
8. J. R. Dixon *et al.*, *Nature* **485**, 376–380 (2012).
9. S. M. Van Belleghem *et al.*, *Nat. Ecol. Evol.* **1**, 0052 (2017).
10. J. J. Lewis *et al.*, *Proc. Natl. Acad. Sci. U.S.A.* **116**, 24174–24183 (2019).
11. A. Mazo-Vargas, R. D. Reed, Deep cis-regulatory homology of the butterfly wing pattern groundplan, dataset, Dryad (2022); https://doi.org/10.5061/dryad.8cz8w9gpr.
12. J. Zhang, Q. Cong, J. Shen, P. A. Opler, N. V. Grishin, bioRxiv 829887 [Preprint] (2019).
13. H. F. Nijhout, *The Development and Evolution of Butterfly Wing Patterns* (Smithsonian Institution Press, 1991).
14. H. F. Nijhout, G. A. Wray, *Biol. J. Linn. Soc. Lond.* **33**, 345–365 (1988).
15. M. Kazemian *et al.*, *Genome Biol. Evol.* **6**, 2301–2320 (2014).
16. L. Minnoye *et al.*, *Genome Res.* **30**, 1815–1834 (2020).
17. A. Sourakov, L. T. Shirai, *Trop. Lepid. Res.* **30**, 4–19 (2020).
18. F. Grosveld, J. van Staalduinen, R. Stadhouders, *Annu. Rev. Genomics Hum. Genet.* **22**, 127–146 (2021).
19. E. Z. Kvon, R. Waymack, M. Gad, Z. Wunderlich, *Nat. Rev. Genet.* **22**, 324–336 (2021).
20. A. Tsai, M. R. Alves, J. Crocker, *eLife* **8**, e45325 (2019).

ACKNOWLEDGMENTS

We thank J. Sanders for experimental and analysis input in addition to building a laboratory in the basement of his house and bringing laboratory equipment that allowed us to perform Nanopore genotyping at the beginning of the COVID-19 pandemic. We thank A. Picard Hastings and A. Agrawal for sharing monarch stocks; J. Hanly, S. Van Belleghem, and R. Papa for comments and experimental input; C. Peng, J. Kwan, B. Brack, R. Geltman, and C. Robertson for assistance rearing caterpillars; L. Livraghi and the personnel from genomics core facilities at Cornell University, Duke University, and the University of Maryland–Baltimore for DNA sequencing; and A. Fungtammasan at DNANexus for preassembling PacBio genomes. **Funding:** This study was supported by National Science Foundation grant DGE-1650441 (to A.M.-V.; Graduate Research Fellowship Program); National Science Foundation grants IOS-1656514, IOS-1753559, and IOS-2128164 (to R.D.R.); and National Science Foundation grant IOS-1656553 (to A.M.). **Authors contributions:** Conceptualization: A.M.-V. and R.D.R. Investigation: A.M.-V. Experiments: A.M.-V. and A.W. Writing – original draft: A.M.-V. and R.D.R. Writing – review & editing: A.M.-V. and R.D.R. Simulation analysis: A.M.L. and P.W.M. Resources: K.R.L.v.d.B., L.Z., J.J.L., A.M., and R.D.R. **Competing interests:** The authors declare no competing interests. **Data and materials availability:** Sequence data from ATAC-seq and Hi-C sequencing that support the findings of this study have been deposited in the National Center for Biotechnology Information BioProject PRJNA695303 under BioSamples accession nos. SAMN17611226 to SAMN17611270 and SRX8598136. Additionally, all butterfly wings showing mutations were scanned and deposited in a Dryad repository (*11*).

SUPPLEMENTARY MATERIALS

science.org/doi/10.1126/science.abi9407
Materials and Methods
Figs. S1 to S11
Tables S1 to S7
References (*21*–*47*)
MDAR Reproducibility Checklist
Data S1 and S2

View/request a protocol for this paper from *Bio-protocol*.

Submitted 17 April 2021; accepted 7 September 2022
10.1126/science.abi9407

Deep cis-regulatory homology of the butterfly wing pattern ground plan

Anyi Mazo-VargasAnna M. LangmüllerAlexis WilderKarin R. L. van der BurgJames J. LewisPhilipp W. MesserLinlin ZhangArnaud MartinRobert D. Reed

Science, 378 (6617), • DOI: 10.1126/science.abi9407

The butterfly's grand ground plan

In the 1920s, biologists proposed that butterfly wing pattern diversity evolved as variations of a ground plan of pattern elements that vary in color, shape, and position between different species. Mazo-Vargas *et al*. found that major aspects of this ground plan are determined by an ancient array of deeply conserved noncoding DNA sequences (see the Perspective by Espeland and Podsiadlowski). These regulatory sequences can have both positive and negative effects, and nuanced interactions between noncoding regions sculpt wing patterns. Deep homology of complex, rapidly evolving traits can thus be reflected in noncoding genomic sequences. —LMZ and DJ

EVOLUTION

How butterfly wings got their pattern

Gene regulatory elements play a crucial role in the pattern formation of butterfly wings

By **Marianne Espeland** *and* **Lars Podsiadlowski**

The development of morphological patterns and structures in organisms is the result of transcription factors and epigenetic regulation in different cells and tissues. Transcription factors, which are proteins that bind to DNA at sites called cis-regulatory elements (CREs), can turn gene expression on or off. The fine-tuned regulation of where, when, and to what extent a gene is expressed is also maintained by epigenetic processes, such as by modulating the accessibility of CREs to transcription factors. On an evolutionary time scale, variation in CREs may modify the expression of a neighboring gene and therefore the phenotype of the organism. On page 304 of this issue, Mazo-Vargas *et al.* (*1*) analyze the evolution of regulatory elements of the gene *WntA*, which is involved in wing pattern formation in Nymphalidae butterflies. Their results illustrate how gene regulatory elements can be conserved over a long time but sometimes quickly undergo adaptive changes.

Butterfly wing patterns provide a prominent model for studying the development and genetic regulation underlying evolutionary changes. This is because slight shifts in gene expression of a few master genes, such as *WntA*, affect the expression of several other genes, which can be directly observed as wing color and pattern variations (*2*–*7*). In the family Nymphalidae, which includes more than 6000 species, patterns from different species deviate from the idealized nymphalid ground plan pattern. This idealized pattern consists of color elements arranged in multiple parallel rows across the wings, known as symmetry systems (*8*). For butterflies of the family Nymphalidae, the *WntA* gene modulates certain elements of these symmetry systems and, specifically, the black coloration in the rather atypically patterned genus *Heliconius* (*2*, *3*, *5*), which does not display any typical elements of the symmetry systems. Because the sequence of the protein-coding region of *WntA* is very similar even in Nymphalidae species with different wing patterns, it was assumed that noncoding CREs play a key role in the variation of wing patterns (*2*).

Evolutionary changes in wing patterns of Nymphalidae butterflies, such as that of the common buckeye butterfly (*Junonia coenia*), are mediated by regulatory elements associated with a few master genes.

Mazo-Vargas *et al.* used comparative sequence analysis and ATAC-seq (assay for transposase-accessible chromatin using sequencing). Combining the data from the two analytical methods, the authors identified CREs that might control *WntA* expression in five different Nymphalidae species. Many of the candidate CREs are located immediately upstream of the *WntA* gene and in the first intron. Mazo-Vargas *et al.* find that some of these candidates show sequence similarity among nymphalid butterflies, implying that the candidates were present in their last common ancestor, whereas other candidates evolved recently.

Gene-editing techniques have been useful for understanding the function of genes in wing patterning. For example, after inactivating *WntA*, variations in colors and pattern elements can be observed, demonstrating that this gene is involved in wing pattern development (*5*, *9*). Instead of inactivating the gene itself, Mazo-Vargas *et al.* inactivated regulatory elements that control the gene using CRISPR-Cas9 to excise small stretches of DNA from the genome. The effect of this deletion on the phenotype of the butterfly could then be studied. Mazo-Vargas *et al.* generated such deletions around 46 *WntA*-associated CREs in five butterfly species covering the diversity of the Nymphalidae family. A similar CRISPR-Cas9 approach has been used in butterfly studies before but only on a small taxonomic scale—e.g., for investigating the wing pattern–regulating master gene *optix* and its regulatory elements of butterflies from the genus *Heliconius*, which are also members of the Nymphalidae family (*10*).

The highly divergent wing patterns of members of the genus *Heliconius* do not display typical elements of the symmetry systems found in other Nymphalidae and have been proposed to either be derived from the nymphalid ground plan pattern or to have originated independently (*11*). If the former is true, one would expect to find the same CREs involved in wing pattern formation in *Heliconius* species as in other Nymphalidae species. If the latter is true, the CREs involved in pattern formation in *Heliconius* would not be found in other Nymphalidae species. Mazo-Vargas *et al.* confirm that both explanations are partly true—both conserved and recently evolved CREs play a role in wing pattern formation. Inactivation of each of the five selected deeply conserved CREs in the species *Heliconius himera* had broad effects on the black coloration. This indicates that although *Heliconius* color patterns look very different from those of other Nymphalidae species, they share the same regulatory elements as those butterflies displaying the nymphalid ground plan pattern. Furthermore, inactivation of CREs that are specific for *Heliconius* butterflies resulted in similar phenotypes, which indicates that recently evolved elements have adopted a role in wing patterning alongside the older, conserved CREs.

According to Mazo-Vargas *et al.*, the inactivation of another less-conserved CRE, which is only found in a single species (*Vanessa cardui*) but not in a close relative (*Vanessa tamerlana*), resulted in changes in multiple wing elements on both wings. This corroborates the idea of recently evolved CREs quickly becoming part of the regulatory

Leibniz Institute for the Analysis of Biodiversity Change, Museum Koenig, Bonn, Germany. Email: m.espeland@leibniz-lib.de; l.podsiadlowski@leibniz-lib.de

PHOTO: LYNN M. STONE/MINDEN PICTURES

pathway in color pattern formation. In some cases, inactivation of a CRE expanded the wing area where *WntA* is expressed, demonstrating that some CREs may negatively control *WntA* transcription.

The five species analyzed by Mazo-Vargas *et al.* represent a large part of the diversity of the Nymphalidae family. The broadness of the sampling allows the authors to address the question of sequence similarity for regulatory elements at a larger scale than has been done by previous studies, which have largely restricted their experiments to a few closely related species. By choosing to study the monarch butterfly (*Danaus plexippus*), which is quite distantly related to the other four species in their experiment, the authors show that some regulatory elements are conserved even in species diverging almost 90 million years ago (*12*). So, how far across the order Lepidoptera does this similarity extend? *WntA* is apparently not expressed in the wings of a previously studied butterfly species from the Pieridae family (*13*). It would be interesting to see whether WntA plays a role in the formation of the wing patterns in other butterflies and moths that share similar wing patterns with unpalatable Nymphalidae species to avoid predation. It is worth investigating whether the patterns in these insects evolved through the same genetic pathways—for example, involving *WntA* and the conserved wing pattern master genes *cortex* and *optix* (*4*, *6*, *14*, *15*)—or whether different pathways are involved.

Mazo-Vargas *et al.* demonstrate that although the regulatory landscape surrounding a gene may be stable over a long time, the loss or gain of CREs may suddenly enable evolutionary change. The approach to manipulate CREs and observe the phenotypic changes opens possibilities for examining other gene regulatory questions in developmental biology, such as those relevant for understanding invertebrate and vertebrate body plans. ■

REFERENCES AND NOTES

1. A. Mazo-Vargas *et al.*, *Science* **378**, 304 (2022).
2. A. Martin *et al.*, *Proc. Natl. Acad. Sci. U.S.A.* **109**, 12632 (2012).
3. A. Martin, R. D. Reed, *Dev. Biol.* **395**, 367 (2014).
4. A. E. van't Hof *et al.* *Nature* **534**, 102 (2016).
5. A. Mazo-Vargas *et al.*, *Proc. Natl. Acad. Sci. U.S.A.* **114**, 10701 (2017).
6. N. J. Nadeau *et al.*, *Nature* **534**, 106 (2016).
7. J. R. Gallant *et al.*, *Nat. Commun.* **5**, 4817 (2014).
8. H. F. Nijhout, *The Development and Evolution of Butterfly Wing Patterns* (Smithsonian Institution Press, 1991).
9. C. Concha *et al.*, *Curr. Biol.* **29**, 3996 (2019).
10. J. J. Lewis *et al.*, *Proc. Natl. Acad. Sci. U.S.A.* **116**, 24174 (2019).
11. C. D. Jiggins, *The Ecology and Evolution of* Heliconius *Butterflies* (Oxford Univ. Press, 2017).
12. M. Espeland *et al.*, *Curr. Biol.* **28**, 770 (2018).
13. J. Fenner *et al.*, *Front. Ecol. Evol.* **8**, 197 (2020).
14. A. Prakash, C. Finet, T. D. Banerjee, V. Saranathan, A. Monteiro, *Cell Rep.* **40**, 111052 (2022).
15. L. Zhang, A. Mazo-Vargas, R. D. Reed, *Proc. Natl. Acad. Sci. U.S.A.* **114**, 10707 (2017).

10.1126/science.ade5689

SPECTROSCOPY

An ultraminiaturized spectrometer

Scaling down spectrometers could allow their application in consumer devices

By **Jorge Quereda**[1] *and* **Andres Castellanos-Gomez**[2]

Optical spectrometers can measure the intensity of light with spectral resolution. Although laboratory benchtop spectrometer systems offer high resolution and wide spectral range, their large size hampers them from being more widely adopted for general consumer products, such as wearable electronics. The miniaturization of spectrometers is crucial to making them cheaper and easier to integrate with other devices, which can help expand the use of such a powerful analytical tool. There is a wide range of potential applications for cheap and small-sized spectrometers, from detecting counterfeit pharmaceuticals and banknotes to monitoring specific biosignals. On page 296 of this issue, Yoon *et al.* (*1*) present a design for an ultraminiaturized spectrometer with performance approaching that of benchtop systems.

"The device has a footprint of 22 μm by 8 μm, which is smaller than the average human skin cell."

Over the past decade, the miniaturization of spectrometers has advanced steadily. However, there are often performance trade-offs when miniaturizing them (*2*). For example, designs that are simply scaled-down versions of benchtop models tend to have relatively poor spectral resolution and light sensitivity. The recent development of "reconstructive-type" spectrometers holds promise to overcome these limitations by using a different operation principle, which could allow researchers to develop high-performance, ultraminiaturized spectrometers.

In conventional spectrometers, a dispersive element, such as a prism or a diffraction grating, is used to spread out the spectrum of a light source. Then, the intensity for the different wavelengths is measured using a large array of identical detectors. By contrast, reconstructive spectrometers do not require the use of a dispersive element. Instead, their operation principle relies on a much smaller number of detectors, where each detector is designed to measure light of a different wavelength range. When measuring the light signal, the different detectors produce signals that can be "reconstructed" using software to produce the overall spectrum (*2*). Besides eliminating the need for dispersive elements, this design also reduces the number of sensors from millions to tens or even fewer, which further facilitates device miniaturization.

The recent discovery of semiconducting nanomaterials with strong light-matter interaction opened an avenue for further reducing the size of reconstructive-type spectrometers. An ultracompact microspectrometer (with a footprint of 10 μm by 150 μm) has been produced with a nanowire, which is engineered to contain segments with different light-absorption spectral profiles (*3*). In addition to nanowires, two-dimensional (2D) semiconductors have also been used to make ultracompact microspectrometers. Because the optical absorption spectra of 2D semiconductors can be changed and controlled by an external electric field (*4*, *5*), this enables a design with just a single detector, whose absorption spectrum can be adjusted to scan a range of wavelengths over time. Previously, 2D black phosphorus was used to build a reconstructive-type infrared spectrometer with a very small footprint of 10 μm by 20 μm (*6*). The device, however, did not work in the visible spectrum and required cryogenic temperatures to function, which limited its applications.

The 2D spectrometer presented by Yoon *et al.* works in the visible spectrum under ambient temperature. The ultraminiaturized spectrometer is created using an overlapping junction of two different semiconducting 2D materials—molybdenum disulfide (MoS_2) and tungsten diselenide (WSe_2). The device has a footprint of 22 μm by 8 μm, which is smaller than the average human skin cell.

[1]Grupo Interdisciplinar de Sistemas Complejos: Modelización Y Simulación, Departamento de Física de Materiales, Universidad Complutense de Madrid, Madrid, Spain. [2]Materials Science Factory, Instituto de Ciencia de Materiales de Madrid, Consejo Superior de Investigaciones Científicas, Madrid, Spain. Email: jorquere@ucm.es; andres.castellanos@csic.es

Science
AAAS

Supplementary Materials for

Deep cis-regulatory homology of the butterfly wing pattern ground plan

Anyi Mazo-Vargas *et al*.

Corresponding authors: Anyi Mazo-Vargas, anyimv@gwu.edu; Robert D. Reed, robertreed@cornell.edu

Science **378**, 304 (2022)
DOI: 10.1126/science.abi9407

The PDF file includes:

Other Supplementary Material for this manuscript includes the following:

Materials and Methods

Butterflies

We sampled five distantly related species of nymphalids for the study: *Danaus plexippus*, the monarch butterfly; *Junonia coenia*, the common buckeye; *Vanessa cardui*, the painted lady; *Agraulis vanillae*, the gulf fritillary; and *Heliconius himera*, a neotropical longwing. All butterfly colonies were reared in the Reed Lab at Cornell University. We used a 16:8 hr light:dark cycle at a temperature of 27-30°C and relative humidity of 60%. Monarch butterflies were a gift of the Anurag Agrawal lab at Cornell University, and larvae fed on *Asclepia curassavica*. The *J. coenia* butterflies derived from a lab colony originated by Fred Nijhout lab at Duke University, and the larvae were fed an artificial diet as described by Nijhout (*21*). *V. cardui* caterpillars and artificial food were purchased from US Commercial Provider, Carolina Biological Supplies, catalog # 144070, and 144040. *A. vanillae* pupae were purchased from Shady Oak Butterfly Farm, and *H. himera* were imported from Ecuador through LPS LLC. Larvae of *A. vanillae* and *H. himera* were fed on *Passiflora biflora*.

Genome assemblies

Here we report a novel genome sequence for *A. vanillae* and an improved assembly for *J. coenia*. For *A. vanillae*, a single female individual was obtained from a commercial breeder in Florida (Shady Oak Farms). High molecular weight DNA was extracted from a whole pupa using Qiagen Genomic-tips 100/G, and sequenced on a PacBio Sequel sequencer at the Institute for Genome Sciences (University of Maryland - Baltimore). An initial sequencing library used Sequel v2.1 chemistry and was sequenced on five SMRT cell 1M runs (30 Gb total yield, 8.7 kb mean subread length), and a second library prepared with Sequel v3 chemistry was sequenced on three additional SMRT cell 1M runs with an increase in read length (23 Gb total yield, 13.5 kb mean subread length). An heterozygous assembly was generated using Arrow and FalconUnzip, before haplotype separation using HaploMerger2 (*22*). The resulting haploid genome sub-assembly 411 Mb and N50 contig length of 509 kb is available on the Dryad repository. For *J. coenia*, we improved the assembly presented in (*23*) using Hi-C data (*24*). First Haplomerger2 was used to resolve haplotype assemblies. Next, Hi-C reads from *J. coenia* wings were aligned and a Hi-C contact map was generated using juicer (*25*). Last, we used 3-d DNA (*26*) to anchor, orient and order or contigs. The resulting assembly has a total length of 502 Mb, and an N50 scaffold length of 17.8 Mb. Of note, 32 scaffolds were larger than 5 Mb, suggesting chromosome level assembly. The assembly is available on lepbase.org as *Jc_v2*.

ATAC-seq

We collected three replicates of the head, forewing, and hindwing tissue from the middle of the last developmental instar, for each species. Nuclei were extracted and processed as previously described (*10*), with the following modifications: For each library, 3-4 larvae were dissected in

ice-cold PBS, and isolated wing or head tissues were homogenized with a dounce homogenizer. Homogenate was then dyed with trypan blue, and nuclei were counted using a hemocytometer. The formula used to calculate the number of nuclei was (size human genome (3.2Gb) / butterfly genome size) x 50,000. Lysis and transposition were done according to the original ATAC-seq protocol (*27*). Qiagen PCR cleanup kits were used to clean transposed DNA, followed by PCR amplification for 10-11 cycles and a final PCR cleanup kit purification step. Libraries were pooled and sent to the BRC Genomics Facility at Cornell University for 2 x 37 bp paired-end (PE) read sequencing on an Illumina NextSeq 500. Read alignment and filtering for samples were performed as previously described (*10*). Briefly, ATAC-seq reads were aligned to each species' reference genome (table S3) using Bowtie2 (*28*). We used ATACseqQC (*29*) and Deeptools (*30*) packages to assess data quality. We evaluated alignment metrics, mapping quality, estimated library complexity, and the fraction of reads in the called peaks or FRiP score (table S4). Alignments were filtered, and duplicates were removed. We measured sample correlations using the multiBigwigSummary / plotCorrelation from Deeptools (*30*). Peak calls were made using Fseq (*31*). For visualization, data was normalized for each replicate and tissue using the bamCoverage RPKM method (*30*). A list of non-redundant peak coordinates was generated for each species data set using bedtools intersect (*32*). These data were used as initial input for DESeq2 (*33*) to assess the changes in ATAC-seq peak signals between tissues. Differential accessibility of peaks was called with Benjamini-Hochberg adjusted p-value < 0.05.

Hi-C-seq

We pooled 26 *J. coenia* forewing imaginal discs collected from 13 larvae in the middle of their final developmental instar. We followed a published in-situ Hi-C protocol (*34*) with modifications as described (*10*). Hi-C sequences were analyzed with HiCExplorer tools *30*, *35*). Reads were mapped against *J. coenia* reference genome (*Jc_v2*) to produce a contact matrix (HicBuildMatrix) at different resolution bins (1kb, 5kb, 10kb, 20kb, 50k, 100kb). Matrices were corrected using hicCorrectMatrix (--correctionMethod 'KR'). Finally, we estimated TAD-separation scores to identify the degree of separation between right and left directions of the analyzed bin with tool hicFindTADs, and visualized them with hicPlotTADs.

Whole-genome alignment and ortholog prediction

We identified evolutionarily conserved, orthologous CREs using a known phylogenetic tree (*36*) and a multiple species alignment. Eleven representative genomes from Nymphalidae, plus a *Papilio* genome as outgroup (table S3), were aligned using progressiveCactus (*37*). HAL tools (*38*) was then used to validate and to export alignments to the MAF format. PhastCons was used to calculate conservation scores and predictions of the "most conserved" elements (*39*). Each of the five species in this study was used as a reference to generate conservation tracks for the *WntA* scaffold. Also, we used HALPER (*40*) to identify open chromatin orthologs between the five

species of interest; this tool allowed us to construct continuous orthologs segments using ATAC-seq peaks coordinates and summits for each species.

CRISPR/Cas9 mosaic shotgun CRE deletions

ATAC-seq signal from heads was subtracted from wings using bamCompare with RPKM normalization from Deeptools (*30*) and inspected in IGV browser. We restricted the focus area to the region around the *WntA* coding sequence, limited by the TAD information resulting from Hi-C analysis and conservation between species. The signal in the focal area was visually inspected in each species for sharp differentially accessible peaks with a positive signal in wings. From those, we selected peaks that did not overlap with exons to be incised from the genome using CRISPR/Cas9. We designed between 2-4 sgRNAs per peak (table S1), following the motif N_{20}NGG, and purchased sgRNAs from Synthego. This "shotgun" approach of injecting multiple sgRNAs to produce a range of different deletion lengths in and around individual CREs (see below) in order to screen for different possible sequence-specific functions of the element. To avoid or reduce off-target effects, we checked sgRNA sequences for either: (1) being unique blast hits in the reference assembly (optimal case) or, (2) with few hits but with more than two mismatches in the first eight nucleotides adjacent to the PAM, and no PAM present. For each species, oviposition was stimulated by placing a host plant in their cage; eggs were collected after 1 – 3 hr. *D. plexippus*, *A. vanillae*, and *H. himera* eggs were injected without further treatment. *J. coenia* and *V. cardui* eggs were washed with 5% benzalkonium chloride (Sigma-Aldrich, St Louis, MO, USA) for 60 and 30 seconds, respectively, and then dried in a desiccation chamber for 10 min. Finally, eggs were glued to a slide and injected using either borosilicate or aluminosilicate needles. Larvae were reared as described above. The final number of injected eggs and surviving caterpillars are in the table S5.

Long-read DNA genotyping

Our CRISPR mosaic "shotgun deletion" strategy uses 2-4 pooled sgRNAs to create indels of different sizes at targeted loci. To confirm the correct targeting of sgRNAs *in vivo*, and to assess relative frequencies of edit lengths, we used Nanopore long-read sequencing. DNA was extracted from bodies (thoracic muscle and legs) of butterflies that showed mutant phenotypes using the Omega Biotek E-Z 96 Tissue DNA Kit. We then PCR amplified DNA using primer pairs at least 400 bps away from the most external sgRNAs for each CRE (table S6). Amplified samples were purified with KAPA pure beads. We pooled samples using the EXP-NBD196 kit, and library preparation was done using the Ligation Sequencing Kit (SQKLSK109) following the manufacturer's specifications (Version: NBA_9102_v109_revB_09Jul2020). The flow cell was placed on MiniON (ONT) and allowed to run for 48 hours. MinKNOW produced FAST5 files, and Guppy (*41*) performed base-calling with a high-accuracy model (--barcode_kits EXP-NBD196, --config dna_r9.4.1_450bps_hac.cfg). Canu (*42*) was then used to map long read

sequences to the amplicon wild type sequence. Assembled contigs were filtered to remove non-specific amplification, and positive hits on the *WntA* scaffold were aligned to the reference locus before the scoring of deletions around sgRNAs cut sites in Geneious Prime 2020.1.2. (https://www.geneious.com). A summary of the deletion alleles found and the average read coverage for each CRE are reported in Data S2 and table S7.

Estimation of the shotgun deletion length distribution

It has been reported that CRISPR/Cas9 genome editing can cause unexpected large deletions spanning several kilobases at a non-negligible frequency (*43*, *44*). Such large deletions would be impossible to detect with PCR if they overlap with primer sites. Thus, any amplicon-based deletion screening will be biased towards shorter deletions, and observed deletion length distributions might not be fully representative of the true underlying deletion length distributions. Since unexpectedly large deletions might affect more than one functional genomic element (e.g., CREs or exons), we sought to estimate the relative distribution of large deletions. To do this we conducted a 2-step simulation approach to infer the true underlying deletion length distribution, informed by the empirically observed deletion data, along with parameters of our genotyping strategy (i.e., amplicon size and position of sgRNA target sites).

The long-read sequencing data (Data S2, table S7) suggest that observed deletions fall into two modes: The first mode reflects very short deletions (≤25 bp, n=66), presumably resulting from cuts at only one sgRNA target site. These short deletions are frequent, and should not significantly contribute to the problem outlined above since they would rarely overlap with PCR primer sites. The second mode has a much broader length distribution with an average of 1.1 kb (n=215) (fig. S8). These longer deletions presumably result when multiple sgRNA target sites are cut simultaneously. Based on these observations, our simulation approach assumed two distinct processes for generating short (≤25 bp) and large deletions (> 25 bp). We first inferred the underlying distribution of the larger deletions (step 1), and then estimated the proportion of short deletions *(p)* afterwards (step 2). This sequential approach was justified because p only determines the relative abundance of short deletions and does not affect the distribution of large deletions.

In step 1, we modeled the true underlying large (>25 bp) deletion length distribution with a gamma distribution defined by a scale parameter k, and a shape parameter θ. Although the gamma distribution is only defined by 2 parameters, it is extremely versatile and includes a variety of standard distributions (e.g., exponential, Erlang, and chi-square) as special cases. The gamma distribution allowed us to model deletion length as a positive, unlimited variable with a distribution of arbitrary skewness and flexible shape. We systematically varied both parameters ($k_{min} = 0.25$, $k_{max} = 5$, $k_{step\ size} = 0.25$; $\theta_{min} = 100$, $\theta_{max} = 3000$, $\theta_{step\ size} = 100$) and screened for the parameter value combination (k^*, θ^*) that resulted in the closest resemblance between simulated and empirical large deletion cumulative distribution when mimicking PCR

screening limitations for the simulated data. Specifically, given a parameter combination (k_i, θ_i), we simulated 500 observable deletions for each observed empirical large deletion. This was done by first sampling the center of each simulated deletion uniformly between the two outmost sgRNA target sites of the given locus and then drawing its length from the gamma distribution with the given (k_i, θ_i) pair. If the deletion had any overlap with a PCR primer site, it was rejected and a new deletion was simulated, until 500 observable deletions were obtained for each observed empirical large deletion. Overall, this resulted in 107,500 observable large deletions for each parameter combination (k_i, θ_i). By simulating a constant number of observable deletions per empirical observation, we retained the empirical relative abundances of different butterfly species and PCR amplicons in the simulated data. For each (k_i, θ_i) pair, we then used a Kolmogorov-Smirnov (KS) test to compare the simulated with the empirical large deletion length distribution (excluding all deletions ≤ 25 bp in both distributions). Among all tested (k_i, θ_i) pairs, $k^* = 2.5$ and $\theta^* = 1000$ resulted in the highest resemblance (i.e., lowest KS test statistic) between the empirical and simulated deletion length distributions (fig. S9).

In step 2, we included a proportion p of short deletions (≤ 25 bp) into our simulation approach. For this, we modeled large deletions with the previously determined best fitting gamma distribution ($k^* = 2.5$ and $\theta^* = 1000$) and then systematically varied the proportion of small deletions that are simulated for each empirical observation ($p_{min} = 0$, $p_{max} = 1$, $p_{step\ size} = 0.01$). For simplicity, we set the length of both – simulated and empirical – short deletions to 0, since we are not interested in the precise length distribution of these short deletions, but only their relative proportion among all deletions. For each value of *p*, the resemblance of the observable simulated and empirical deletion length distribution – both now consisting of short and large deletions – was again assessed with the KS test. Among all tested proportions, $p^* = 0.22$ resulted in the highest resemblance (i.e., lowest KS test statistic, fig. S10). Finally, to estimate the frequency of overlooked large deletions in our data, we simulated 1,000,000 deletions using the inferred parameters of our best fitting true deletion length model (22 % short deletions and long deletions drawn from a gamma distribution with $k^* = 2.5$ and $\theta^* = 1000$), but without mimicking PCR screening limitations. For this distribution, 64 % of all deletions were smaller than the average amplicon size (2339 bp) in our deletion sequencing data (fig. S11), suggesting that they should be detectable by the PCR screening approach. From this simulated distribution we calculated P30-P90 values, which indicate the percentage of deletions expected to be under a certain length (e.g., a P50 of 1.7 kb means that 50% of deletions are 1.7kb or less), and graphically mapped these values at each deletion target (fig. S3).

It is important to note that this simulation approach has some limitations. First, it assumes that all large deletions, both observed and unobserved, are generated by the same underlying process. We cannot absolutely rule out that there could exist some additional process that generates exceptionally large, unobservable deletions. It is not clear, however, what such a process would be. The power of our analysis is also limited by the amount of empirical data (281 deletions),

which results in some uncertainty for parameter fitting (fig. S9). While $p^* = 22\ \%, k^* = 2.5$ and $\theta^* = 1000$ yielded the best fit (i.e., lowest KS test statistic) among all tested parameter combinations, but there is some noise in this analysis. We therefore cannot exclude that a different parameter combination could provide a better fit if there were more data. From the data we do have, however, there is no reason to assume that we are dramatically underestimating long deletions. This is also consistent with the fact that we do not observe a strong truncation at the right tail of the empirical deletion length distribution, which we would expect if most deletions were in fact too long for us to detect. Thus, while we cannot rule out that very long deletions may be occurring at some rate, all empirical data and simulations suggest that the majority of deletions should be observed with our PCR screening approach.

Generation and genotyping of *V. cardui CRE 23* F_1 and F_2 mutants

V. cardui eggs were injected within a maximum of one hour after being laid using the three sgRNAs (table S1). Caterpillars were reared as described above. We crossed G_0 crispants in pools of 10-20 butterflies in single cages with a 50:50 sex ratio to obtain F_1 individuals. Eggs were collected for the next generation, with a subsequent cross of ten F_1 butterflies, 50:50 sex ratio. DNA was extracted from the thorax of F_1 and F_2 adult butterflies with mutant phenotypes on their wings. PE150 libraries were sequenced in an Illumina NovaSeq6000 S4 Flow cell at the Institute for Genome Sciences (University of Maryland - Baltimore). Read alignments to the *V. cardui* reference genome (Table S3) were generated using BWA-MEM (*45*). Mosdepth (*46*) calculated the median genome-wide sequencing coverage for 10bp fixed-size windows along the scaffold that includes *WntA*. To normalize the data, coverage values for each window were divided by the average depth for the complete scaffold. Two CRISPR/Cas9 deletion alleles were observed around the gRNA target sites in each of the sequenced butterflies after inspection of the coverage plots and the alignments on IGV 2.13 (*47*) (fig. S7). Although we sequenced a limited number of progeny, it is worth noting that between the eight alleles observed there were ten deletion events 90% smaller than the simulated P30 deletion length (818bp), which is consistent with the predicted deletion length distribution described above. Fluctuations in coverage profiles outside the target region result from population variation compared to the reference genome.

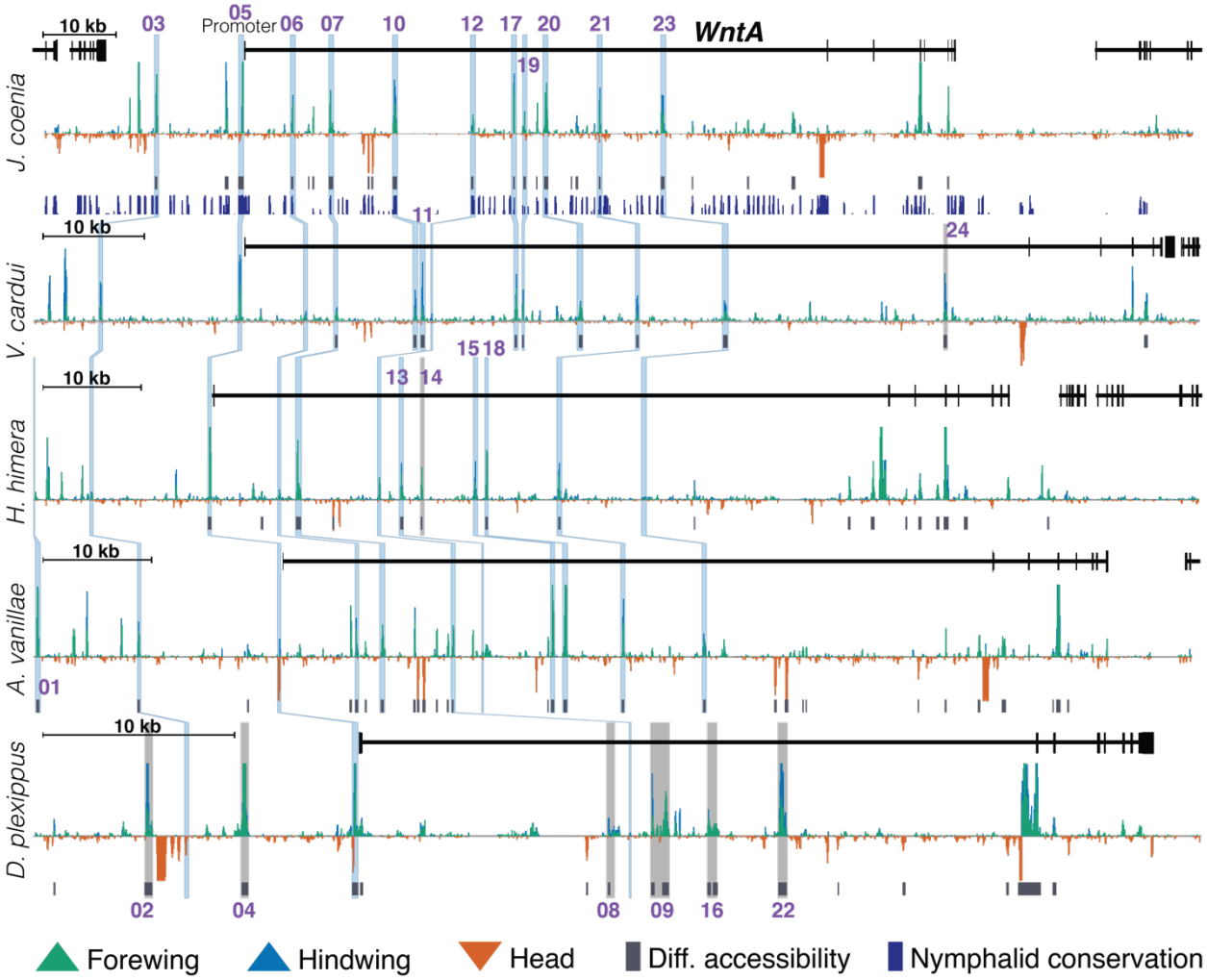

Fig. S1. Chromatin accessibility tracks (ATAC-seq) for each species sampled in this study. Orthologous CREs assessed in this study are highlighted in blue while lineage-specific elements are highlighted in grey. Purple numbers are the IDs for each CRE knocked out in this study.

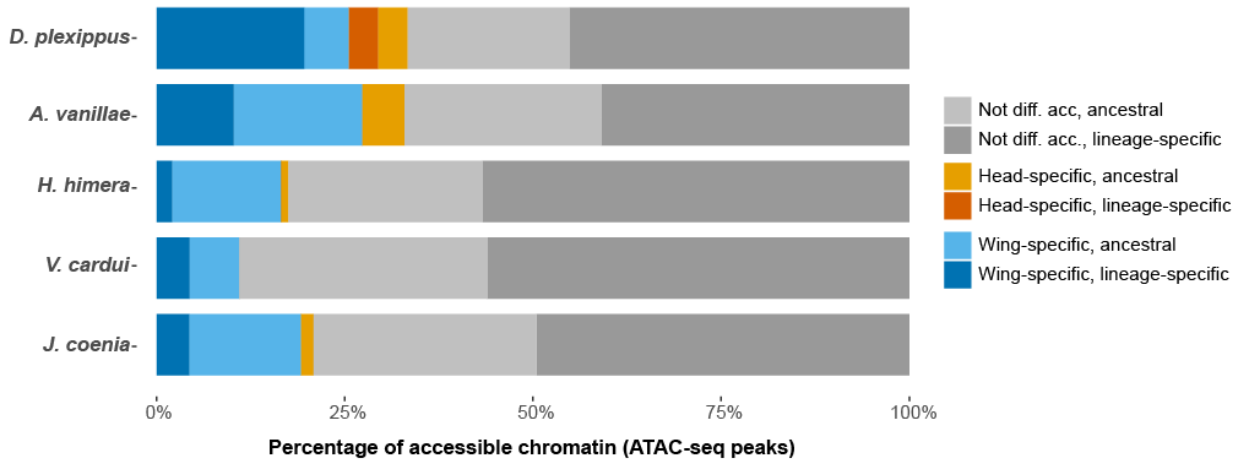

Fig. S2. Distribution of accessible chromatin regions in ancestral and lineage-specific *WntA* TAD sequences. Proportion of peak calls from ATAC-seq profiles overlapping with the 'most conserved' DNA regions were calculated by PhastCons. Most of the ATAC-seq peaks are not differentially accessible between head and wing tissue (grey), but of the differentially accessible peaks, most are wing-specific (blue).

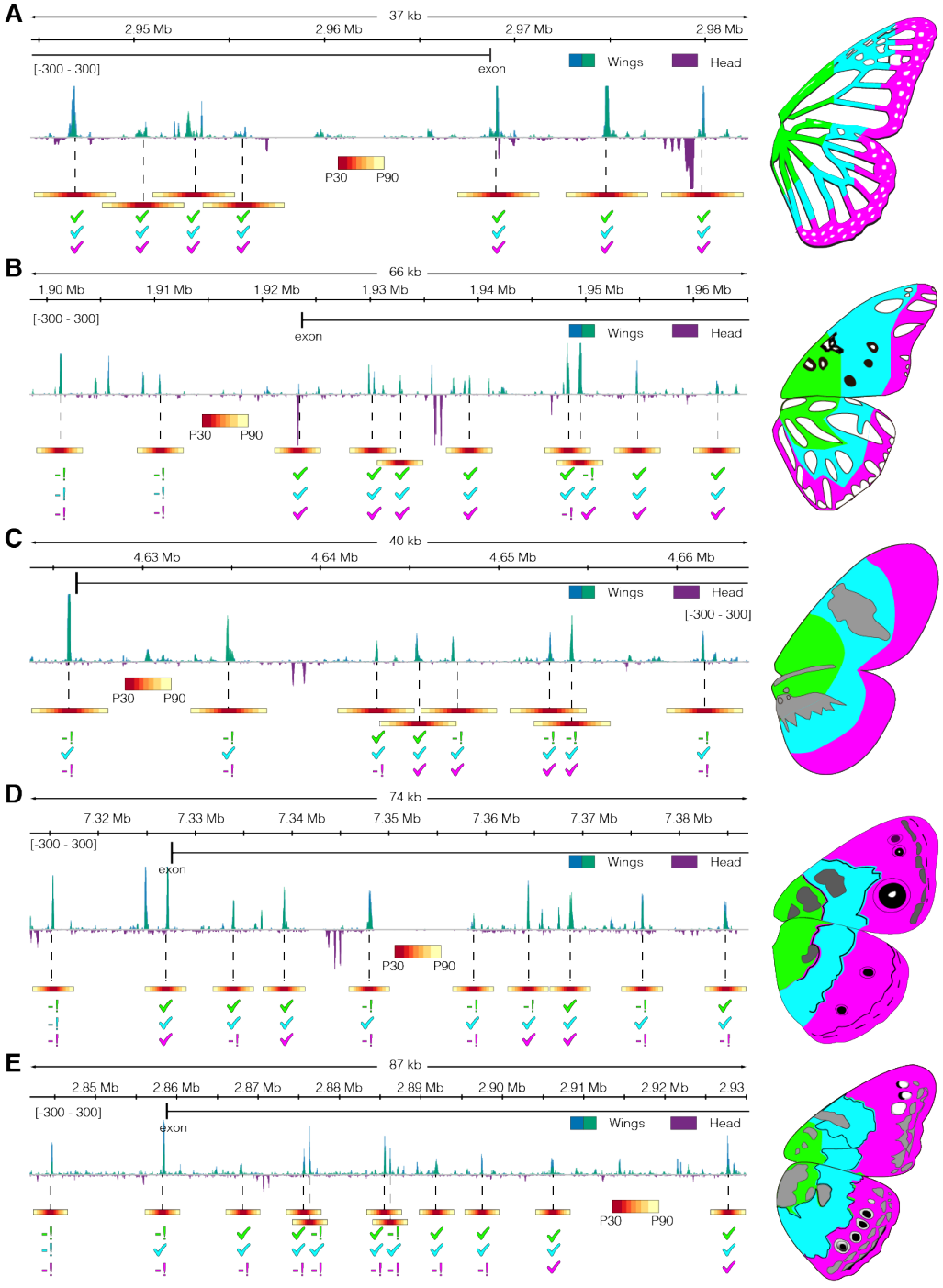

Fig. S3 (previous page). Predicted P30-P90 intervals for expected deletion sizes for each target CRE and the presence of mutant clones in wings. ATAC-seq profiles for (**A**) *D. plexippus,* (**B**) *A. vanillae*, (**C**) *H. himera*, (**D**) *J. coenia*, and (**E**) *V. cardui*. Dotted lines are the middle portion of the expected sgRNAs deletion range with a heatmap with the percentile (P30-P90) sizes of the predicted deletions. We recorded the presence (✓) and absence (-!) of mutant clones in the basal (green), median (cyan), and distal (magenta) regions of butterfly wings. Gray and black colors in the butterfly cartoons are for pattern reference.

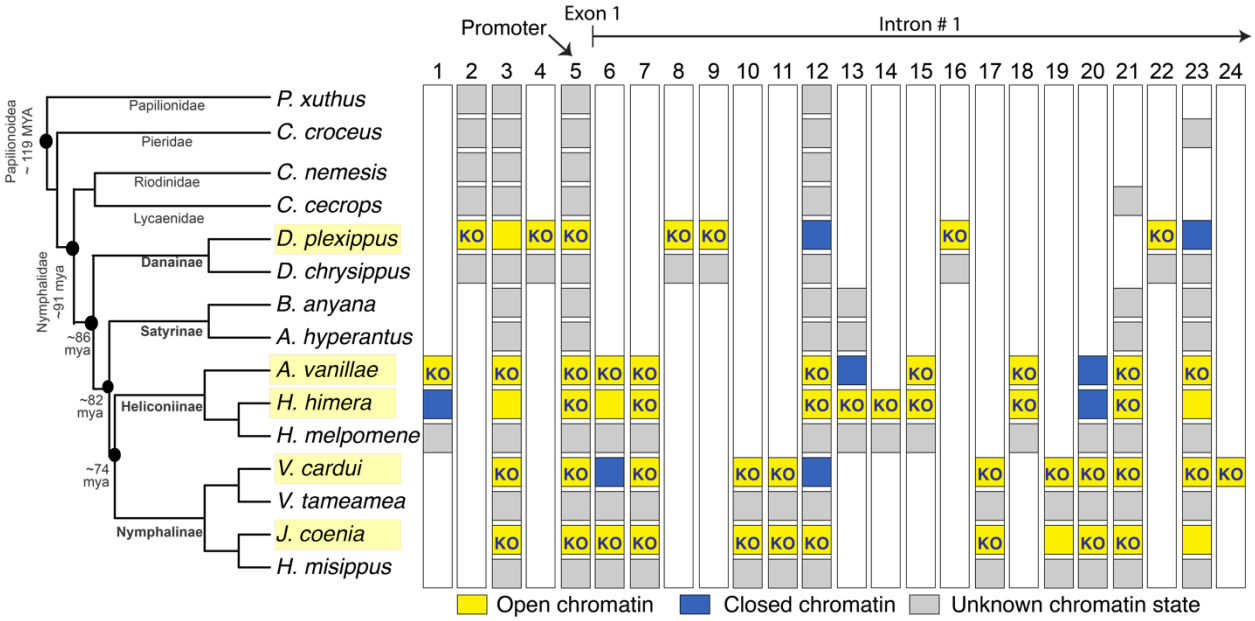

Fig. S4. Phylogenetic histories of *WntA* CREs in this study. Sequence conservation of an expanded selection of butterflies reveals deep conservation of many *WntA* CREs, as well as a handful of recently derived elements in several lineages. Solid color boxes indicate orthologous regions. Divergence times from Espeland *et al.* (*47*).

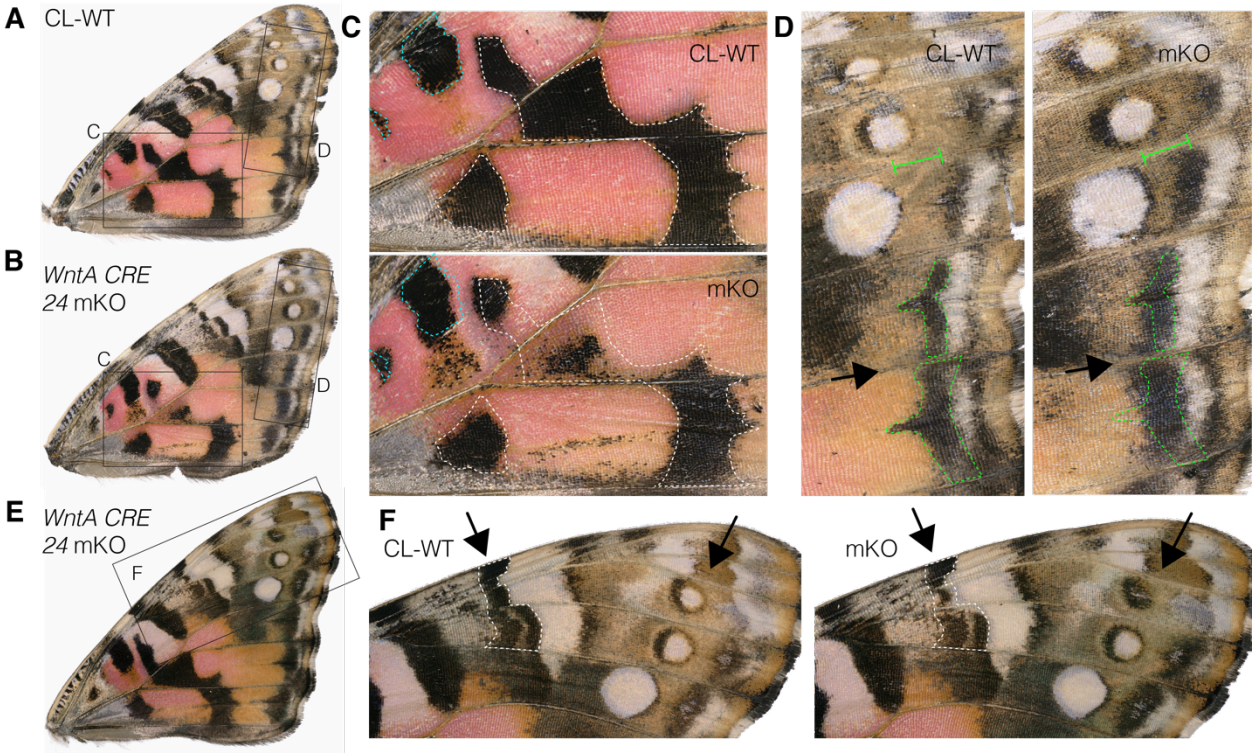

Fig. S5. A recently derived, species-specific CRE regulates multiple ancestral wing patterns. **(A)** *V. cardui* wild type. (**B-F**) *WntA CRE 24* mosaic knockout (mKO) shows effects across multiple pattern elements. Wild type (WT), and mKaO phenotypes are from contralateral (CL) wings of the same individual in **A-D** and **E-F**. The arrows point to mutant changes in pattern between contralateral wings.

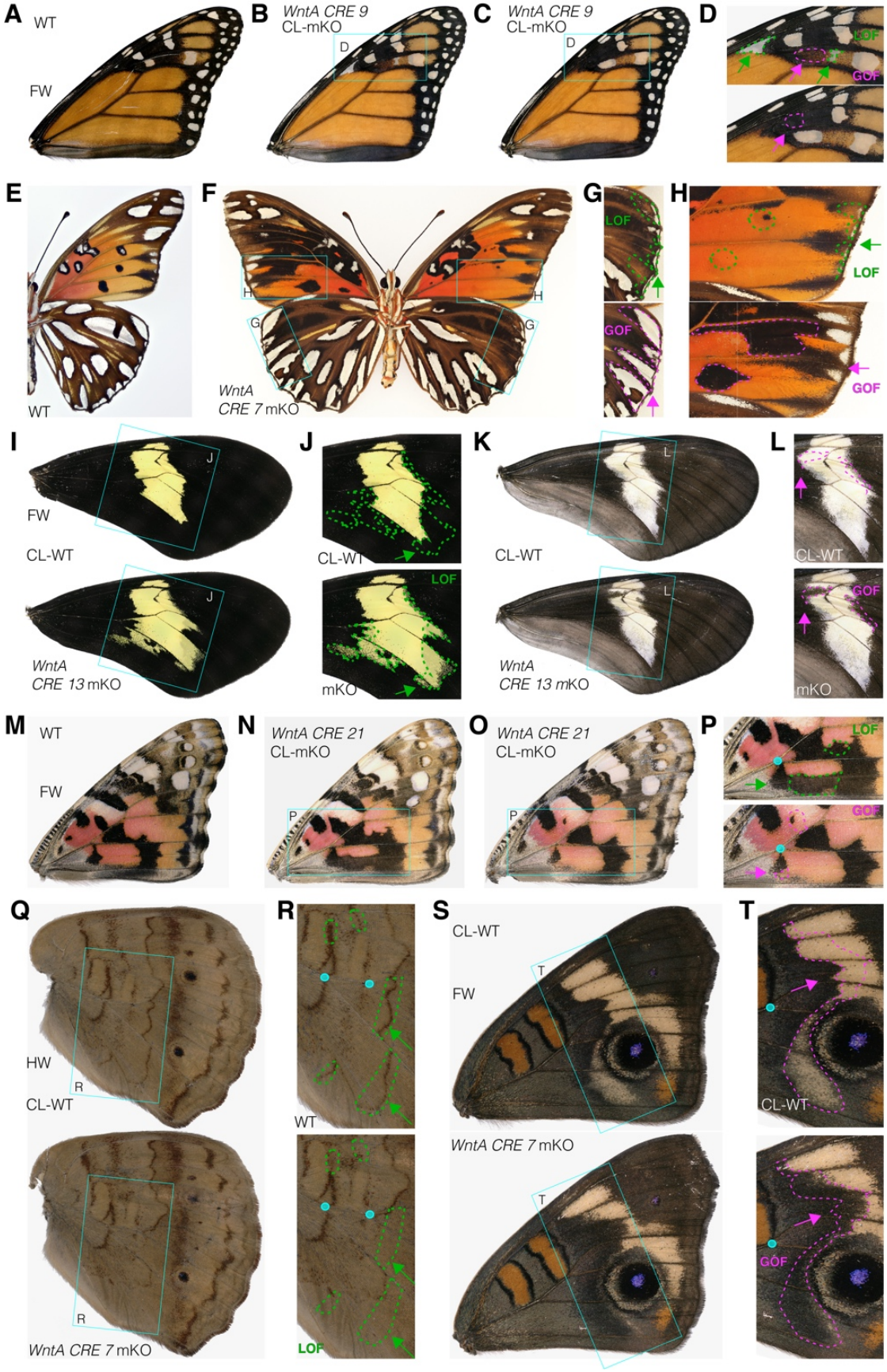
A
WT
FW
B
WntA CRE 9
CL-mKO
D
C
WntA CRE 9
CL-mKO
D
D
LOF
GOF
E
WT
F
H
H
G
G
WntA
CRE 7 mKO
G
LOF
GOF
H
LOF
GOF
I
J
FW
CL-WT
J
WntA
CRE 13 mKO
J
CL-WT
LOF
mKO
K
L
CL-WT
L
WntA
CRE 13 mKO
L
CL-WT
GOF
mKO
M
WT
FW
N
WntA CRE 21
CL-mKO
P
O
WntA CRE 21
CL-mKO
P
P
LOF
GOF
Q
HW
R
CL-WT
R
WntA CRE 7 mKO
R
WT
LOF
S
CL-WT
T
FW
WntA CRE 7 mKO
T
T
CL-WT
GOF

Fig. S6 (previous page). Examples of gain- and loss-of-function from *WntA* CRE knockouts in five nymphalid species. (A) *D. plexippus* ventral wild type wings. (**B-D**) ventral wings of *WntA CRE 9 mKO*. **(E)** *A. vanillae* ventral wild type wings, (**F-H**) wings of a *WntA CRE 7 mKO* crispant showing both *WntA* GOF and LOF clonal effects. (**I-J)** dorsal and (**K-L)** ventral forewings of *H. himera WntA CRE 13 mKO*. (**M**) *V. cardui* wild type ventral forewing. (**N-P**) *V. cardui WntA CRE 21 mKO* effects in the ventral forewing. *J. coenia WntA CRE 7 mKO*, (**Q-R**) in ventral hindwing, (**S-T**) and dorsal forewings. Cyan dots are vein-based wing landmarks. Magenta lines and arrows highlight the gain-of-function (GOF) phenotypic effects, while green colors indicate loss-of-function (LOF) effects.

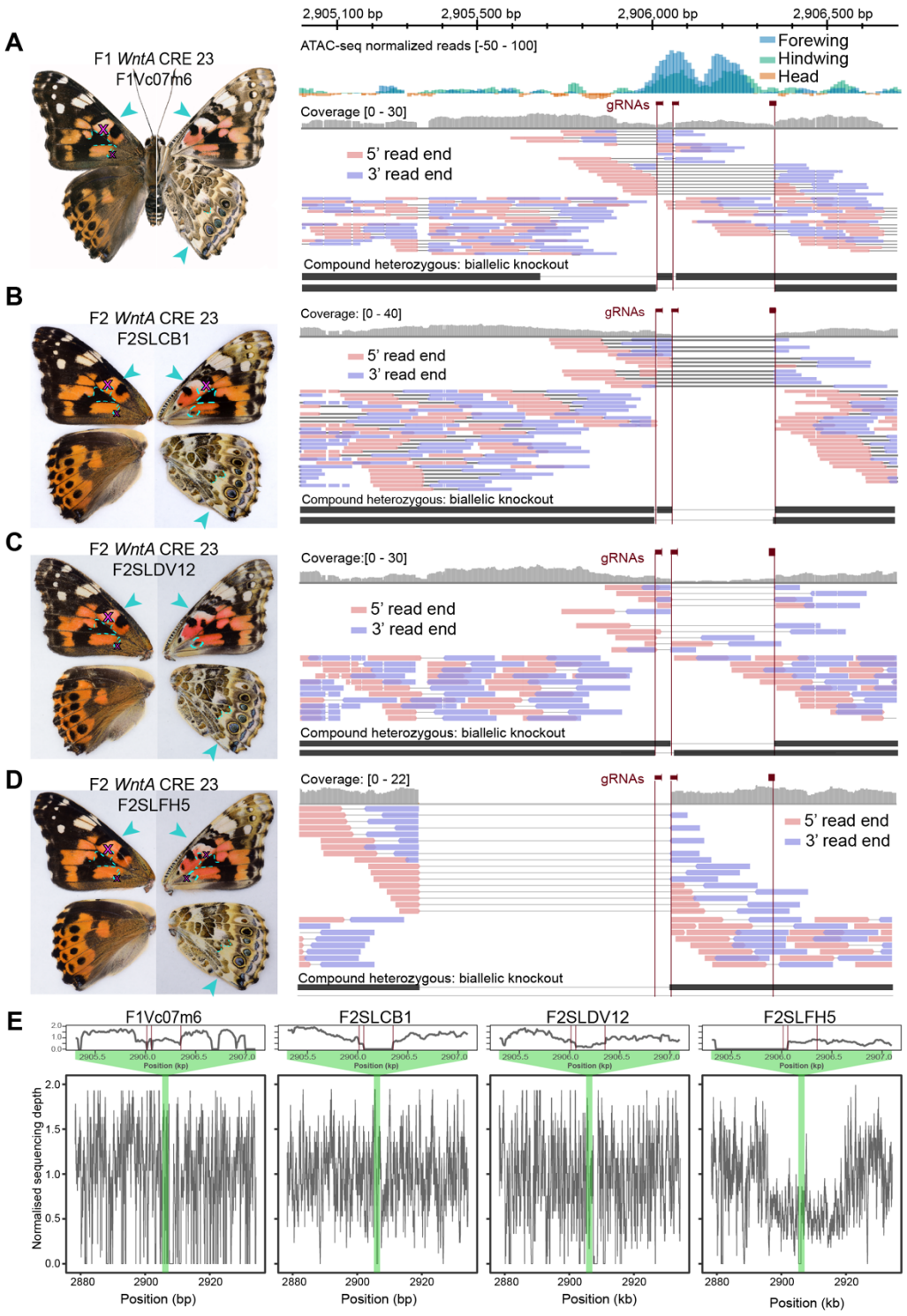

Fig. S7. F_1 and F_2 *WntA CRE 23* mutant genotypes. Genotyping by whole-genome resequencing of **(A)** one F_1 and **(B-D)** three F_2 *V. cardui WntA CRE 23* mutants presenting gain- and/or loss-of-function effects in butterfly color patterns (see Fig 3) with aligned PE150 Illumina reads revealing different knockout alleles. A-D represent compound heterozygosity of two deletion alleles at the targeted site. Cyan arrowheads and dashed annotations show regions with color pattern effects. (E) Normalized mean sequencing coverage around the target site.

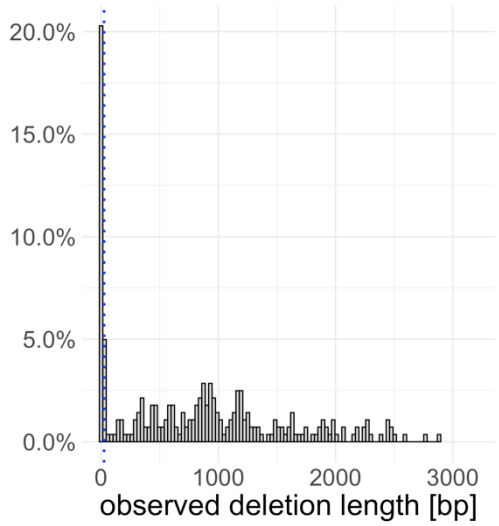

Fig. S8. Empirical deletion length distribution. Shotgun deletion sequencing data, n=281 deletion alleles. A deletion length of 25 bp – the chosen threshold separating short and large deletions in our simulation approach – is highlighted as a vertical dotted line.

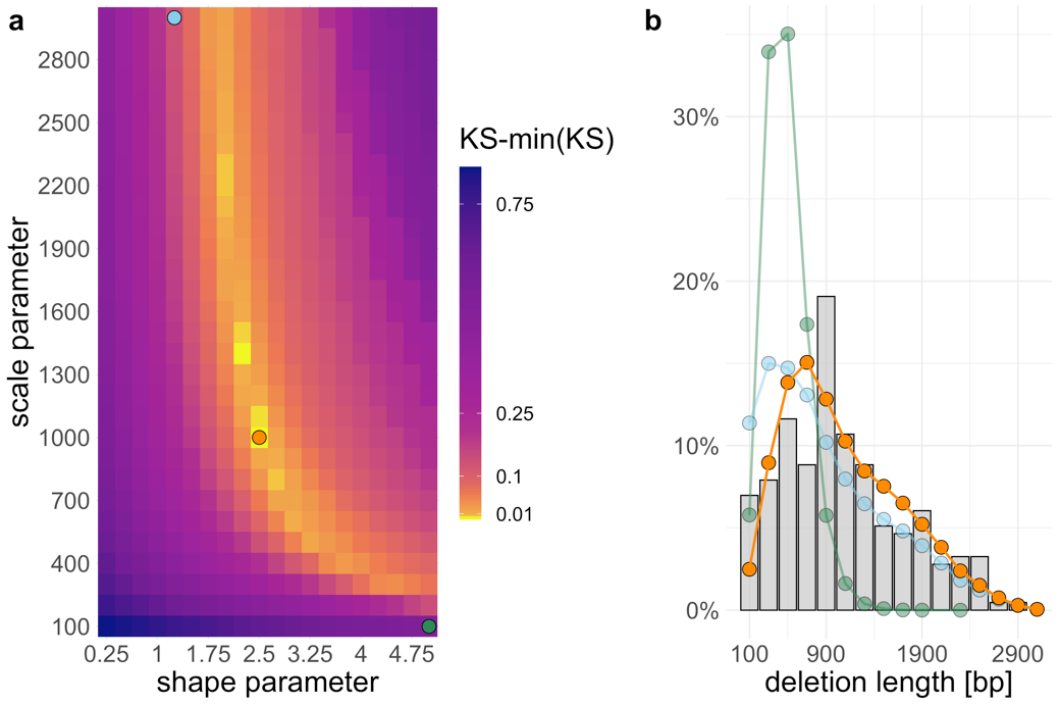

Fig. S9. Large deletion simulations (step 1). (**A**) Difference in Kolmogorov-Smirnov test statistic (KS) between the gamma distribution with the closest resemblance (orange dot, min (KS)=0.06) and other gamma distributions when compared to the empirical large deletion data. Two additional randomly chosen parameter combinations are highlighted in sky-blue and sea-green respectively. (**B**) Standardized empirical (histogram) vs. simulated (dots) large deletion length distributions. Dots are colored according to the used shape and scale parameters (see fig. S9A).

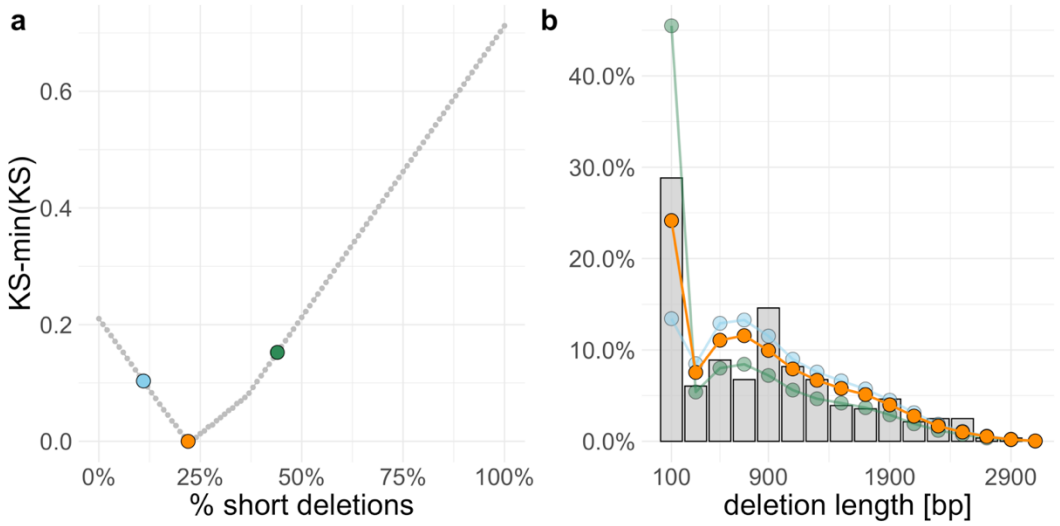

Fig. S10. Small deletion simulations (step 2). (**A**) Difference in Kolmogorov-Smirnov test statistic (KS) between the gamma distribution with the closest resemblance (orange dot, min (KS) = 0.05) and other gamma distributions when contrasted to the empirical deletion data. While the proportion of short deletions varied (x-axis), large deletions were simulated with a gamma distribution using a shape parameter of 2.5, and a scale parameter of 1000. Two additional randomly chosen parameter values are highlighted in sky-blue and sea-green respectively. (**B**) Standardized empirical (histogram) vs. observable simulated (dots) deletion length distributions. Dots are colored according to the used proportion parameter *p* (see fig. S10A).

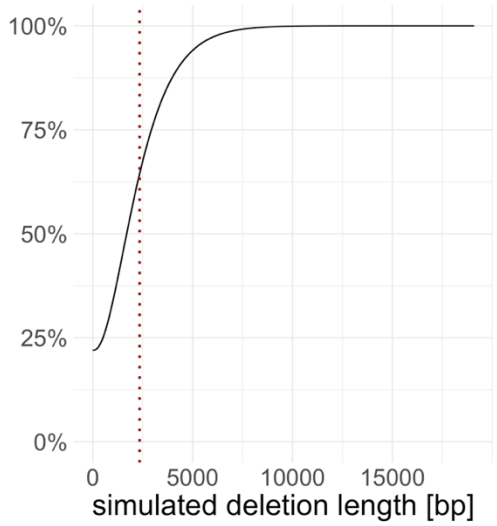

Fig. S11. Cumulative distribution of 1,000,000 simulated deletions. (22 % short deletions, large deletions drawn from a gamma distribution with shape parameter of 2.5 and a scale parameter of 1000) without considering PCR screening limitations. The average PCR amplicon size (2339 bp) of our deletion sequencing data is highlighted as a vertical dotted line.

Table S1.

List of sgRNAs used in CRISPR-Cas9 knock-out experiments. wCRE= *WntA cis*-regulatory element. Vc: *Vanessa cardui*, Jc: *Junonia coenia*, Av: *Agraulis vanillae*, Dp: *Danaus plexippus*, Hhim: *Heliconius himera*.

Element	guide RNA ID	sgRNA sequence
wCREVc01	wCREVc01_01	CGAGGTAAGTGAAACGCACA
wCREVc01	wCREVc01_02	CGTCGACACGTAAAAAGGAA
wCREVc01	wCREVc01_03	TTACATACCGACGATTTCTG
wCREVc01	wCREVc01_04	GATTAATATACTCTAGTGGA
wCREVc02	wCREVc02_01	GCTTTCTCGATTCTGTATAA
wCREVc02	wCREVc02_02	ATTCGTAACGCTATCGAAAC
wCREVc02	wCREVc02_03	GTACGAAGAGGCGGTACGGT
wCREVc02	wCREVc02_04	GCCGCTCTGGTCAAGCGGAT
wCREVc03	wCREVc03_01	CGCCCGCGGATTCATGTTTC
wCREVc03	wCREVc03_02	ACGCCAATAATACGTCGTGG
wCREVc03	wCREVc03_03	AATAACATCGCAAACAGCCT
wCREVc04	wCREVc04_01	GGACGCGTGAACGGGGGTTC
wCREVc04	wCREVc04_02	GGCGGTGGGCATTGTACTTA
wCREVc04	wCREVc04_03	AACACATCTCAATAATCCGA
wCREVc04	wCREVc04_04	ACATGTAACCTCATTCACTT
wCREVc05	wCREVc05_01	ACATTTGCCATCCTTATACG
wCREVc05	wCREVc05_02	AATAAACTCTGTACCTCTGT
wCREVc05	wCREVc05_03	TTACGAATGTGTGAGTGTCG
wCREVc06	wCREVc06_01	ACTGAGATAAAAGACGTCTC
wCREVc06	wCREVc06_02	CTAACTAATGAAATCTACAT
wCREVc06	wCREVc06_03	CATTGACTTGACAGCCTCTA
wCREVc06	wCREVc06_04	AGAGGCCTTGTGTTTAAAGT
wCREVc07	wCREVc07_01	AATCGCCGCTTTGACCACTA
wCREVc07	wCREVc07_02	ATTGGAAGGGGAGTCAGTTT
wCREVc07	wCREVc07_03	TGTGTACCAAGAAAGTGTTA
wCREVc08	wCREVc08_01	GtGACCGTTTCATATGTTTCA
wCREVc08	wCREVc08_02	TGAAAAAGGAACGCGGTCAG
wCREVc08	wCREVc08_03	TTGGGATAAGGCTTCGTAAC
wCREVc08	wCREVc08_04	CGGGCGATGACGTTCGCGCC
wCREVc09	wCREVc09_01	tgaTTCAATTTGAAACAACG
wCREVc09	wCREVc09_02	ATTGTTTTGGCGGGACGCGA
wCREVc09	wCREVc09_03	TGTTTACAAAAGATCTATTG
wCREVc09	wCREVc09_04	TATGTGACTGTTCATTCATT
wCREVc10	wCREVc10_01	GAATGCTGCGAGTATAGATC
wCREVc10	wCREVc10_02	GGCTAGCTGATGCTTATGGT
wCREVc10	wCREVc10_03	CGACGCGCCTGCGATCCGCG
wCREVc10	wCREVc10_04	acaTaaacacaGAACTGAAC
wCREVc11	wCREVc11_01	AAAGTTCGAAATTGATGGTC
wCREVc11	wCREVc11_02	AGCAACCCTGTATCTGGCTA
wCREVc11	wCREVc11_03	ATATTGAAAGCGAATTATTA
wCREJc01	wCREJc01_01	TATGCAAACGTATGTAGTCG
wCREJc01	wCREJc01_02	GGAGTAATAGGTCCCATTAG
wCREJc01	wCREJc01_03	CAGATTACTGACATGACTTT
wCREJc02	wCREJc02_01	TAGGGACAGCTAAAAACGAG
wCREJc02	wCREJc02_02	ACTCGTTTTATTGTTTTGAG
wCREJc02	wCREJc02_03	TACATAAGTCCTTACCAGAC
wCREJc03	wCREJc03_01	ACTATCAACGGTTTTAAGTT
wCREJc03	wCREJc03_02	TAACAATGTTTCGCTTTACG
wCREJc03	wCREJc03_03	CTCTGTATTTACAGCTACAG
wCREJc04	wCREJc04_01	AAATCACGATGTCAGAATAT
wCREJc04	wCREJc04_02	TGCGCGAAACGTCAGCCGCG
wCREJc04	wCREJc04_03	ATGTTGTGTGAAGCGGCTAG
wCREJc05	wCREJc05_01	TTTTATTACAATGCATAGTA
wCREJc05	wCREJc05_02	ACACTTAATAAGGATCTCAT
wCREJc05	wCREJc05_03	GTAATTACGGTGCACTTATT
wCREJc05	wCREJc05_04	TAGATCAGACTTACCTGCAG
wCREJc06	wCREJc06_01	CTACTCAGTTCGTTTTAGAT
wCREJc06	wCREJc06_02	GATATCTTATGAGAGTTATT
wCREJc06	wCREJc06_03	TGACTAGCAGAAAAGCTGAA

Element	guide RNA ID	sgRNA sequence
wCREAv01	wCREAv01_03	AATATACAGTCTTGCCTTTT
wCREAv02	wCREAv02_01	TATGGCCAACTCTAAGTGAC
wCREAv02	wCREAv02_02	CCGGCATGATCGGTACGCTA
wCREAv02	wCREAv02_03	CCTTTAATCTTGGTGACATA
wCREAv03	wCREAv03_01	GCACACTTTGGAAATGGCCG
wCREAv03	wCREAv03_02	CACACATCGCCTGCATATTG
wCREAv04	wCREAv04_01	TGTTGTCAACACTAATTCAA
wCREAv04	wCREAv04_02	ATTGCGACGTCACTTGTCAA
wCREAv04	wCREAv04_03	TTGAAAACATTGCTAAGCTT
wCREAv05	wCREAv05_01	TCTGCATAAAGTGCGTGCGT
wCREAv05	wCREAv05_02	TCCTCTACTTTTCGCTTAAA
wCREAv05	wCREAv05_03	TGCGCGAAACGTCAGTCACA
wCREAv05	wCREAv05_04	GTGTTGTATGGCTTGAACGG
wCREAv06	wCREAv06_01	ATATGTGATACCTTCGAAAT
wCREAv06	wCREAv06_02	GGGTGGACCACCTCTGACTT
wCREAv06	wCREAv06_03	CATTAATTTTAGATCACGGC
wCREAv06	wCREAv06_04	CTGGATAGTGAGATGTCACA
wCREAv07	wCREAv07_01	ACAAGCATAAAGGTACGTAT
wCREAv07	wCREAv07_02	AATATTGTATAGAGTGGGAT
wCREAv07	wCREAv07_03	CCAAATATGTCCCAGAAGAT
wCREAv07	wCREAv07_04	CGAACTATATTAAAAATTCG
wCREAv08	wCREAv08_01	TAATGTAATCGAAATCCAGA
wCREAv08	wCREAv08_02	ACAGTGATGACGTTCGCGCC
wCREAv08	wCREAv08_03	TATATAATCGGATCGGATTT
wCREAv09	wCREAv09_01	ATTTTGCCTCAGCATTTCAC
wCREAv09	wCREAv09_02	AGTTTAAGCCAAAGCACTTC
wCREAv10	wCREAv10_01	ATTACTTTAGTAACAGCTAT
wCREAv10	wCREAv10_02	AGGCTTCTTAGTAAGGGTTA
wCREAv10	wCREAv10_03	TTTCCGACCGCGCGGATCGC
wCREDp01	wCREDp01_01	GAGCTAACGATATACGATTG
wCREDp01	wCREDp01_02	TCTGACATTTCCGTTGTTGA
wCREDp02	wCREDp02_01	CCGGGTGAGAAGAATGCTAA
wCREDp02	wCREDp02_02	GCTTTAAAATTCTCTTATAG
wCREDp03	wCREDp03_01	ATAAACGTAAATCTACCAGA
wCREDp03	wCREDp03_02	CAACAATAGCATTTGTGGAA
wCREDp04	wCREDp04_01	AAGCGGTAACACTCTTATAG
wCREDp04	wCREDp04_02	CCGCCATCACGGCGGCAGCA
wCREDp04	wCREDp04_03	GAGACGGATCCCTACTCAAA
wCREDp04	wCREDp04_04	TGTTCAAACAAGTCTCCCAT
wCREDp05	wCREDp05_01	AATACTTCACCTTGGTCACG
wCREDp05	wCREDp05_02	ACGGAACAGGATGTGCTGTT
wCREDp05	wCREDp05_03	CGCATATTAAATACGTGTGT
wCREDp05	wCREDp05_04	TAAGTATCTCGAGCTGAACA
wCREDp06	wCREDp06_01	GTCATCGGTTTAAGAATCAA
wCREDp06	wCREDp06_02	CCCCGGGACATGTATGGAGC
wCREDp06	wCREDp06_03	CTTTTACAAGGTGCTTATAC
wCREDp07	wCREDp07_01	TCATTGGACCACTTAAGTGT
wCREDp07	wCREDp07_02	CCATAGGATTCGCTAAGGGA
wCREDp07	wCREDp07_03	CGCAGGCGCGTTACCACTCT
wCREDp07	wCREDp07_04	GAAAACTTTCGTGAAGTTGC
wCREHhim1	wCREHhim1_01	GACCAGGCGCTCTGATCTCC
wCREHhim1	wCREHhim1_02	TTTATGACGGCCTAATATCA
wCREHhim1	wCREHhim1_03	GCATACGAGTCTTCTTAATA
wCREHhim1	wCREHhim1_04	TAGACGTTACGTTACAGTGG
wCREHhim2	wCREHhim2_01	CAATGCCTATGCTTATACAT
wCREHhim2	wCREHhim2_02	GGTCCGCCACGGACCGTAGC
wCREHhim2	wCREHhim2_03	TAATATTCAGCTTAGGTTTT
wCREHhim3	wCREHhim3_01	CGTGTTAAGTGCTCAACGCC
wCREHhim3	wCREHhim3_02	GCAAGTACCAAATACGATGA

continuation table S1….

Element	guide RNA ID	sgRNA sequence
wCREJc06	wCREJc06_04	GAGCATTACTTTGCATGTCG
wCREJc07	wCREJc07_01	ACTAATTGAAATTAGAACAT
wCREJc07	wCREJc07_02	CAATCGCTCTATAACCATAG
wCREJc07	wCREJc07_03	ATTTGTCAGTTGAAAGCGAT
wCREJc07	wCREJc07_04	TTAAACCTACGAGAGCTAAA
wCREJc08	wCREJc08_01	CGAATAAAAACATTGCGTTC
wCREJc08	wCREJc08_02	AAATTGATCACACGGTGGCC
wCREJc08	wCREJc08_03	AACTTTTGAGAAAAGGAACG
wCREJc09	wCREJc09_01	TAAAACGATCAACATTTTAG
wCREJc09	wCREJc09_02	AGACGGAATTTATCTACGGC
wCREJc09	wCREJc09_03	TCTGTTGACAACACCTGCCG
wCREJc09	wCREJc09_04	AGATGTCTGGTGAACTTGTT
wCREJc10	wCREJc10_01	TTTGCCCGTCGTACATATTG
wCREJc10	wCREJc10_02	GTTGATCGAAAGAAGATTAA
wCREJc10	wCREJc10_03	GCTGTTGCTTATTCTTGGTG
wCREJc10	wCREJc10_04	GTAATAAACGCGTATCGAAT
wCREAv01	wCREAv01_01	TTAATTTACGTAGGGCTTAA
wCREAv01	wCREAv01_02	GTACGAAGAGGCGGGACGGT

Element	guide RNA ID	sgRNA sequence
wCREHhim3	wCREHhim3_03	GAAGGAATGTGTTACGCATG
wCREHhim4	wCREHhim4_01	TTAAAAAAGATCTATTGTGG
wCREHhim4	wCREHhim4_02	ATTGTTTTGGCGGGACGTGG
wCREHhim4	wCREHhim4_03	TCATGTGAAAGGGATCGCC
wCREHhim6	wCREHhim6_01	AATGTGGCAGCCCATTTCAA
wCREHhim6	wCREHhim6_02	CGAATCTTTCTACCTAAGGG
wCREHhim6	wCREHhim6_03	TATGTGTTTTGATAATATGC
wCREHhim7	wCREHhim7_01	TTACTCGAAGGCATTGAGTA
wCREHhim7	wCREHhim7_02	TAGCTTATTGAAACCGGTTA
wCREHhim7	wCREHhim7_03	AATAGTGCGTTAAGATCTTG
wCREHhim8	wCREHhim8_01	TAGCAATAATTATCTATATT
wCREHhim8	wCREHhim8_02	AAAGCTCTGTTTATGCTTCC
wCREHhim8	wCREHhim8_03	CGTGACACGCGCCGCACCT
wCREHhim8	wCREHhim8_04	CCAAATACTGAGAGCATATC
wCREHhim10	wCREHhim10_01	CTGTTGCTAATGTAATTATA
wCREHhim10	wCREHhim10_02	TAATGTAGGCTTCTTAGTAA
wCREHhim10	wCREHhim10_03	TTTCCTACCGCGCGGATCGC
wCREHhim10	wCREHhim10_04	TGCCGTGATGTGTTGAAGAT

Table S2.

Genome coordinates of target ATAC-seq peaks per each species.

Species	Ortholog CRE #	Species CRE ID	Genome	CRE - Peak call	Maximum targeted deletion size
A. vanillae	CRE #07	wcreAv01	Av.v0	Av_Sc0000002: 1932623-1932905	Av_Sc0000002: 1932650-1932916
A. vanillae	CRE #18	wcreAv02		Av_Sc0000002: 1949300-1949683	Av_Sc0000002: 1949278-1949695
A. vanillae	CRE #15	wcreAv03		Av_Sc0000002: 1948212-1948501	Av_Sc0000002: 1948303-1948416
A. vanillae	CRE #21	wcreAv04		Av_Sc0000002: 1954651-1954871	Av_Sc0000002: 1954571-1954983
A. vanillae	CRE #06	wcreAv05		Av_Sc0000002: 1929801-1930549	Av_Sc0000002: 1929925-1930616
A. vanillae	CRE #12	wcreAv06		Av_Sc0000002: 1939131-1939322	Av_Sc0000002: 1939053-1939355
A. vanillae	CRE #23	wcreAv07		Av_Sc0000002: 1962064-1962330	Av_Sc0000002: 1961973-1962351
A. vanillae	CRE #03	wcreAv08		Av_Sc0000002: 1910389-1910612	Av_Sc0000002: 1910396-1910739
A. vanillae	CRE #01	wcreAv09		Av_Sc0000002: 1901162-1901423	Av_Sc0000002: 1901103-1901344
A. vanillae	CRE #05, Promoter	wcreAv10		Av_Sc0000002: 1923176-1923504	Av_Sc0000002: 1923180-1923418
D. plexippus	CRE #04	wcreDp01	GCF_009731565.1	NC_045826.1: 2974656-2975017	NC_045826.1: 2974707-2974983
D. plexippus	CRE #08	wcreDp02		NC_045826.1: 2955767-2955900	NC_045826.1: 2955660-2955883
D. plexippus	CRE #22	wcreDp03		NC_045826.1: 2946559-2947009	NC_045826.1: 2946617-2947176
D. plexippus	CRE #09	wcreDp04		NC_045826.1: 2952729-2953642	NC_045826.1: 2952716-2953585
D. plexippus	CRE #16	wcreDp05		NC_045826.1: 2950182-2950708	NC_045826.1: 2950239-2950722
D. plexippus	CRE #02	wcreDp06		NC_045826.1: 2979646-2980077	NC_045826.1: 2979666-2980077
D. plexippus	CRE #05, Promoter	wcreDp07		NC_045826.1: 2968925-2969247	NC_045826.1: 2968975-2969309
H. himera	CRE #07	wcreHhim01	Heliconius_erato_demophoon	Herato1001: 4634641-4635171	Herato1001: 4634558-4635168
H. himera	CRE #18	wcreHhim02		Herato1001: 4653966-4654231	Herato1001: 4654069-4654179
H. himera	CRE #15	wcreHhim03		Herato1001: 4652782-4653011	Herato1001: 4652584-4653184
H. himera	CRE #21	wcreHhim04		Herato1001: 4661349-4661614	Herato1001: 4661350-4661775
H. himera	CRE #12	wcreHhim06		Herato1001: 4643046-4643256	Herato1001: 4642987-4643269
H. himera	CRE #13	wcreHhim07		Herato1001: 4645303-4645590	Herato1001: 4645366-4645719
H. himera	CRE #14	wcreHhim08		Herato1001: 4647340-4647553	Herato1001: 4647192-4648338
H. himera	CRE #05, Promoter	wcreHhim10		Herato1001: 4625668-4626032	Herato1001: 4625664-4626179
J. coenia	CRE #10	wcreJc01	jcgen_v2	HiC_scaffold_25: 7347758-7348287	HiC_scaffold_25: 7347721-7348256
J. coenia	CRE #07	wcreJc02		HiC_scaffold_25: 7339018-7339554	HiC_scaffold_25: 7338956-7339393
J. coenia	CRE #21	wcreJc03		HiC_scaffold_25: 7376018-7376320	HiC_scaffold_25: 7375944-7376376
J. coenia	CRE #06	wcreJc04		HiC_scaffold_25: 7333798-7334121	HiC_scaffold_25: 7333769-7334127
J. coenia	CRE #20	wcreJc05		HiC_scaffold_25: 7368495-7369086	HiC_scaffold_25: 7368415-7369069
J. coenia	CRE #17	wcreJc06		HiC_scaffold_25: 7364251-7364531	HiC_scaffold_25: 7364128-7364640
J. coenia	CRE #23	wcreJc07		HiC_scaffold_25: 7384549-7385071	HiC_scaffold_25: 7384349-7385198
J. coenia	CRE #03	wcreJc08		HiC_scaffold_25: 7315140-7315467	HiC_scaffold_25: 7315290-7315403
J. coenia	CRE #12	wcreJc09		HiC_scaffold_25: 7358525-7358856	HiC_scaffold_25: 7358533-7358898
J. coenia	CRE #05, Promoter	wcreJc10		HiC_scaffold_25: 7326569-7327307	HiC_scaffold_25: 7326646-7327283
V. cardui	CRE #10	wcreVc01	Vcar.v1.scaf	VCAR10162: 2875489-2875788	VCAR10162: 2875477-2875743
V. cardui	CRE #07	wcreVc02		VCAR10162: 2867740-2868028	VCAR10162: 2867757-2868563
V. cardui	CRE #24	wcreVc03		VCAR10162: 2927583-2927957	VCAR10162: 2927561-2927924
V. cardui	CRE #11	wcreVc04		VCAR10162: 2876174-2876534	VCAR10162: 2876208-2876551
V. cardui	CRE #20	wcreVc05		VCAR10162: 2891739-2892112	VCAR10162: 2891691-2892160
V. cardui	CRE #17	wcreVc06		VCAR10162: 2885429-2885687	VCAR10162: 2885248-2885739
V. cardui	CRE #23	wcreVc07		VCAR10162: 2905955-2906344	VCAR10162: 2906104-2906353
V. cardui	CRE #03	wcreVc08		VCAR10162: 2844553-2844814	VCAR10162: 2844226-2844756
V. cardui	CRE #21	wcreVc09		VCAR10162: 2897375-2897624	VCAR10162: 2897333-2897665
V. cardui	CRE #05, Promoter	wcreVc10		VCAR10162: 2858195-2858584	VCAR10162: 2857851-2858697
V. cardui	CRE #19	wcreVc11		VCAR10162: 2886165-2886336	VCAR10162: 2886085-2886349

Table S3.

List of species and genome sequence sources used in this study.

Papilio xuthus	Papilionidae - Papilioninae	lepbase.org	Pxut_1.0	Nishikawa *et al.* 2005
Danaeus plexippus	Nymphalidae - Danainae	NCBI	GCF_009731565.1 - Dplex_v4	Gu *et al.* 2019
Danaeus chrysippus	Nymphalidae - Danainae	NCBI	GCA_004959915.1 - KIT_Dchrysippus_v1.3	Martin *et al.* 2020
Bicyclus anyana	Nymphalidae - Satyrinae	lepbase.org	Bicyclus_anynana_v1.2	Nowell *et al.* 2017
Aphantopus hyperantus	Nymphalidae - Satyrinae	NCBI	GCA_902806685.1 - iAphHyp1.1	BioProject: PRJEB36757
Agraulis vanillae	Nymphalidae - Heliconiinae	Dryad	AvanFL_v0.fa	This manuscript
Heliconius erato demophoon	Nymphalidae - Heliconiinae	lepbase.org	Heliconius_erato_demophoon_v1	Van Belleghem *et al.* 2017
Heliconius himera	Nymphalidae - Heliconiinae	lepbase.org	Heliconius_himera_helico3	Edelman *et al.* 2019
Helicinius melpomene	Nymphalidae - Heliconiinae	lepbase.org	Hmel2.5.scaffolds	Pinharanda *et al.* 2018
Hypolimnas misippus	Nymphalidae - Nymphalinae	NCBI	UofC_Hmis_v1.0	VanKuren *et al.* 2019
Junonia coenia	Nymphalidae - Nymphalinae	lepbase.org	jcgen_v2.fa	This manuscript
Vanessa cardui	Nymphalidae - Nymphalinae	lepbase.org	Vcar.v1.scaf.fa	Zhang *et al.* 2021
Vanessa tameamea	Nymphalidae - Nymphalinae	NCBI	ASM293899v1	BioProject: PRJNA493654

Table S4.

ATAC-seq samples with the alignment and quality control statistics. Non-Redundant Fraction (NRF), PCR Bottlenecking Coefficients 1 and 2 (PBC1, PBC2), fraction of reads in called peak region (FRip)

Species	Sample name	Sequencing depth	% mapped	NRF	PBC1	PBC2	FRip
D. plexippus	ATAC001_DpM5thFw1	22,576,990	88%	0.8	0.9	11	0.70
	ATAC023_DpM5thFw2	16,738,827	81%	0.8	0.9	17	0.70
	ATAC025_DpM5thFw3	11,962,082	83%	0.7	0.8	7	0.89
	ATAC002_DpM5thHw1	19,418,685	87%	0.8	0.9	9	0.72
	ATAC024_DpM5thHw2	14,673,669	86%	0.7	0.9	8	0.84
	ATAC026_DpM5thHw3	12,508,804	87%	0.7	0.9	8	0.88
	ATAC027_DpM5thHD1	13,479,773	71%	0.8	0.9	18	0.72
	ATAC028_DpM5thHD2	27,142,322	77%	0.7	0.9	9	0.75
	ATAC029_DpM5thHD3	19,927,620	76%	0.8	0.9	11	0.71
A. vanillae	ATAC034_AvM5thFw1	17,295,707	92%	0.7	0.9	10	0.82
	ATAC037_AvM5thFw2	20,685,695	92%	0.6	0.8	5	0.83
	ATAC040_AvM5thFw3	17,341,680	89%	0.8	0.9	10	0.79
	ATAC035_AvM5thHw1	24,273,551	92%	0.6	0.8	6	0.81
	ATAC038_AvM5thHw2	15,974,424	91%	0.6	0.8	6	0.86
	ATAC041_AvM5thHw3	15,760,591	89%	0.7	0.9	8	0.80
	ATAC036_AvM5thHD1	26,929,395	90%	0.6	0.8	6	0.75
	ATAC039_AvM5thHD2	16,887,692	91%	0.7	0.9	8	0.84
	ATAC042_AvM5thHD3	18,830,151	87%	0.7	0.8	7	0.77
H. himera	ATAC013_HhimM5thFw1	28,390,780	75%	0.8	0.9	17	0.61
	ATAC043_HhimM5thFw2	58,720,883	81%	0.7	0.9	10	0.69
	ATAC048_HhimM5thFw3	32,965,627	78%	0.7	0.9	12	0.67
	ATAC014_HhimM5thHw1	45,342,569	72%	0.8	0.9	19	0.49
	ATAC044_HhimM5thHw2	39,683,955	76%	0.7	0.9	12	0.68
	ATAC049_HhimM5thHw3	32,898,390	79%	0.7	0.9	11	0.75
	ATAC015_HhimM5thHD1	25,895,251	78%	0.8	0.9	23	0.60
	ATAC045_HhimM5thHD2	35,444,279	80%	0.8	0.9	13	0.63
	ATAC050_HhimM5thHD3	31,950,874	79%	0.8	0.9	13	0.68
V. cardui	ATAC004_VcM5thFw1	9,348,925	92%	0.8	0.9	24	0.66
	ATAC010_VcM5thFw2	56,685,433	94%	0.7	0.9	22	0.44
	ATAC030_VcM5thFw3	18,345,041	88%	0.8	0.9	15	0.70
	ATAC005_VcM5thHw1	22,214,567	93%	0.7	0.9	17	0.67
	ATAC011_VcM5thHw2	42,159,245	93%	0.7	0.9	17	0.50
	ATAC031_VcM5thHw3	31,986,703	89%	0.6	0.8	6	0.74
	ATAC012_VcM5thHD1	46,265,224	88%	0.7	0.9	22	0.44
	ATAC032_VcM5thHD2	15,041,762	80%	0.7	0.9	8	0.75
	ATAC033_VcM5thHD3	16,400,602	82%	0.8	0.9	11	0.72
J. coenia	ATAC006_JcM5thFw1	13,878,937	81%	0.9	0.9	18	0.78
	ATAC016_JcM5thFw2	16,126,659	88%	0.9	0.9	16	0.79
	ATAC019_JcM5thFw3	52,718,382	86%	0.9	0.9	18	0.61
	ATAC017_JcM5thHw2	18,205,610	75%	0.9	1.0	27	0.60
	ATAC020_JcM5thHw3	30,218,065	77%	0.9	0.9	22	0.60
	ATAC046_JcM5thHw4	51,718,806	87%	0.7	0.9	8	0.79
	ATAC018_JcM5thHD1	23,298,731	79%	0.9	1.0	29	0.48
	ATAC021_JcM5thHD2	20,697,385	81%	0.8	0.9	10	0.63
	ATAC047_JcM5thHD4	32,603,886	82%	0.9	0.9	18	0.55

Table S5.

Summary of CRISPR/Cas9 experiments and number of mosaic mutant adults.

Species	Ortholog CRE #	Species CRE ID	Number of sgRNAs	Concentration each sgRNA	Time APC	# eggs	Hatched larvae	Hatching rate	Number of mutant adults	Genotyping method
A. vanillae	CRE #07	wcreAv01	3	475	2 h	130	96	74	19	Amplicon - Nanopore
	CRE #18	wcreAv02	3	250	2h 30 m	143	74	52	7	Amplicon - Nanopore
	CRE #15	wcreAv03	2	250	2h 30 m	139	18	13	4	Amplicon - Nanopore
	CRE #21	wcreAv04	3	250	3 h	60	36	60	15	Amplicon - Nanopore
	CRE #06	wcreAv05	4	250	3 h	80	27	34	6	Amplicon - Nanopore
	CRE #12	wcreAv06	4	250	3 h	100	55	55	35	Genome wide - Nanopore
	CRE #23	wcreAv07	4	250	3 h	94	46	49	23	Amplicon - Nanopore
	CRE #03	wcreAv08	3	250	3h 30 m	55	35	64	0	Genome wide - Nanopore
	CRE #01	wcreAv09	2	250	3h 30 m	99	41	41	3	Genome wide - Nanopore
	CRE #05, Promoter	wcreAv10	3	250	3 h	47	25	53	8	Amplicon - Nanopore
D. plexippus	CRE #04	wcreDp01	2	250-400	2h 30 m	150	93	62	7	Amplicon - Nanopore
	CRE #08	wcreDp02	2	250	2h 36m	116	66	57	29	Amplicon - Nanopore
	CRE #22	wcreDp03	2	250	2h 5m	75	54	72	5	Amplicon - Nanopore
	CRE #09	wcreDp04	4	250	2h 5m	102	68	67	10	Amplicon - Nanopore
	CRE #16	wcreDp05	4	250	2h 30 m	167	87	52	2	Amplicon - Nanopore
	CRE #02	wcreDp06	3	250	2h 30 m	191	65	34	12	Amplicon - Nanopore
	CRE #05, Promoter	wcreDp07	4	250	2h 30 m	240	90	38	19	Amplicon - Nanopore
H. himera	CRE #07	wcreHhim01	4	250	3 h	72	13	18	6	Amplicon - Nanopore
	CRE #18	wcreHhim02	3	250	3 h	30	13	43	7	Genome wide - Nanopore
	CRE #15	wcreHhim03	3	250	3 h	55	20	36	4	Amplicon - Nanopore
	CRE #21	wcreHhim04	3	250	3 h	60	21	35	3	Amplicon - Nanopore
	CRE #12	wcreHhim06	3	250	2h 45 m	68	24	35	3	Genome wide - Nanopore
	CRE #13	wcreHhim07	3	250	2h 45 m	55	16	29	4	Amplicon - Nanopore
	CRE #14	wcreHhim08	4	250	2h 45 m	58	12	21	3	Genome wide - PacBio
	CRE #05, Promoter	wcreHhim10	4	250	2h 45 m	30	10	33	1	Amplicon - Nanopore
J. coenia	CRE #10	wcreJc01	3	250	2-3 h	1177	172	15	7	Genome wide - Nanopore
	CRE #07	wcreJc02	3	125 - 250	2-3 h	1307	223	17	4	Amplicon - Nanopore
	CRE #21	wcreJc03	3	125 - 250	2-3 h	1019	206	20	7	Amplicon - Nanopore
	CRE #06	wcreJc04	3	100 - 250	2-3 h	803	112	14	2	Amplicon - Nanopore
	CRE #20	wcreJc05	4	100-125-250	2-3 h	1842	167	9	17	Amplicon - Nanopore
	CRE #17	wcreJc06	4	125 - 250	2-3 h	1349	189	14	4	Genome wide - Nanopore
	CRE #23	wcreJc07	4	125-150-250	2-3 h	1326	121	9	3	Amplicon - Nanopore
	CRE #03	wcreJc08	3	125-250	2-3 h	495	176	36	0	Amplicon - Nanopore
	CRE #12	wcreJc09	4	250	2-3 h	302	125	41	7	Genome wide - Nanopore
	CRE #05, Promoter	wcreJc10	4	250	2-3 h	287	95	33	27	Amplicon - Nanopore
V. cardui	CRE #10	wcreVc01	4	250	3 h	257	131	51	6	Amplicon - Nanopore
	CRE #07	wcreVc02	3	250	3 h	704	44	6	1	Amplicon - Nanopore
	CRE #07	wcreVc02	4	75	3h 15 m	529	100	19	7	Amplicon - Nanopore
	CRE #24	wcreVc03	4	250	2h 30 m	270	91	34	16	Amplicon - Nanopore
	CRE #11	wcreVc04	4	250	3 h	562	191	34	5	Amplicon - Nanopore
	CRE #20	wcreVc05	3	250	2h 30 m	338	88	26	12	Amplicon - Nanopore
	CRE #17	wcreVc06	4	250	4 h	562	248	44	11	Amplicon - Nanopore
	CRE #23	wcreVc07	3	250	2h 30 m	400	224	56	42	Amplicon - Nanopore
	CRE #03	wcreVc08	4	250	2h 10m	150	66	44	0	Amplicon - Nanopore
	CRE #21	wcreVc09	2	100	2h 30 m	719	315	44	15	Amplicon - Nanopore
	CRE #05, Promoter	wcreVc10	4	250	2h	144	35	24	1	Amplicon - Nanopore
	CRE #19	wcreVc11	3	250	2h 12m	236	94	40	6	Amplicon - Nanopore

Table S6.

List of oligos used to amplify regions containing target CREs

Element	primer name	sequence
wcreAv01	NP_Av01_FWD	ATACTGTCCCACTGGGCGCT
wcreAv01	NP_Av01_REV	TCTGCCCTCAAACGCAACGG
wcreAv02	wcreAv02FWD	GAGATTGAGATCGAGAATCGAGA
wcreAv02	NP_Av02_REV	AACCATACGCACGAAGCTGCA
wcreAv03	NP_Av03_FWD	GGTACGTGAGCGCGTCTTCA
wcreAv03	NP_Av03_REV	TCAGATGCCCTCTCGGTGGA
wcreAv04	NP_Av04_FWD	GGCAATCCGAAATGGCCGTA
wcreAv04	NP_Av04_REV	CCACCTTTCCGTGGCATTGC
wcreAv06	NP_Av06_FWD	GCATTACTCCCGTCGCCGTT
wcreAv06	NP_Av06_REV	ACAGTGACGTACCGCAACCA
wcreAv07	NP_Av07_FWD	CTCAGCGCCGTGGTTGTCTA
wcreAv07	NP_Av07_REV	TTGCCCCCTTAGCCTTCTCA
wcreAv10	NP_Av10_FWD	CGGAATGCTGCCAATGATATGC
wcreAv10	NP_Av10_REV	CCCGACAGTCTGAGGAAGTCAT
wcreDp01	NP_Dp01_FWD	AGATTTTGTGGAGGCCCGGC
wcreDp01	NP_Dp01_REV	AAACCCTCCAGAGACGCCGT
wcreDp02	NP_Dp02_FWD	GCGGCTTCTTGTGGCTTCTC
wcreDp02	wcreDp02FWD	GGCCGTAACAAGCTGAGGCA
wcreDp03	NP_Dp03_FWD	CGCATCGGACGTCCAAGCAA
wcreDp03	NP_Dp03_REV	AGACCGCACACACGTCAAGA
wcreDp04	wcreDp04FWD	TCGCAGAGGATACAGCCGTC
wcreDp04	wcreDp04REV	ACGCCGCTATCATCAAACGC
wcreDp05	NP_Dp05_REV	GCATAGCACAAGTTTGCCCGA
wcreDp05	wcreDp05FWD	TCCAGGCTTGTAGAAACAATGTCA
wcreDp06	NP_Dp06_FWD	GACGCAAGAACCTTGCAGGC
wcreDp06	NP_Dp06_REV	GCACTCAATCAACGCGGCTG
wcreDp07	NP_Dp07_FWD	ATTCCTGGACGCTCCACATG
wcreDp07	NP_Dp07_REV	AGGTTTCGATACATGGAGTGCA
wcreHhim02	NP_Hhim02_FWD	AAACCGACGATGAGGAGGCG
wcreHhim02	NP_Hhim02_REV	ACCAGACAACCTTTGGGTTAGGA
wcreHhim03	NP_Hhim03_FWD	CCGATAGCGCAGAGTGCACC
wcreHhim03	NP_Hhim03_REV	CGTCTAACGACCCACGCCTC
wcreHhim04	NP_Hhim04_FWD	GAGTGCCGCCACAATGCTTC
wcreHhim04	NP_Hhim04_REV	GCCTCCAGCAAAGTCGGGAA
wcreHhim07	NP_Hhim07_FWD	GTCCGGTGTGGTCGAAGTGA
wcreHhim07	NP_Hhim07_REV	AACTGCCCGAATACAGGGCGT
wcreHhim10	NP_Hhim10_FWD	GCTGCATCCCGTACACCACAA
wcreHhim10	NP_Hhim10_REV	AAACAGTCTCCCTACCCCGCA
wcreJc02	NP_Jc02_FWD	AGGGCTGATACGCACTAGCGG
wcreJc02	NP_Jc02_REV	GGTCGAGCGGTGTGTCGAA
wcreJc03	NP_Jc03_FWD	ACCCTACAACTGACTCGCCAA

Element	primer name	sequence
wcreJc03	NP_Jc03_REV	AGACGTCCCGACGAACAACCA
wcreJc04	NP_Jc04_FWD	CGCGCGCACGAAATAGCTT
wcreJc04	NP_Jc04_REV	AGGTTTAACAAGCGCGTTGGG
wcreJc05	NP_Jc05_FWD	GGTCGGCGACACATACGTGA
wcreJc05	NP_Jc05_REV	TCGCGCTGAAGTGGATGTGT
wcreJc07	NP_Jc07_FWD	ACAAACCGCCGCGCTGAAATA
wcreJc07	NP_Jc07_REV	AAACGGATCGTGCCATCTCCA
wcreJc08	wcreJc08FWD	CGTCGCGTCACTAGTAATCAGTACA
wcreJc08	NP_Jc08_REV	CTGGTGCCGAGCCCAAGATA
wcreJc10	NP_Jc10_FWD	AAAATGAGCATCTGCCTGCGGT
wcreJc10	NP_Jc10_REV	GTTTCAACCGTGCTTACGTGCG
wcreVc01	NP_Vc01_FWD	AGAGATCACCAAGTTGACCGT
wcreVc01	NP_Vc01_REV	GCACTATGGACCTGTCGCCA
wcreVc02	NP_Vc02_FWD	GCGCATGGTTCACTAACGCC
wcreVc02	NP_Vc02_REV	AGTGTCGTGTGGCAAGTCGAG
wcreVc03	wcreVc03FWD2	CCGTCTGGGTAGCACCAACT
wcreVc03	wcreVc03REV	GACAGCATCCCTTCCAACAC
wcreVc04	wcreVc04FWD	TCTGCCCACGTTGTACGCTT
wcreVc04	NP_Vc04_REV	TGACAACACCTGCCGTGGTT
wcreVc05	NP_Vc05_FWD	ACGCTGTCTCACTCACGCTA
wcreVc05	NP_Vc05_REV	TCAGTGCAGGCGTGACTGATC
wcreVc07	wcreVc07_FWD	CAGGTGTAGTGCACGTCGAT
wcreVc07	NP_Vc07_FWD02	GGCGGCTTTGAGTGACAGGAA
wcreVc07	NP_Vc07_FWD03	GTGATCCACGGTTACGCTCGT
wcreVc07	NP_Vc07_FWD04	TCGCGCGTGATATACACCGA
wcreVc07	NP_Vc07_FWD05	GGGACTCTGACCCTCTCCAGGTG
wcreVc07	wcreVc07_REV	TCTGTGTCCTCTTGGAGCCG
wcreVc07	NP_Vc07_REV	CCACAGTGGGGCCAGAACAT
wcreVc07	NP_Vc07_REV02	ATGCCTAAGACTCGCGGACA
wcreVc07	NP_Vc07_REV03	ACGAGAATGCTGAAGAATACGAGAA
wcreVc07	NP_Vc07_REV04	ACGACGCGGTCATGACTGGATCAGC
wcreVc06	NP_Vc06_FWD	CCCTACGGCGACTTCGTACG
wcreVc06	NP_Vc06_REV	CGCAAACGGGAGAGTTGACTG
wcreVc08	NP_Vc08_FWD	ATATGGAGCGCGGTTGTGCC
wcreVc08	NP_Vc08_REV	GTCGACAGACGTCATCTGCCTAGT
wcreVc09	NP_Vc09_FWD	GATGGCGCGCCTTTCCAAGT
wcreVc09	wcreVc09REV	AAGCGGTAACGCCTCGTTAAA
wcreVc10	NP_Vc10_FWD	AAAGGACTTGCTACCCGCCAC
wcreVc10	NP_Vc10_REV	TCGCAAGCTGGCATCGAAGA
wcreVc11	wcreVc06FWD	CGCATCGATTCACTGGCAGA
wcreVc11	NP_Vc11_REV	TCAACTCACGGTGACACGCT

Table S7.

Nanopore sequencing coverage statistics.

							Coverage statistics - Canu Nanopore amplicon reads assemblies				
Species	Ortholog CRE #	Species CRE ID	WT Amplicon size	Target deletion size	ratio KO/Amplified	# samples	# alleles	mean	max	min	sd
A. vanillae	CRE #07	wcreAv01	1807	266	0.15	3	3	80.10	95.68	68.27	14.09
A. vanillae	CRE #18	wcreAv02	1520	417	0.27	3	3	93.31	113.91	71.38	21.30
A. vanillae	CRE #15	wcreAv03	2187	113	0.05	3	9	64.76	125.05	23.88	37.19
A. vanillae	CRE #21	wcreAv04	2990	412	0.14	2	5	61.44	207.59	7.36	84.52
A. vanillae	CRE #12	wcreAv06	2061	302	0.15	3	7	73.01	276.60	10.90	95.75
A. vanillae	CRE #23	wcreAv07	2302	378	0.16	3	6	64.15	198.19	14.46	69.79
A. vanillae	CRE #03	wcreAv08	2986	343	0.11	1	1	56.05	56.05	56.05	NA
A. vanillae	CRE #01	wcreAv09	3017	241	0.08	1	1	107.15	107.15	107.15	NA
A. vanillae	CRE #05, Promoter	wcreAv10	2308	238	0.10	3	9	112.54	532.61	7.23	172.86
D. plexippus	CRE #04	wcreDp01	1574	276	0.18	3	6	35.64	89.42	15.23	27.49
D. plexippus	CRE #08	wcreDp02	1974	223	0.11	3	17	45.15	194.22	5.26	48.87
D. plexippus	CRE #22	wcreDp03	2852	559	0.20	2	3	38.21	69.84	9.12	30.44
D. plexippus	CRE #09	wcreDp04	3065	869	0.28	2	5	42.85	97.84	19.24	32.71
D. plexippus	CRE #16	wcreDp05	1520	483	0.32	2	7	46.51	86.98	12.16	28.80
D. plexippus	CRE #02	wcreDp06	2792	411	0.15	3	9	52.96	107.53	12.96	32.23
D. plexippus	CRE #05, Promoter	wcreDp07	3147	334	0.11	3	14	86.14	600.98	9.05	158.07
H. himera	CRE #07	wcreHhim01	2984	620	0.21						
H. himera	CRE #18	wcreHhim02	1912	258	0.13	2	5	48.57	89.62	7.80	38.75
H. himera	CRE #15	wcreHhim03	2828	533	0.19	3	12	29.98	99.68	4.84	29.94
H. himera	CRE #21	wcreHhim04	2684	414	0.15	3	10	62.01	219.70	2.84	63.89
H. himera	CRE #12	wcreHhim06	1775	282	0.16						
H. himera	CRE #13	wcreHhim07	1695	321	0.19	2	7	40.91	81.47	13.16	31.40
H. himera	CRE #05, Promoter	wcreHhim10	2281	515	0.23	1	4	41.30	78.04	6.43	33.67
J. coenia	CRE #10	wcreJc01	2019	535	0.26						
J. coenia	CRE #07	wcreJc02	2488	437	0.18	5	11	46.71	76.10	3.61	20.88
J. coenia	CRE #21	wcreJc03	1643	432	0.26	3	6	51.88	110.66	11.07	38.97
J. coenia	CRE #06	wcreJc04	2170	358	0.16	3	3	127.22	145.97	105.78	20.23
J. coenia	CRE #20	wcreJc05	2490	654	0.26	3	10	55.46	113.71	12.82	28.44
J. coenia	CRE #17	wcreJc06	2575	512	0.20	2	4	86.80	134.50	13.65	56.87
J. coenia	CRE #23	wcreJc07	1479	849	0.57	2	11	39.93	152.77	7.35	45.58
J. coenia	CRE #03	wcreJc08	995	113	0.11						
J. coenia	CRE #05, Promoter	wcreJc10	2529	637	0.25	3	8	46.68	84.19	23.53	21.01
V. cardui	CRE #10	wcreVc01	1663	266	0.16	2	2	114.58	117.46	111.70	4.07
V. cardui	CRE #07	wcreVc02	3144	806	0.26	2	4	60.84	98.16	21.27	43.08
V. cardui	CRE #24	wcreVc03	1327	363	0.27	3	3	108.82	111.33	105.22	3.20
V. cardui	CRE #11	wcreVc04	1426	343	0.24	3	4	69.14	114.54	9.89	48.71
V. cardui	CRE #20	wcreVc05	2648	469	0.18	3	11	45.11	102.74	5.88	32.16
V. cardui	CRE #17	wcreVc06	2799	491	0.18	3	15	47.78	154.22	10.26	41.48
V. cardui	CRE #23	wcreVc07	1669	249	0.15	12	30	96.75	348.93	11.03	117.54
V. cardui	CRE #03	wcreVc08	2794	530	0.19	2	2	89.44	89.76	89.11	0.46
V. cardui	CRE #21	wcreVc09	2225	332	0.15	3	5	61.94	87.55	5.62	33.51
V. cardui	CRE #05, Promoter	wcreVc10	3053	846	0.28	1	3	86.80	94.94	76.20	9.61
V. cardui	CRE #19	wcreVc11	2822	264	0.09	3	3	77.44	93.97	55.98	19.47
		Average	2284	425	0.19	2.8	7.1	66.6	147.7	29.9	44.2
		SD	589	184	0.09	1.7	5.4	25.0	113.6	34.2	37.7
		Median	2302	411	0.18	3.0	6.0	61.4	107.5	12.8	32.7
		Max	3147	869	0.57	12.0	30.0	127.2	601.0	111.7	172.9
		Min	995	113	0.05	1.0	1.0	30.0	56.1	2.8	0.5

References and Notes

1. M. Rebeiz, M. Tsiantis, Enhancer evolution and the origins of morphological novelty. *Curr. Opin. Genet. Dev.* **45**, 115–123 (2017). doi:10.1016/j.gde.2017.04.006 Medline

2. A. Monteiro, M. D. Gupta, Identifying coopted networks and causative mutations in the origin of novel complex traits. *Curr. Top. Dev. Biol.* **119**, 205–226 (2016). doi:10.1016/bs.ctdb.2016.03.003 Medline

3. C. Concha, R. W. R. Wallbank, J. J. Hanly, J. Fenner, L. Livraghi, E. S. Rivera, D. F. Paulo, C. Arias, M. Vargas, M. Sanjeev, C. Morrison, D. Tian, P. Aguirre, S. Ferrara, J. Foley, C. Pardo-Diaz, C. Salazar, M. Linares, D. Massardo, B. A. Counterman, M. J. Scott, C. D. Jiggins, R. Papa, A. Martin, W. O. McMillan, Interplay between developmental flexibility and determinism in the evolution of mimetic *Heliconius* wing patterns. *Curr. Biol.* **29**, 3996–4009.e4 (2019). doi:10.1016/j.cub.2019.10.010 Medline

4. A. Martin, R. Papa, N. J. Nadeau, R. I. Hill, B. A. Counterman, G. Halder, C. D. Jiggins, M. R. Kronforst, A. D. Long, W. O. McMillan, R. D. Reed, Diversification of complex butterfly wing patterns by repeated regulatory evolution of a *Wnt* ligand. *Proc. Natl. Acad. Sci. U.S.A.* **109**, 12632–12637 (2012). doi:10.1073/pnas.1204800109 Medline

5. A. Martin, R. D. Reed, *Wnt* signaling underlies evolution and development of the butterfly wing pattern symmetry systems. *Dev. Biol.* **395**, 367–378 (2014). doi:10.1016/j.ydbio.2014.08.031 Medline

6. A. Mazo-Vargas, C. Concha, L. Livraghi, D. Massardo, R. W. R. Wallbank, L. Zhang, J. D. Papador, D. Martinez-Najera, C. D. Jiggins, M. R. Kronforst, C. J. Breuker, R. D. Reed, N. H. Patel, W. O. McMillan, A. Martin, Macroevolutionary shifts of *WntA* function potentiate butterfly wing-pattern diversity. *Proc. Natl. Acad. Sci. U.S.A.* **114**, 10701–10706 (2017). doi:10.1073/pnas.1708149114 Medline

7. J. R. Gallant, V. E. Imhoff, A. Martin, W. K. Savage, N. L. Chamberlain, B. L. Pote, C. Peterson, G. E. Smith, B. Evans, R. D. Reed, M. R. Kronforst, S. P. Mullen, Ancient homology underlies adaptive mimetic diversity across butterflies. *Nat. Commun.* **5**, 4817–4827 (2014). doi:10.1038/ncomms5817 Medline

8. J. R. Dixon, S. Selvaraj, F. Yue, A. Kim, Y. Li, Y. Shen, M. Hu, J. S. Liu, B. Ren, Topological domains in mammalian genomes identified by analysis of chromatin interactions. *Nature* **485**, 376–380 (2012). doi:10.1038/nature11082 Medline

9. S. M. Van Belleghem, P. Rastas, A. Papanicolaou, S. H. Martin, C. F. Arias, M. A. Supple, J. J. Hanly, J. Mallet, J. J. Lewis, H. M. Hines, M. Ruiz, C. Salazar, M. Linares, G. R. P. Moreira, C. D. Jiggins, B. A. Counterman, W. O. McMillan, R. Papa, Complex modular architecture around a simple toolkit of wing pattern genes. *Nat. Ecol. Evol.* **1**, 0052 (2017). doi:10.1038/s41559-016-0052 Medline

10. J. J. Lewis, R. C. Geltman, P. C. Pollak, K. E. Rondem, S. M. Van Belleghem, M. J. Hubisz, P. R. Munn, L. Zhang, C. Benson, A. Mazo-Vargas, C. G. Danko, B. A. Counterman, R. Papa, R. D. Reed, Parallel evolution of ancient, pleiotropic enhancers underlies butterfly wing pattern mimicry. *Proc. Natl. Acad. Sci. U.S.A.* **116**, 24174–24183 (2019). doi:10.1073/pnas.1907068116 Medline

11. A. Mazo-Vargas, R. D. Reed, Deep cis-regulatory homology of the butterfly wing pattern groundplan, dataset, Dryad (2022); https://doi.org/10.5061/dryad.8cz8w9gpr.

12. J. Zhang, Q. Cong, J. Shen, P. A. Opler, N. V. Grishin, Genomics of a complete butterfly continent. bioRxiv 829887 [Preprint] (2019). https://doi.org/10.1101/829887.

13. H. F. Nijhout, *The Development and Evolution of Butterfly Wing Patterns* (Smithsonian Institution Press, 1991).

14. H. F. Nijhout, G. A. Wray, Homologies in the colour patterns of the genus *Heliconius* (Lepidoptera: Nymphalidae). *Biol. J. Linn. Soc. Lond.* **33**, 345–365 (1988). doi:10.1111/j.1095-8312.1988.tb00449.x

15. M. Kazemian, K. Suryamohan, J.-Y. Chen, Y. Zhang, M. A. H. Samee, M. S. Halfon, S. Sinha, Evidence for deep regulatory similarities in early developmental programs across highly diverged insects. *Genome Biol. Evol.* **6**, 2301–2320 (2014). doi:10.1093/gbe/evu184 Medline

16. L. Minnoye, I. I. Taskiran, D. Mauduit, M. Fazio, L. Van Aerschot, G. Hulselmans, V. Christiaens, S. Makhzami, M. Seltenhammer, P. Karras, A. Primot, E. Cadieu, E. van Rooijen, J.-C. Marine, G. Egidy, G.-E. Ghanem, L. Zon, J. Wouters, S. Aerts, Cross-species analysis of enhancer logic using deep learning. *Genome Res.* **30**, 1815–1834 (2020). doi:10.1101/gr.260844.120 Medline

17. A. Sourakov, L. T. Shirai, Pharmacological and surgical experiments on wing pattern development of Lepidoptera, with a focus on the eyespots of saturniid moths. *Trop. Lepid. Res.* **30**, 4–19 (2020).

18. F. Grosveld, J. van Staalduinen, R. Stadhouders, Transcriptional regulation by (super)enhancers: From discovery to mechanisms. *Annu. Rev. Genomics Hum. Genet.* **22**, 127–146 (2021). doi:10.1146/annurev-genom-122220-093818 Medline

19. E. Z. Kvon, R. Waymack, M. Gad, Z. Wunderlich, Enhancer redundancy in development and disease. *Nat. Rev. Genet.* **22**, 324–336 (2021). doi:10.1038/s41576-020-00311-x Medline

20. A. Tsai, M. R. Alves, J. Crocker, Multi-enhancer transcriptional hubs confer phenotypic robustness. *eLife* **8**, e45325 (2019). doi:10.7554/eLife.45325 Medline

21. H. F. Nijhout, Ontogeny of the color pattern on the wings of *Precis coenia* (Lepidoptera: Nymphalidae). *Dev. Biol.* **80**, 275–288 (1980). doi:10.1016/0012-1606(80)90404-2 Medline

22. S. Huang, M. Kang, A. Xu, HaploMerger2: Rebuilding both haploid sub-assemblies from high-heterozygosity diploid genome assembly. *Bioinformatics* **33**, 2577–2579 (2017). doi:10.1093/bioinformatics/btx220 Medline

23. K. R. L. van der Burg, J. J. Lewis, A. Martin, H. F. Nijhout, C. G. Danko, R. D. Reed, Contrasting roles of transcription factors spineless and EcR in the highly dynamic chromatin landscape of butterfly wing metamorphosis. *Cell Rep.* **27**, 1027–1038.e3 (2019). doi:10.1016/j.celrep.2019.03.092 Medline

24. K. R. L. van der Burg, J. J. Lewis, B. J. Brack, R. A. Fandino, A. Mazo-Vargas, R. D. Reed, Genomic architecture of a genetically assimilated seasonal color pattern. *Science* **370**, 721–725 (2020). doi:10.1126/science.aaz3017 Medline

25. N. C. Durand, J. T. Robinson, M. S. Shamim, I. Machol, J. P. Mesirov, E. S. Lander, E. L. Aiden, Juicebox provides a visualization system for Hi-C contact maps with unlimited zoom. *Cell Syst.* **3**, 99–101 (2016). doi:10.1016/j.cels.2015.07.012 Medline

26. O. Dudchenko, S. S. Batra, A. D. Omer, S. K. Nyquist, M. Hoeger, N. C. Durand, M. S. Shamim, I. Machol, E. S. Lander, A. P. Aiden, E. L. Aiden, De novo assembly of the *Aedes aegypti* genome using Hi-C yields chromosome-length scaffolds. *Science* **356**, 92–95 (2017). doi:10.1126/science.aal3327 Medline

27. J. D. Buenrostro, P. G. Giresi, L. C. Zaba, H. Y. Chang, W. J. Greenleaf, Transposition of native chromatin for fast and sensitive epigenomic profiling of open chromatin, DNA-binding proteins and nucleosome position. *Nat. Methods* **10**, 1213–1218 (2013). doi:10.1038/nmeth.2688 Medline

28. B. Langmead, S. L. Salzberg, Fast gapped-read alignment with Bowtie 2. *Nat. Methods* **9**, 357–359 (2012). doi:10.1038/nmeth.1923 Medline

29. J. Ou, H. Liu, J. Yu, M. A. Kelliher, L. H. Castilla, N. D. Lawson, L. J. Zhu, ATACseqQC: A Bioconductor package for post-alignment quality assessment of ATAC-seq data. *BMC Genomics* **19**, 169–182 (2018). doi:10.1186/s12864-018-4559-3 Medline

30. F. Ramírez, D. P. Ryan, B. Grüning, V. Bhardwaj, F. Kilpert, A. S. Richter, S. Heyne, F. Dündar, T. Manke, deepTools2: A next generation web server for deep-sequencing data analysis. *Nucleic Acids Res.* **44**, W160–W165 (2016). doi:10.1093/nar/gkw257 Medline

31. A. P. Boyle, J. Guinney, G. E. Crawford, T. S. Furey, F-Seq: A feature density estimator for high-throughput sequence tags. *Bioinformatics* **24**, 2537–2538 (2008). doi:10.1093/bioinformatics/btn480 Medline

32. A. R. Quinlan, I. M. Hall, BEDTools: A flexible suite of utilities for comparing genomic features. *Bioinformatics* **26**, 841–842 (2010). doi:10.1093/bioinformatics/btq033 Medline

33. M. I. Love, W. Huber, S. Anders, Moderated estimation of fold change and dispersion for RNA-seq data with DESeq2. *Genome Biol.* **15**, 550–571 (2014). doi:10.1186/s13059-014-0550-8 Medline

34. S. S. Rao, M. H. Huntley, N. C. Durand, E. K. Stamenova, I. D. Bochkov, J. T. Robinson, A. L. Sanborn, I. Machol, A. D. Omer, E. S. Lander, E. L. Aiden, A 3D map of the human genome at kilobase resolution reveals principles of chromatin looping. *Cell* **159**, 1665–1680 (2014). doi:10.1016/j.cell.2014.11.021 Medline

35. J. Wolff, V. Bhardwaj, S. Nothjunge, G. Richard, G. Renschler, R. Gilsbach, T. Manke, R. Backofen, F. Ramírez, B. A. Grüning, Galaxy HiCExplorer: A web server for reproducible Hi-C data analysis, quality control and visualization. *Nucleic Acids Res.* **46**, W11–W16 (2018). doi:10.1093/nar/gky504 Medline

36. M. Espeland, J. Breinholt, K. R. Willmott, A. D. Warren, R. Vila, E. F. A. Toussaint, S. C. Maunsell, K. Aduse-Poku, G. Talavera, R. Eastwood, M. A. Jarzyna, R. Guralnick, D. J. Lohman, N. E. Pierce, A. Y. Kawahara, A comprehensive and dated phylogenomic analysis of butterflies. *Curr. Biol.* **28**, 770–778.e5 (2018). doi:10.1016/j.cub.2018.01.061 Medline

37. B. Paten, D. Earl, N. Nguyen, M. Diekhans, D. Zerbino, D. Haussler, Cactus: Algorithms for genome multiple sequence alignment. *Genome Res.* **21**, 1512–1528 (2011). doi:10.1101/gr.123356.111 Medline

38. G. Hickey, B. Paten, D. Earl, D. Zerbino, D. Haussler, HAL: A hierarchical format for storing and analyzing multiple genome alignments. *Bioinformatics* **29**, 1341–1342 (2013). doi:10.1093/bioinformatics/btt128 Medline

39. A. Siepel, G. Bejerano, J. S. Pedersen, A. S. Hinrichs, M. Hou, K. Rosenbloom, H. Clawson, J. Spieth, L. W. Hillier, S. Richards, G. M. Weinstock, R. K. Wilson, R. A. Gibbs, W. J. Kent, W. Miller, D. Haussler, Evolutionarily conserved elements in vertebrate, insect, worm, and yeast genomes. *Genome Res.* **15**, 1034–1050 (2005). doi:10.1101/gr.3715005 Medline

40. X. Zhang, I. M. Kaplow, M. Wirthlin, T. Y. Park, A. R. Pfenning, HALPER facilitates the identification of regulatory element orthologs across species. *Bioinformatics* **36**, 4339–4340 (2020). doi:10.1093/bioinformatics/btaa493 Medline

41. R. R. Wick, L. M. Judd, K. E. Holt, Performance of neural network basecalling tools for Oxford Nanopore sequencing. *Genome Biol.* **20**, 129–139 (2019). doi:10.1186/s13059-019-1727-y Medline

42. S. Koren, B. P. Walenz, K. Berlin, J. R. Miller, N. H. Bergman, A. M. Phillippy, Canu: Scalable and accurate long-read assembly via adaptive *k*-mer weighting and repeat separation. *Genome Res.* **27**, 722–736 (2017). doi:10.1101/gr.215087.116 Medline

43. M. Kosicki, K. Tomberg, A. Bradley, Repair of double-strand breaks induced by CRISPR-Cas9 leads to large deletions and complex rearrangements. *Nat. Biotechnol.* **36**, 765–771 (2018). doi:10.1038/nbt.4192 Medline

44. H. Y. Shin, C. Wang, H. K. Lee, K. H. Yoo, X. Zeng, T. Kuhns, C. M. Yang, T. Mohr, C. Liu, L. Hennighausen, CRISPR/Cas9 targeting events cause complex deletions and insertions at 17 sites in the mouse genome. *Nat. Commun.* **8**, 15464–15474 (2017). doi:10.1038/ncomms15464 Medline

45. H. Li, Aligning sequence reads, clone sequences and assembly contigs with BWA-MEM. arXiv:1303.3997 [q-bio.GN] (2013).

46. B. S. Pedersen, A. R. Quinlan, Mosdepth: Quick coverage calculation for genomes and exomes. *Bioinformatics* **34**, 867–868 (2018). doi:10.1093/bioinformatics/btx699 Medline

47. H. Thorvaldsdóttir, J. T. Robinson, J. P. Mesirov, Integrative Genomics Viewer (IGV): High-performance genomics data visualization and exploration. *Brief. Bioinform.* **14**, 178–192 (2013). doi:10.1093/bib/bbs017 Medline

Data S1. (separate xlxs file - sheet 1)
List of all mKOs obtained from CRE shotgun CRISPR/Cas9 experiments. Knock-out effect in adult wings is code as Loss-of-function (L), Gain-of-function (G), presence of Loss-of-Function and Gain-of-Function effects on the same wing surface (T), ambiguous effects (A). No phenotype effects (NP). DFw=Dorsal Forewing, DHw=Dorsal Hindwing, VFw= Ventral Forewing, VHw=Ventral Hindwing

Dats S2. (separate xlxs file - sheet 2)
List of deletion alleles found in mKO butterflies using long-read sequencing.

Data S1. List of all mKOs obtained from CRE shotgun CRISPR/Cas9 experiments. Knock-out effect in adult wings is code as Loss-of-Function (**L**), Gain-of-Function (**G**), presence of Loss-of-Function and Gain-of-Function effects on the same wing surface (**T**), ambiguous effects (**A**). No phenotype effects (**NP**). DFw=Dorsal Forewing, DHw=Dorsal Hindwing, VFw= Ventral Forewing, VHw=Ventral Hindwing

Species	Ortholog CRE #	Species CRE ID	Mutant - ID	DFw	DHw	VFw	VHw	Size mutant clones
A vanillae	CRE# 07	wcreAv01	wcreAv01-01	G	G	G	G	Medium to large
A vanillae	CRE# 07	wcreAv01	wcreAv01-02	G	G	T	G	Medium to large
A vanillae	CRE# 07	wcreAv01	wcreAv01-03	G	G	G	G	Medium to large
A vanillae	CRE# 07	wcreAv01	wcreAv01-04	G	T	T	G	Medium to large
A vanillae	CRE# 07	wcreAv01	wcreAv01-05	G	G	G	G	Medium to large
A vanillae	CRE# 07	wcreAv01	wcreAv01-06	G	G	G	G	Medium to large
A vanillae	CRE# 07	wcreAv01	wcreAv01-07	G	G	G	G	Medium to large
A vanillae	CRE# 07	wcreAv01	wcreAv01-08	G	G	G	G	Medium to large
A vanillae	CRE# 07	wcreAv01	wcreAv01-09	G	NP	G	G	Medium to large
A vanillae	CRE# 07	wcreAv01	wcreAv01-10	G	G	G	G	Medium to large
A vanillae	CRE# 07	wcreAv01	wcreAv01-11	G	G	G	G	Medium to large
A vanillae	CRE# 07	wcreAv01	wcreAv01-12	G	G	T	G	Medium to large
A vanillae	CRE# 07	wcreAv01	wcreAv01-13	G	G	G	G	Medium to large
A vanillae	CRE# 07	wcreAv01	wcreAv01-14	G	G	G	G	Medium to large
A vanillae	CRE# 07	wcreAv01	wcreAv01-15	G	G	G	G	Medium to large
A vanillae	CRE# 07	wcreAv01	wcreAv01-16	G	G	G	G	Medium to large
A vanillae	CRE# 07	wcreAv01	wcreAv01-17	G	G	G	T	Medium to large
A vanillae	CRE# 07	wcreAv01	wcreAv01-m1	G	G	T	T	Medium to large
A vanillae	CRE# 07	wcreAv01	wcreAv01-m2	T	G	T	G	Medium to large
A vanillae	CRE# 18	wcreAv02	wcreAv02-01	G	G	T	G	Medium to large
A vanillae	CRE# 18	wcreAv02	wcreAv02-02	G	G	G	G	Small
A vanillae	CRE# 18	wcreAv02	wcreAv02-03	NP	NP	T	G	Small
A vanillae	CRE# 18	wcreAv02	wcreAv02-04	L	NP	G	NP	Small
A vanillae	CRE# 18	wcreAv02	wcreAv02-05	L	G	T	T	Medium to large
A vanillae	CRE# 18	wcreAv02	wcreAv02-06	G	G	NP	L	Medium to large
A vanillae	CRE# 18	wcreAv02	wcreAv02-07	G	G	L	G	Medium to large
A vanillae	CRE# 15	wcreAv03	wcreAv03-01	NP	NP	NP	G	Small
A vanillae	CRE# 15	wcreAv03	wcreAv03-02	L	L	L	L	Medium to large
A vanillae	CRE# 15	wcreAv03	wcreAv03-03	G	G	G	G	Medium to large
A vanillae	CRE# 15	wcreAv03	wcreAv03-04	L	G	L	G	Medium to large
A vanillae	CRE# 21	wcreAv04	wcreAv04-01	G	NP	G	G	Small
A vanillae	CRE# 21	wcreAv04	wcreAv04-02	G	NP	G	NP	damage mutant
A vanillae	CRE# 21	wcreAv04	wcreAv04-03	L	L	L	L	Medium to large
A vanillae	CRE# 21	wcreAv04	wcreAv04-04	L	L	T	L	Medium to large
A vanillae	CRE# 21	wcreAv04	wcreAv04-05	L	L	L	L	Medium to large
A vanillae	CRE# 21	wcreAv04	wcreAv04-06	NP	L	NP	NP	Small
A vanillae	CRE# 21	wcreAv04	wcreAv04-07	NP	NP	G	NP	Small
A vanillae	CRE# 21	wcreAv04	wcreAv04-08	NP	NP	T	L	Small
A vanillae	CRE# 21	wcreAv04	wcreAv04-09	G	L	NP	NP	Small
A vanillae	CRE# 21	wcreAv04	wcreAv04-10	L	L	G	L	Small
A vanillae	CRE# 21	wcreAv04	wcreAv04-11	G	G	G	G	Small
A vanillae	CRE# 21	wcreAv04	wcreAv04-12	NP	NP	G	G	Small
A vanillae	CRE# 21	wcreAv04	wcreAv04-13	NP	NP	L	NP	Small
A vanillae	CRE# 21	wcreAv04	wcreAv04-15	NP	L	L	L	Small
A vanillae	CRE# 21	wcreAv04	wcreAv04-16	NP	NP	L	NP	Small
A vanillae	CRE# 06	wcreAv05	wcreAv05-01	NP	NP	L	L	Medium to large
A vanillae	CRE# 06	wcreAv05	wcreAv05-02	NP	NP	NP	G	Small
A vanillae	CRE# 06	wcreAv05	wcreAv05-03	NP	G	T	G	Medium to large
A vanillae	CRE# 06	wcreAv05	wcreAv05-04	NP	NP	G	G	Medium to large
A vanillae	CRE# 06	wcreAv05	wcreAv05-07	L	L	T	L	Small
A vanillae	CRE# 06	wcreAv05	wcreAv05-08	NP	G	NP	L	Small
A vanillae	CRE# 12	wcreAv06	wcreAv06-01	G	A	T	T	Medium to large
A vanillae	CRE# 12	wcreAv06	wcreAv06-02	A	G	G	T	Medium to large
A vanillae	CRE# 12	wcreAv06	wcreAv06-03	G	NP	NP	NP	Medium to large

A vanillae	CRE# 12	wcreAv06	wcreAv06-04	G	G	T	NP	Medium to large
A vanillae	CRE# 12	wcreAv06	wcreAv06-05	G	NP	T	L	Medium to large
A vanillae	CRE# 12	wcreAv06	wcreAv06-06	NP	G	T	NP	Medium to large
A vanillae	CRE# 12	wcreAv06	wcreAv06-07	NP	NP	NP	T	Medium to large
A vanillae	CRE# 12	wcreAv06	wcreAv06-08	G	A	T	G	Medium to large
A vanillae	CRE# 12	wcreAv06	wcreAv06-09	T	L	T	G	Medium to large
A vanillae	CRE# 12	wcreAv06	wcreAv06-10	G	G	L	G	Medium to large
A vanillae	CRE# 12	wcreAv06	wcreAv06-11	G	G	G	NP	Medium to large
A vanillae	CRE# 12	wcreAv06	wcreAv06-12	T	A	T	NP	Medium to large
A vanillae	CRE# 12	wcreAv06	wcreAv06-13	NP	G	G	T	Medium to large
A vanillae	CRE# 12	wcreAv06	wcreAv06-14	G	G	G	G	Medium to large
A vanillae	CRE# 12	wcreAv06	wcreAv06-15	L	L	L	A	Medium to large
A vanillae	CRE# 12	wcreAv06	wcreAv06-16	G	G	A	G	Medium to large
A vanillae	CRE# 12	wcreAv06	wcreAv06-17	L	A	L	L	Medium to large
A vanillae	CRE# 12	wcreAv06	wcreAv06-18	G	G	G	NP	Medium to large
A vanillae	CRE# 12	wcreAv06	wcreAv06-20	G	G	A	T	Medium to large
A vanillae	CRE# 12	wcreAv06	wcreAv06-21	G	G	L	A	Medium to large
A vanillae	CRE# 12	wcreAv06	wcreAv06-22	G	G	L	T	Medium to large
A vanillae	CRE# 12	wcreAv06	wcreAv06-23	NP	NP	G	T	Medium to large
A vanillae	CRE# 12	wcreAv06	wcreAv06-24	G	A	NP	A	Medium to large
A vanillae	CRE# 12	wcreAv06	wcreAv06-25	G	G	T	A	Medium to large
A vanillae	CRE# 12	wcreAv06	wcreAv06-26	A	G	T	L	Medium to large
A vanillae	CRE# 12	wcreAv06	wcreAv06-27	NP	A	NP	G	Medium to large
A vanillae	CRE# 12	wcreAv06	wcreAv06-28	G	NP	G	NP	Medium to large
A vanillae	CRE# 12	wcreAv06	wcreAv06-29	A	A	T	G	Medium to large
A vanillae	CRE# 12	wcreAv06	wcreAv06-30	L	NP	T	T	Medium to large
A vanillae	CRE# 12	wcreAv06	wcreAv06-31	G	G	G	NP	Medium to large
A vanillae	CRE# 12	wcreAv06	wcreAv06-32	G	G	T	G	Medium to large
A vanillae	CRE# 12	wcreAv06	wcreAv06-33	L	G	T	NP	Medium to large
A vanillae	CRE# 12	wcreAv06	wcreAv06-34	A	G	T	NP	Medium to large
A vanillae	CRE# 12	wcreAv06	wcreAv06-35	NP	G	NP	NP	Medium to large
A vanillae	CRE# 12	wcreAv06	wcreAv06-37	NP	NP	NP	T	Medium to large
A vanillae	CRE# 23	wcreAv07	wcreAv07-01	NP	NP	NP	L	Medium to large
A vanillae	CRE# 23	wcreAv07	wcreAv07-03	NP	L	L	L	Medium to large
A vanillae	CRE# 23	wcreAv07	wcreAv07-04	L	L	T	G	Medium to large
A vanillae	CRE# 23	wcreAv07	wcreAv07-05	NP	NP	NP	L	Medium to large
A vanillae	CRE# 23	wcreAv07	wcreAv07-06	A	L	L	L	Medium to large
A vanillae	CRE# 23	wcreAv07	wcreAv07-08	L	NP	L	G	Medium to large
A vanillae	CRE# 23	wcreAv07	wcreAv07-09	L	L	L	L	Medium to large
A vanillae	CRE# 23	wcreAv07	wcreAv07-10	L	NP	L	A	Medium to large
A vanillae	CRE# 23	wcreAv07	wcreAv07-11	NP	NP	L	NP	Small
A vanillae	CRE# 23	wcreAv07	wcreAv07-12	NP	NP	L	G	Medium to large
A vanillae	CRE# 23	wcreAv07	wcreAv07-13	L	L	L	A	Medium to large
A vanillae	CRE# 23	wcreAv07	wcreAv07-14	L	L	L	NP	Medium to large
A vanillae	CRE# 23	wcreAv07	wcreAv07-15	NP	L	NP	T	Medium to large
A vanillae	CRE# 23	wcreAv07	wcreAv07-16	NP	L	L	NP	Medium to large
A vanillae	CRE# 23	wcreAv07	wcreAv07-17	L	NP	L	NP	Medium to large
A vanillae	CRE# 23	wcreAv07	wcreAv07-18	NP	L	G	L	Medium to large
A vanillae	CRE# 23	wcreAv07	wcreAv07-20	L	L	L	G	Medium to large
A vanillae	CRE# 23	wcreAv07	wcreAv07-23	NP	NP	L	NP	Small
A vanillae	CRE# 23	wcreAv07	wcreAv07-25	NP	NP	L	NP	Small
A vanillae	CRE# 23	wcreAv07	wcreAv07-26	A	A	L	NP	Small
A vanillae	CRE# 23	wcreAv07	wcreAv07-27	NP	NP	L	NP	Small
A vanillae	CRE# 23	wcreAv07	wcreAv07-28	NP	NP	L	NP	Medium to large
A vanillae	CRE# 23	wcreAv07	wcreAv07-29	A	G	NP	NP	Medium to large
A vanillae	CRE# 01	wcreAv09	wcreAv09-01	G	NP	NP	G	Small
A vanillae	CRE# 01	wcreAv09	wcreAv09-02	NP	NP	T	A	Small
A vanillae	CRE# 01	wcreAv09	wcreAv09-04	NP	NP	L	NP	Small
A vanillae	CRE# 05	wcreAv10	wcreAv10-01	L	NP	L	L	Medium to large

A vanillae	CRE# 05	wcreAv10	wcreAv10-02	L	L	L	L	Medium to large
A vanillae	CRE# 05	wcreAv10	wcreAv10-03	L	NP	L	L	Medium to large
A vanillae	CRE# 05	wcreAv10	wcreAv10-04	L	L	L	L	Medium to large
A vanillae	CRE# 05	wcreAv10	wcreAv10-05	A	L	L	NP	Medium to large
A vanillae	CRE# 05	wcreAv10	wcreAv10-06	L	L	L	L	Medium to large
A vanillae	CRE# 05	wcreAv10	wcreAv10-07	L	L	L	L	Medium to large
A vanillae	CRE# 05	wcreAv10	wcreAv10-08	L	L	L	L	Medium to large
D plexippus	CRE# 04	wcreDp01	wcreDp01-01	G	L	L	L	Medium to large
D plexippus	CRE# 04	wcreDp01	wcreDp01-02	T	G	L	L	Medium to large
D plexippus	CRE# 04	wcreDp01	wcreDp01-03	G	NP	L	L	Medium to large
D plexippus	CRE# 04	wcreDp01	wcreDp01-06	NP	L	L	L	Medium to large
D plexippus	CRE# 04	wcreDp01	wcreDp01-07	NP	L	L	NP	Medium to large
D plexippus	CRE# 04	wcreDp01	wcreDp01-08	A	NP	A	L	Small
D plexippus	CRE# 04	wcreDp01	wcreDp01-10	NP	NP	L	L	Medium to large
D plexippus	CRE# 08	wcreDp02	wcreDp02-01	G	NP	L	NP	Small
D plexippus	CRE# 08	wcreDp02	wcreDp02-03	G	NP	T	L	Medium to large
D plexippus	CRE# 08	wcreDp02	wcreDp02-04	G	NP	T	L	Medium to large
D plexippus	CRE# 08	wcreDp02	wcreDp02-05	L	NP	T	T	Medium to large
D plexippus	CRE# 08	wcreDp02	wcreDp02-06	G	NP	G	T	Small
D plexippus	CRE# 08	wcreDp02	wcreDp02-07	G	G	NP	G	medium to large
D plexippus	CRE# 08	wcreDp02	wcreDp02-09	G	G	NP	NP	Small
D plexippus	CRE# 08	wcreDp02	wcreDp02-11	G	G	G	G	Medium to large
D plexippus	CRE# 08	wcreDp02	wcreDp02-12	L	NP	L	L	Medium to large
D plexippus	CRE# 08	wcreDp02	wcreDp02-13	NP	NP	G	L	Medium to large
D plexippus	CRE# 08	wcreDp02	wcreDp02-14	G	NP	NP	NP	Medium to large
D plexippus	CRE# 08	wcreDp02	wcreDp02-18	G	G	G	NP	Small
D plexippus	CRE# 08	wcreDp02	wcreDp02-20	G	T	T	L	Medium to large
D plexippus	CRE# 08	wcreDp02	wcreDp02-22	G	A	A	L	Small
D plexippus	CRE# 08	wcreDp02	wcreDp02-23	G	G	G	T	Small
D plexippus	CRE# 08	wcreDp02	wcreDp02-24	G	A	G	T	Small
D plexippus	CRE# 08	wcreDp02	wcreDp02-25	G	NP	G	L	Small
D plexippus	CRE# 08	wcreDp02	wcreDp02-26	T	L	L	NP	Medium to large
D plexippus	CRE# 08	wcreDp02	wcreDp02-31	T	T	G	L	Small
D plexippus	CRE# 08	wcreDp02	wcreDp02-34	T	NP	T	L	Small
D plexippus	CRE# 08	wcreDp02	wcreDp02-40	G	L	T	NP	Medium to large
D plexippus	CRE# 08	wcreDp02	wcreDp02-41	NP	G	A	L	Small
D plexippus	CRE# 08	wcreDp02	wcreDp02-45	G	NP	G	NP	Small
D plexippus	CRE# 08	wcreDp02	wcreDp02-47	G	A	NP	G	Small
D plexippus	CRE# 08	wcreDp02	wcreDp02-48	G	NP	G	NP	Small
D plexippus	CRE# 08	wcreDp02	wcreDp02-49	G	NP	G	L	Medium to large
D plexippus	CRE# 08	wcreDp02	wcreDp02-50	G	G	G	L	Medium to large
D plexippus	CRE# 08	wcreDp02	wcreDp02-51	G	A	L	G	Medium to large
D plexippus	CRE# 08	wcreDp02	wcreDp02-52	G	NP	NP	L	Medium to large
D plexippus	CRE# 22	wcreDp03	wcreDp03-02	G	G	T	L	Medium to large
D plexippus	CRE# 22	wcreDp03	wcreDp03-14	NP	NP	L	L	Medium to large
D plexippus	CRE# 22	wcreDp03	wcreDp03-19	G	NP	NP	NP	Small
D plexippus	CRE# 22	wcreDp03	wcreDp03-25	G	NP	L	NP	Medium to large
D plexippus	CRE# 22	wcreDp03	wcreDp03-27	L	NP	L	L	Medium to large
D plexippus	CRE# 09	wcreDp04	wcreDp04-01	NP	L	NP	L	Small
D plexippus	CRE# 09	wcreDp04	wcreDp04-07	G	G	T	L	Medium to large
D plexippus	CRE# 09	wcreDp04	wcreDp04-09	G	NP	G	L	Medium to large
D plexippus	CRE# 09	wcreDp04	wcreDp04-11	G	NP	T	L	Medium to large
D plexippus	CRE# 09	wcreDp04	wcreDp04-15	NP	G	G	L	Medium to large
D plexippus	CRE# 09	wcreDp04	wcreDp04-17	G	NP	G	NP	Medium to large
D plexippus	CRE# 09	wcreDp04	wcreDp04-18	NP	G	L	L	Medium to large
D plexippus	CRE# 09	wcreDp04	wcreDp04-21	NP	G	G	NP	Medium to large
D plexippus	CRE# 09	wcreDp04	wcreDp04-24	G	G	NP	NP	Medium to large
D plexippus	CRE# 09	wcreDp04	wcreDp04-28	G	NP	T	T	Medium to large
D plexippus	CRE# 16	wcreDp05	wcreDp05-01	T	L	L	L	Medium to large

D plexippus	CRE# 16	wcreDp05	wcreDp05-09	G	A	L	L	Small
D plexippus	CRE# 02	wcreDp06	wcreDp06-01	A	L	L	L	Medium to large
D plexippus	CRE# 02	wcreDp06	wcreDp06-02	G	NP	NP	L	Medium to large
D plexippus	CRE# 02	wcreDp06	wcreDp06-03	NP	G	NP	L	Small
D plexippus	CRE# 02	wcreDp06	wcreDp06-04	G	NP	L	L	Medium to large
D plexippus	CRE# 02	wcreDp06	wcreDp06-06	T	G	NP	L	Medium to large
D plexippus	CRE# 02	wcreDp06	wcreDp06-09	G	G	G	L	Medium to large
D plexippus	CRE# 02	wcreDp06	wcreDp06-10	L	NP	L	L	Small
D plexippus	CRE# 02	wcreDp06	wcreDp06-11	NP	L	NP	L	Medium to large
D plexippus	CRE# 02	wcreDp06	wcreDp06-12	L	L	NP	L	Small
D plexippus	CRE# 02	wcreDp06	wcreDp06-13	T	L	NP	L	Medium to large
D plexippus	CRE# 02	wcreDp06	wcreDp06-22	NP	G	NP	NP	Small
D plexippus	CRE# 02	wcreDp06	wcreDp06-23	G	NP	NP	L	Small
D plexippus	CRE# 05	wcreDp07	wcreDp07-01	L	L	L	L	Medium to large
D plexippus	CRE# 05	wcreDp07	wcreDp07-02	L	L	L	L	Medium to large
D plexippus	CRE# 05	wcreDp07	wcreDp07-03	L	L	L	L	Medium to large
D plexippus	CRE# 05	wcreDp07	wcreDp07-04	L	L	L	L	Medium to large
D plexippus	CRE# 05	wcreDp07	wcreDp07-05	L	L	L	L	Medium to large
D plexippus	CRE# 05	wcreDp07	wcreDp07-06	L	L	L	L	Medium to large
D plexippus	CRE# 05	wcreDp07	wcreDp07-07	L	L	L	L	Medium to large
D plexippus	CRE# 05	wcreDp07	wcreDp07-08	L	L	L	L	Medium to large
D plexippus	CRE# 05	wcreDp07	wcreDp07-10	L	L	L	L	Medium to large
D plexippus	CRE# 05	wcreDp07	wcreDp07-11	L	L	L	L	Medium to large
D plexippus	CRE# 05	wcreDp07	wcreDp07-12	L	NP	L	L	Small
D plexippus	CRE# 05	wcreDp07	wcreDp07-18	L	L	L	L	Medium to large
D plexippus	CRE# 05	wcreDp07	wcreDp07-20	NP	NP	NP	L	Medium to large
D plexippus	CRE# 05	wcreDp07	wcreDp07-22	L	L	L	L	Medium to large
D plexippus	CRE# 05	wcreDp07	wcreDp07-23	L	L	L	L	Medium to large
D plexippus	CRE# 05	wcreDp07	wcreDp07-24	L	L	L	L	Medium to large
D plexippus	CRE# 05	wcreDp07	wcreDp07-25	L	L	L	L	Medium to large
D plexippus	CRE# 05	wcreDp07	wcreDp07-26	L	L	L	L	Medium to large
D plexippus	CRE# 05	wcreDp07	wcreDp07-27	L	L	L	L	Medium to large
H himera	CRE# 07	wcreHhim01	wcreHhim01-01	G	NP	G	NP	Medium to large
H himera	CRE# 07	wcreHhim01	wcreHhim01-02	L	NP	L	NP	Medium to large
H himera	CRE# 07	wcreHhim01	wcreHhim01-04	G	NP	A	NP	Small
H himera	CRE# 07	wcreHhim01	wcreHhim01-05	A	NP	A	NP	doubful mutant
H himera	CRE# 07	wcreHhim01	wcreHhim01-06	L	NP	L	NP	Small
H himera	CRE# 07	wcreHhim01	wcreHhim01-m1	G	NP	G	NP	Medium to large
H himera	CRE# 18	wcreHhim02	wcreHhim02-01	T	NP	T	NP	Medium to large
H himera	CRE# 18	wcreHhim02	wcreHhim02-02	G	NP	G	NP	Medium to large
H himera	CRE# 18	wcreHhim02	wcreHhim02-03	G	NP	T	NP	Medium to large
H himera	CRE# 18	wcreHhim02	wcreHhim02-04	T	NP	T	NP	Medium to large
H himera	CRE# 18	wcreHhim02	wcreHhim02-05	G	NP	G	NP	Small
H himera	CRE# 18	wcreHhim02	wcreHhim02-06	A	NP	A	NP	doubful mutant
H himera	CRE# 18	wcreHhim02	wcreHhim02-m1	G	NP	G	NP	Medium to large
H himera	CRE# 15	wcreHhim03	wcreHhim03-02	G	NP	G	NP	Medium to large
H himera	CRE# 15	wcreHhim03	wcreHhim03-03	T	NP	T	NP	Medium to large
H himera	CRE# 15	wcreHhim03	wcreHhim03-04	T	NP	G	NP	Medium to large
H himera	CRE# 15	wcreHhim03	wcreHhim03-05	A	NP	T	NP	Medium to large
H himera	CRE# 21	wcreHhim04	wcreHhim04-01	A	NP	A	NP	doubful mutant
H himera	CRE# 21	wcreHhim04	wcreHhim04-03	A	NP	A	NP	doubful mutant
H himera	CRE# 21	wcreHhim04	wcreHhim04-05	A	NP	A	NP	doubful mutant
H himera	CRE# 12	wcreHhim06	wcreHhim06-01	T	NP	T	L	Small
H himera	CRE# 12	wcreHhim06	wcreHhim06-02	G	NP	G	NP	Small
H himera	CRE# 12	wcreHhim06	wcreHhim06-05	A	NP	L	NP	Medium to large
H himera	CRE# 13	wcreHhim07	wcreHhim07-01	A	NP	G	NP	Small
H himera	CRE# 13	wcreHhim07	wcreHhim07-02	A	NP	NP	NP	Small
H himera	CRE# 13	wcreHhim07	wcreHhim07-03	L	L	L	L	Medium to large
H himera	CRE# 13	wcreHhim07	wcreHhim07-04	T	NP	L	A	Medium to large

H himera	CRE# 14	wcreHhim08	wcreHhim08-01	G	NP	G	NP	Medium to large
H himera	CRE# 14	wcreHhim08	wcreHhim08-02	A	NP	G	NP	Small
H himera	CRE# 14	wcreHhim08	wcreHhim08-03	G	NP	G	NP	Small
H himera	CRE# 05	wcreHhim10	wcreHhim10-m1	L	NP	L	NP	Medium to large
J coenia	CRE# 10	wcreJc01	wcreJc01-27	G	G	NP	L	Small
J coenia	CRE# 10	wcreJc01	wcreJc01-30	NP	NP	NP	A	Small
J coenia	CRE# 10	wcreJc01	wcreJc01-31	A	NP	NP	NP	Small
J coenia	CRE# 10	wcreJc01	wcreJc01-32	A	NP	NP	NP	Small
J coenia	CRE# 10	wcreJc01	wcreJc01-33	A	NP	NP	NP	Small
J coenia	CRE# 10	wcreJc01	wcreJc01-37	A	NP	L	NP	Small
J coenia	CRE# 10	wcreJc01	wcreJc01-43	NP	NP	A	NP	Small
J coenia	CRE# 07	wcreJc02	wcreJc02-59	NP	NP	NP	L	Small
J coenia	CRE# 07	wcreJc02	wcreJc02-64	NP	NP	NP	A	Small
J coenia	CRE# 07	wcreJc02	wcreJc02-65	NP	NP	NP	L	Small
J coenia	CRE# 07	wcreJc02	wcreJc02-66	G	NP	NP	NP	Small
J coenia	CRE# 21	wcreJc03	wcreJc03-01	NP	NP	L	NP	Medium to large
J coenia	CRE# 21	wcreJc03	wcreJc03-34	A	NP	NP	NP	Small
J coenia	CRE# 21	wcreJc03	wcreJc03-49	NP	NP	G	NP	Small
J coenia	CRE# 21	wcreJc03	wcreJc03-50	L	NP	NP	NP	Small
J coenia	CRE# 21	wcreJc03	wcreJc03-52	NP	NP	NP	L	small
J coenia	CRE# 21	wcreJc03	wcreJc03-54	L	NP	NP	NP	small
J coenia	CRE# 21	wcreJc03	wcreJc03-56	L	NP	NP	NP	Small
J coenia	CRE# 06	wcreJc04	wcreJc04-14	A	NP	NP	L	Small
J coenia	CRE# 06	wcreJc04	wcreJc04-15	NP	NP	L	NP	Small
J coenia	CRE# 20	wcreJc05	wcreJc05-04	NP	NP	G	NP	Small
J coenia	CRE# 20	wcreJc05	wcreJc05-06	NP	NP	G	NP	Small
J coenia	CRE# 20	wcreJc05	wcreJc05-09	NP	NP	A	NP	Small
J coenia	CRE# 20	wcreJc05	wcreJc05-10	NP	A	NP	NP	Small
J coenia	CRE# 20	wcreJc05	wcreJc05-17a	NP	NP	A	A	Medium to large
J coenia	CRE# 20	wcreJc05	wcreJc05-17b	L	NP	NP	A	Small
J coenia	CRE# 20	wcreJc05	wcreJc05-18	NP	NP	NP	L	Medium to large
J coenia	CRE# 20	wcreJc05	wcreJc05-20	G	NP	L	L	Medium to large
J coenia	CRE# 20	wcreJc05	wcreJc05-21	NP	NP	NP	L	Medium to large
J coenia	CRE# 20	wcreJc05	wcreJc05-24	NP	NP	L	NP	Small
J coenia	CRE# 20	wcreJc05	wcreJc05-25	NP	NP	NP	NP	Small
J coenia	CRE# 20	wcreJc05	wcreJc05-26	NP	NP	G	NP	Small
J coenia	CRE# 20	wcreJc05	wcreJc05-27	NP	NP	NP	NP	Small
J coenia	CRE# 20	wcreJc05	wcreJc05-29	NP	NP	A	L	Medium to large
J coenia	CRE# 20	wcreJc05	wcreJc05-30	G	NP	NP	NP	Small
J coenia	CRE# 20	wcreJc05	wcreJc05-32	G	NP	NP	NP	Small
J coenia	CRE# 20	wcreJc05	wcreJc05-33	NP	NP	L	NP	Small
J coenia	CRE# 17	wcreJc06	wcreJc06-24	NP	NP	A	A	Small
J coenia	CRE# 17	wcreJc06	wcreJc06-30	NP	G	NP	NP	Medium to large
J coenia	CRE# 17	wcreJc06	wcreJc06-38	A	NP	NP	NP	Small
J coenia	CRE# 17	wcreJc06	wcreJc06-40	L	NP	NP	A	small
J coenia	CRE# 17	wcreJc06	wcreJc06-41	NP	NP	L	NP	Small
J coenia	CRE# 23	wcreJc07	wcreJc07-13	NP	NP	L	L	Small
J coenia	CRE# 23	wcreJc07	wcreJc07-15	NP	NP	L	NP	Small
J coenia	CRE# 23	wcreJc07	wcreJc07-16	NP	NP	L	NP	Small
J coenia	CRE# 12	wcreJc09	wcreJc09-01	NP	NP	L	L	Medium to large
J coenia	CRE# 12	wcreJc09	wcreJc09-02	NP	NP	NP	L	Medium to large
J coenia	CRE# 12	wcreJc09	wcreJc09-03	NP	NP	L	L	Medium to large
J coenia	CRE# 12	wcreJc09	wcreJc09-04	NP	NP	L	NP	Medium to large
J coenia	CRE# 12	wcreJc09	wcreJc09-05	NP	NP	NP	L	Medium to large
J coenia	CRE# 12	wcreJc09	wcreJc09-06	NP	NP	A	NP	Small
J coenia	CRE# 12	wcreJc09	wcreJc09-07	NP	NP	A	NP	Small
J coenia	CRE# 05	wcreJc10	wcreJc10-01	L	NP	L	L	Medium to large
J coenia	CRE# 05	wcreJc10	wcreJc10-02	L	NP	L	NP	Medium to large
J coenia	CRE# 05	wcreJc10	wcreJc10-03	L	NP	L	L	Medium to large

J coenia	CRE# 05	wcreJc10	wcreJc10-04	L	NP	L	NP	Medium to large
J coenia	CRE# 05	wcreJc10	wcreJc10-05	L	NP	L	L	Medium to large
J coenia	CRE# 05	wcreJc10	wcreJc10-06	NP	NP	L	L	Medium to large
J coenia	CRE# 05	wcreJc10	wcreJc10-07	L	NP	L	L	Medium to large
J coenia	CRE# 05	wcreJc10	wcreJc10-08	L	NP	L	L	Medium to large
J coenia	CRE# 05	wcreJc10	wcreJc10-09	L	NP	L	L	Medium to large
J coenia	CRE# 05	wcreJc10	wcreJc10-10	NP	NP	L	L	Medium to large
J coenia	CRE# 05	wcreJc10	wcreJc10-11	L	NP	L	NP	Medium to large
J coenia	CRE# 05	wcreJc10	wcreJc10-12	L	NP	L	L	Medium to large
J coenia	CRE# 05	wcreJc10	wcreJc10-13	NP	NP	L	L	Medium to large
J coenia	CRE# 05	wcreJc10	wcreJc10-14	L	NP	L	L	Medium to large
J coenia	CRE# 05	wcreJc10	wcreJc10-15	L	NP	L	L	Medium to large
J coenia	CRE# 05	wcreJc10	wcreJc10-16	L	NP	L	L	Medium to large
J coenia	CRE# 05	wcreJc10	wcreJc10-17	L	NP	L	L	Medium to large
J coenia	CRE# 05	wcreJc10	wcreJc10-18	L	NP	L	L	Medium to large
J coenia	CRE# 05	wcreJc10	wcreJc10-19	L	NP	L	L	Medium to large
J coenia	CRE# 05	wcreJc10	wcreJc10-20	L	NP	L	L	Medium to large
J coenia	CRE# 05	wcreJc10	wcreJc10-21	L	NP	L	L	Medium to large
J coenia	CRE# 05	wcreJc10	wcreJc10-22	L	NP	L	L	Medium to large
J coenia	CRE# 05	wcreJc10	wcreJc10-23	L	NP	L	L	Medium to large
J coenia	CRE# 05	wcreJc10	wcreJc10-24	NP	NP	NP	L	Medium to large
J coenia	CRE# 05	wcreJc10	wcreJc10-25	L	NP	L	L	Medium to large
J coenia	CRE# 05	wcreJc10	wcreJc10-26	L	NP	L	L	Medium to large
J coenia	CRE# 05	wcreJc10	wcreJc10-27	L	NP	L	L	Medium to large
V cardui	CRE# 10	wcreVc01	wcreVc01-12	NP	NP	G	NP	medium to large
V cardui	CRE# 10	wcreVc01	wcreVc01-13	A	NP	G	A	Small
V cardui	CRE# 10	wcreVc01	wcreVc01-15	A	NP	NP	A	Small
V cardui	CRE# 10	wcreVc01	wcreVc01-16	NP	NP	A	NP	Small
V cardui	CRE# 10	wcreVc01	wcreVc01-17	NP	NP	NP	G	Small
V cardui	CRE# 10	wcreVc01	wcreVc01-23	NP	NP	L	NP	Small
V cardui	CRE# 07	wcreVc02	wcreVc02-03	L	L	NP	NP	Small
V cardui	CRE# 07	wcreVc02	wcreVc02-04	A	NP	NP	NP	Small
V cardui	CRE# 07	wcreVc02	wcreVc02-05	NP	NP	L	NP	Small
V cardui	CRE# 07	wcreVc02	wcreVc02-06	A	NP	A	NP	Small
V cardui	CRE# 07	wcreVc02	wcreVc02-07	A	NP	NP	L	Small
V cardui	CRE# 07	wcreVc02	wcreVc02-10	NP	NP	NP	L	Small
V cardui	CRE# 07	wcreVc02	wcreVc02-20	A	NP	A	L	Medium to large
V cardui	CRE# 07	wcreVc02	wcreVc02-21	NP	NP	A	NP	Small
V cardui	CRE# 24	wcreVc03	wcreVc03-08	L	A	A	NP	Medium to large
V cardui	CRE# 24	wcreVc03	wcreVc03-12	NP	NP	A	NP	Small
V cardui	CRE# 24	wcreVc03	wcreVc03-17	NP	NP	G	NP	Small
V cardui	CRE# 24	wcreVc03	wcreVc03-18	NP	NP	A	A	Small
V cardui	CRE# 24	wcreVc03	wcreVc03-20	NP	NP	NP	L	Small
V cardui	CRE# 24	wcreVc03	wcreVc03-21	NP	NP	NP	G	Small
V cardui	CRE# 24	wcreVc03	wcreVc03-23	NP	NP	A	G	Small
V cardui	CRE# 24	wcreVc03	wcreVc03-29	NP	NP	L	NP	Medium to large
V cardui	CRE# 24	wcreVc03	wcreVc03-34	A	NP	L	L	Medium to large
V cardui	CRE# 24	wcreVc03	wcreVc03-35	NP	NP	A	A	Small
V cardui	CRE# 24	wcreVc03	wcreVc03-39	NP	NP	NP	L	Small
V cardui	CRE# 24	wcreVc03	wcreVc03-41	G	NP	NP	L	Small
V cardui	CRE# 24	wcreVc03	wcreVc03-46	NP	NP	L	NP	Small
V cardui	CRE# 24	wcreVc03	wcreVc03-53	G	G	G	G	Medium to large
V cardui	CRE# 24	wcreVc03	wcreVc03-57	L	G	A	G	Medium to large
V cardui	CRE# 24	wcreVc03	wcreVc03-62	L	NP	L	L	Small
V cardui	CRE# 11	wcreVc04	wcreVc04-06	L	NP	L	NP	Small
V cardui	CRE# 11	wcreVc04	wcreVc04-15	NP	NP	G	NP	Small
V cardui	CRE# 11	wcreVc04	wcreVc04-21	L	NP	NP	NP	Small
V cardui	CRE# 11	wcreVc04	wcreVc04-32	NP	NP	G	NP	Small
V cardui	CRE# 11	wcreVc04	wcreVc04-34	NP	NP	NP	G	Medium to large

V cardui	CRE# 20	wcreVc05	wcreVc05-01	NP	NP	NP	L	Small
V cardui	CRE# 20	wcreVc05	wcreVc05-03	L	NP	G	G	Small
V cardui	CRE# 20	wcreVc05	wcreVc05-09	NP	NP	NP	L	Small
V cardui	CRE# 20	wcreVc05	wcreVc05-12	L	NP	T	NP	Small
V cardui	CRE# 20	wcreVc05	wcreVc05-13	L	NP	A	A	Small
V cardui	CRE# 20	wcreVc05	wcreVc05-17	G	NP	L	L	Medium to large
V cardui	CRE# 20	wcreVc05	wcreVc05-18	L	NP	NP	NP	Medium to large
V cardui	CRE# 20	wcreVc05	wcreVc05-22	L	NP	A	NP	Small
V cardui	CRE# 20	wcreVc05	wcreVc05-23	NP	NP	A	L	Small
V cardui	CRE# 20	wcreVc05	wcreVc05-24	G	NP	A	L	Medium to large
V cardui	CRE# 20	wcreVc05	wcreVc05-26	L	NP	L	NP	Small
V cardui	CRE# 20	wcreVc05	wcreVc05-28	NP	NP	NP	A	Medium to large
V cardui	CRE# 17	wcreVc06	wcreVc06-01	G	NP	G	NP	Medium to large
V cardui	CRE# 17	wcreVc06	wcreVc06-02	G	NP	NP	NP	Medium to large
V cardui	CRE# 17	wcreVc06	wcreVc06-03	G	NP	G	NP	Medium to large
V cardui	CRE# 17	wcreVc06	wcreVc06-06	G	NP	G	L	Medium to large
V cardui	CRE# 17	wcreVc06	wcreVc06-10	NP	NP	NP	L	Medium to large
V cardui	CRE# 17	wcreVc06	wcreVc06-12	NP	NP	G	NP	Medium to large
V cardui	CRE# 17	wcreVc06	wcreVc06-13	NP	NP	G	NP	Medium to large
V cardui	CRE# 17	wcreVc06	wcreVc06-14	G	NP	G	NP	Medium to large
V cardui	CRE# 17	wcreVc06	wcreVc06-15	T	NP	G	G	Medium to large
V cardui	CRE# 17	wcreVc06	wcreVc06-16	G	NP	G	NP	Medium to large
V cardui	CRE# 17	wcreVc06	wcreVc06-19	G	NP	G	G	Medium to large
V cardui	CRE# 23	wcreVc07	wcreVc07-01	T	NP	T	L	Medium to large
V cardui	CRE# 23	wcreVc07	wcreVc07-02	G	NP	G	L	Medium to large
V cardui	CRE# 23	wcreVc07	wcreVc07-06	L	NP	G	A	Medium to large
V cardui	CRE# 23	wcreVc07	wcreVc07-07	G	NP	G	L	Medium to large
V cardui	CRE# 23	wcreVc07	wcreVc07-08	G	NP	G	NP	Medium to large
V cardui	CRE# 23	wcreVc07	wcreVc07-09	G	NP	G	A	Medium to large
V cardui	CRE# 23	wcreVc07	wcreVc07-10	G	NP	G	L	Medium to large
V cardui	CRE# 23	wcreVc07	wcreVc07-11	NP	NP	G	NP	Medium to large
V cardui	CRE# 23	wcreVc07	wcreVc07-12	G	NP	G	NP	Medium to large
V cardui	CRE# 23	wcreVc07	wcreVc07-13	G	NP	NP	NP	Small
V cardui	CRE# 23	wcreVc07	wcreVc07-14	NP	NP	A	A	Small
V cardui	CRE# 23	wcreVc07	wcreVc07-17	G	NP	G	NP	Medium to large
V cardui	CRE# 23	wcreVc07	wcreVc07-18	G	L	G	L	Medium to large
V cardui	CRE# 23	wcreVc07	wcreVc07-19	G	NP	G	L	Medium to large
V cardui	CRE# 23	wcreVc07	wcreVc07-21	G	NP	G	L	Medium to large
V cardui	CRE# 23	wcreVc07	wcreVc07-24	NP	NP	G	NP	Medium to large
V cardui	CRE# 23	wcreVc07	wcreVc07-25	G	NP	G	A	Medium to large
V cardui	CRE# 23	wcreVc07	wcreVc07-31	G	NP	G	L	Medium to large
V cardui	CRE# 23	wcreVc07	wcreVc07-32	G	NP	T	NP	Medium to large
V cardui	CRE# 23	wcreVc07	wcreVc07-33	G	NP	G	L	Medium to large
V cardui	CRE# 23	wcreVc07	wcreVc07-35	NP	NP	T	NP	Medium to large
V cardui	CRE# 23	wcreVc07	wcreVc07-36	G	NP	G	A	Medium to large
V cardui	CRE# 23	wcreVc07	wcreVc07-40	G	A	G	NP	Medium to large
V cardui	CRE# 23	wcreVc07	wcreVc07-42	G	NP	G	A	Medium to large
V cardui	CRE# 23	wcreVc07	wcreVc07-48	G	NP	G	NP	Medium to large
V cardui	CRE# 23	wcreVc07	wcreVc07-51	G	NP	G	NP	Medium to large
V cardui	CRE# 23	wcreVc07	wcreVc07-52	G	NP	G	NP	Medium to large
V cardui	CRE# 23	wcreVc07	wcreVc07-54	T	L	G	NP	Medium to large
V cardui	CRE# 23	wcreVc07	wcreVc07-55	G	NP	G	NP	Medium to large
V cardui	CRE# 23	wcreVc07	wcreVc07-57	G	NP	G	A	Medium to large
V cardui	CRE# 23	wcreVc07	wcreVc07-58	NP	NP	G	NP	Small
V cardui	CRE# 23	wcreVc07	wcreVc07-60	NP	NP	G	NP	Small
V cardui	CRE# 23	wcreVc07	wcreVc07-62	G	NP	G	NP	Medium to large
V cardui	CRE# 23	wcreVc07	wcreVc07-66	G	NP	G	A	Medium to large
V cardui	CRE# 23	wcreVc07	wcreVc07-68	NP	NP	G	NP	Medium to large
V cardui	CRE# 23	wcreVc07	wcreVc07-69	G	NP	G	L	Medium to large

V cardui	CRE# 23	wcreVc07	wcreVc07-70	NP	NP	G	NP	Medium to large
V cardui	CRE# 23	wcreVc07	wcreVc07-73	G	NP	G	L	Medium to large
V cardui	CRE# 23	wcreVc07	wcreVc07-78	G	NP	G	A	Medium to large
V cardui	CRE# 23	wcreVc07	wcreVc07-80a	G	NP	NP	G	Medium to large
V cardui	CRE# 23	wcreVc07	wcreVc07-80b	G	NP	G	NP	Medium to large
V cardui	CRE# 23	wcreVc07	wcreVc07-82	G	NP	G	NP	Medium to large
V cardui	CRE# 21	wcreVc09	wcreVc09-02	G	NP	G	NP	Medium to large
V cardui	CRE# 21	wcreVc09	wcreVc09-13	NP	NP	NP	A	Small
V cardui	CRE# 21	wcreVc09	wcreVc09-23	NP	NP	NP	A	Small
V cardui	CRE# 21	wcreVc09	wcreVc09-27	NP	NP	A	NP	Small
V cardui	CRE# 21	wcreVc09	wcreVc09-29	NP	NP	G	NP	Small
V cardui	CRE# 21	wcreVc09	wcreVc09-36	NP	NP	L	NP	Medium to large
V cardui	CRE# 21	wcreVc09	wcreVc09-37	G	NP	NP	NP	Medium to large
V cardui	CRE# 21	wcreVc09	wcreVc09-40	NP	NP	G	G	Small
V cardui	CRE# 21	wcreVc09	wcreVc09-41	G	NP	G	A	Small
V cardui	CRE# 21	wcreVc09	wcreVc09-42	NP	NP	NP	L	Small
V cardui	CRE# 21	wcreVc09	wcreVc09-43	NP	NP	G	NP	Small
V cardui	CRE# 21	wcreVc09	wcreVc09-44	G	NP	G	NP	Medium to large
V cardui	CRE# 21	wcreVc09	wcreVc09-45	G	NP	G	A	Medium to large
V cardui	CRE# 21	wcreVc09	wcreVc09-47	A	NP	G	NP	Small
V cardui	CRE# 21	wcreVc09	wcreVc09-48	G	NP	G	NP	Small
V cardui	CRE# 05	wcreVc10	wcreVc10-01	L	L	L	NP	Small
V cardui	CRE# 19	wcreVc11	wcreVc11-01	G	NP	G	NP	Medium to large
V cardui	CRE# 19	wcreVc11	wcreVc11-03	NP	NP	G	NP	Medium to large
V cardui	CRE# 19	wcreVc11	wcreVc11-05	G	NP	NP	NP	Small
V cardui	CRE# 19	wcreVc11	wcreVc11-06	NP	NP	NP	G	Medium to large
V cardui	CRE# 19	wcreVc11	wcreVc11-07	G	NP	G	NP	Medium to large
V cardui	CRE# 19	wcreVc11	wcreVc11-08	G	A	G	NP	Medium to large

Dats S2. List of deletion alleles found in mKO butterflies using long-read sequencing.

Species	Element	Deletion Size	Canu output tig name	WT amplicon size (bp)	Distance from 5' oligo to most 5' gRNA cut site
Av	wcreAv01	4	wcreAv01_04_tig00000001	1807	1435
Av	wcreAv01	8	wcreAv01_04_tig00000001	1807	1435
Av	wcreAv01	1006	wcreAv01_04_tig00000002	1807	1435
Av	wcreAv01	1264	wcreAv01_04_tig00000003	1807	1435
Av	wcreAv01	1111	wcreAv01_04_tig00000004	1807	1435
Av	wcreAv01	7	wcreAv01_04_tig00000004	1807	1435
Av	wcreAv01	1526	wcreAv01_04_tig00000005	1807	1435
Av	wcreAv01	7	wcreAv01_04_tig00000005	1807	1435
Av	wcreAv01	6	wcreAv01_06_tig00000001	1807	1435
Av	wcreAv01	8	wcreAv01_06_tig00000001	1807	1435
Av	wcreAv01	8	wcreAv01_09_tig00000001	1807	1435
Av	wcreAv01	1170	wcreAv01_09_tig00000001	1807	1435
Av	wcreAv01	1197	wcreAv01_09_tig00000003	1807	1435
Av	wcreAv02	686	wcreAv02_01_tig00000001	1520	105
Av	wcreAv02	867	wcreAv02_01_tig00000002	1520	105
Av	wcreAv02	5	wcreAv02_01_tig00000003	1520	105
Av	wcreAv02	5	wcreAv02_05_tig00000001	1520	105
Av	wcreAv02	5	wcreAv02_06_tig00000001	1520	105
Av	wcreAv02	825	wcreAv02_01_tig00000005	1520	105
Av	wcreAv02	944	wcreAv02_01_tig00000006	1520	105
Av	wcreAv02	1118	wcreAv02_01_tig00000007	1520	105
Av	wcreAv02	472	wcreAv02_05_tig00000002	1520	105
Av	wcreAv02	848	wcreAv02_06_tig00000002	1520	105
Av	wcreAv03	1013	wcreAv03_02_tig00000003	2187	907
Av	wcreAv03	6	wcreAv03_03_tig00000001	2187	907
Av	wcreAv03	2	wcreAv03_03_tig00000001	2187	907
Av	wcreAv03	824	wcreAv03_03_tig00000002	2187	907
Av	wcreAv03	473	wcreAv03_03_tig00000003	2187	907
Av	wcreAv03	587	wcreAv03_04_tig00000001	2187	907
Av	wcreAv03	7	wcreAv03_04_tig00000002	2187	907
Av	wcreAv03	7	wcreAv03_04_tig00000004	2187	907
Av	wcreAv03	5	wcreAv03_04_tig00000002	2187	907
Av	wcreAv03	938	wcreAv03_04_tig00000004	2187	907
Av	wcreAv03	7	wcreAv03_04_tig00000004	2187	907
Av	wcreAv03	909	wcreAv03_04_tig00000005	2187	907
Av	wcreAv03	54	wcreAv03_04_tig00000005	2187	907
Av	wcreAv04	415	wcreAv04_03_tig00000001	2990	1364
Av	wcreAv04	2282	wcreAv04_03_tig00000005	2990	1364
Av	wcreAv04	2263	wcreAv04_03_tig00000006	2990	1364
Av	wcreAv04	16	wcreAv04_04_tig00000002	2990	1364
Av	wcreAv04	2171	wcreAv04_04_tig00000003	2990	1364

Av	wcreAv06	340	wcreAv06_01_tig00000001	2061	1140
Av	wcreAv06	4	wcreAv06_01_tig00000001	2061	1140
Av	wcreAv06	852	wcreAv06_01_tig00000002	2061	1140
Av	wcreAv06	835	wcreAv06_01_tig00000003	2061	1140
Av	wcreAv06	81	wcreAv06_01_tig00000003	2061	1140
Av	wcreAv06	867	wcreAv06_01_tig00000004	2061	1140
Av	wcreAv06	21	wcreAv06_11_tig00000001	2061	1140
Av	wcreAv07	380	wcreAv07_01_tig00000001	2302	693
Av	wcreAv07	139	wcreAv07_01_tig00000002	2302	693
Av	wcreAv07	6	wcreAv07_01_tig00000002	2302	693
Av	wcreAv07	554	wcreAv07_01_tig00000004	2302	693
Av	wcreAv07	34	wcreAv07_01_tig00000004	2302	693
Av	wcreAv07	13	wcreAv07_04_tig00000002	2302	693
Av	wcreAv07	317	wcreAv07_09_tig00000001	2302	693
Av	wcreAv07	1249	wcreAv07_09_tig00000002	2302	693
Av	wcreAv08	8	wcreAv08_03_tig00000002	3005	1423
Av	wcreAv09	2600	wcreAv09_01_tig00000003	3036	1304
Av	wcreAv10	468	wcreAv10_02_tig00000001	2308	1015
Av	wcreAv10	573	wcreAv10_02_tig00000002	2308	1015
Av	wcreAv10	239	wcreAv10_02_tig00000003	2308	1015
Av	wcreAv10	1134	wcreAv10_02_tig00000004	2308	1015
Av	wcreAv10	805	wcreAv10_02_tig00000005	2308	1015
Av	wcreAv10	6	wcreAv10_02_tig00000005	2308	1015
Av	wcreAv10	1735	wcreAv10_03_tig00000001	2308	1015
Av	wcreAv10	7	wcreAv10_03_tig00000002	2308	1015
Av	wcreAv10	7	wcreAv10_03_tig00000002	2308	1015
Av	wcreAv10	7	wcreAv10_03_tig00000002	2308	1015
Av	wcreAv10	1197	wcreAv10_07_tig00000001	2308	1015
Av	wcreAv10	1816	wcreAv10_07_tig00000002	2308	1015
Dp	wcreDp01	5	wcreDp01_01_tig00000001	1614	936
Dp	wcreDp01	385	wcreDp01_01_tig00000005	1614	936
Dp	wcreDp01	142	wcreDp01_01_tig00000005	1614	936
Dp	wcreDp01	1430	wcreDp01_02_tig00000001	1614	936
Dp	wcreDp01	1058	wcreDp01_06_tig00000002	1614	936
Dp	wcreDp02	1145	wcreDp02_04_tig00000002	1993	245
Dp	wcreDp02	1600	wcreDp02_04_tig00000003	1993	245
Dp	wcreDp02	1499	wcreDp02_04_tig00000004	1993	245
Dp	wcreDp02	925	wcreDp02_04_tig00000005	1993	245
Dp	wcreDp02	958	wcreDp02_04_tig00000006	1993	245
Dp	wcreDp02	1169	wcreDp02_12_tig00000001	1993	245
Dp	wcreDp02	7	wcreDp02_12_tig00000001	1993	245
Dp	wcreDp02	1159	wcreDp02_12_tig00000002	1993	245
Dp	wcreDp02	1602	wcreDp02_12_tig00000003	1993	245
Dp	wcreDp02	17	wcreDp02_12_tig00000004	1993	245
Dp	wcreDp02	1650	wcreDp02_12_tig00000006	1993	245

Dp	wcreDp02	1354	wcreDp02_12_tig00000008	1993	245
Dp	wcreDp02	1316	wcreDp02_51_tig00000001	1993	245
Dp	wcreDp02	1640	wcreDp02_51_tig00000002	1993	245
Dp	wcreDp02	1015	wcreDp02_51_tig00000003	1993	245
Dp	wcreDp02	930	wcreDp02_51_tig00000004	1993	245
Dp	wcreDp02	10	wcreDp02_51_tig00000004	1993	245
Dp	wcreDp03	915	wcreDp03_27_tig00000002	2871	1095
Dp	wcreDp04	931	wcreDp04_09_tig00000002	3083	1160
Dp	wcreDp04	1065	wcreDp04_09_tig00000003	3083	1160
Dp	wcreDp04	1905	wcreDp04_09_tig00000004	3083	1160
Dp	wcreDp04	2452	wcreDp04_28_tig00000001	3083	1160
Dp	wcreDp04	1985	wcreDp04_28_tig00000003	3083	1160
Dp	wcreDp05	1204	wcreDp05_01_tig00000001	1543	87
Dp	wcreDp05	1003	wcreDp05_09_tig00000001	1543	87
Dp	wcreDp05	1099	wcreDp05_09_tig00000003	1543	87
Dp	wcreDp05	1203	wcreDp05_09_tig00000004	1543	87
Dp	wcreDp05	543	wcreDp05_09_tig00000005	1543	87
Dp	wcreDp06	2237	wcreDp06_01_tig00000001	2811	976
Dp	wcreDp06	32	wcreDp06_01_tig00000002	2811	976
Dp	wcreDp06	30	wcreDp06_01_tig00000002	2811	976
Dp	wcreDp06	1281	wcreDp06_01_tig00000004	2811	976
Dp	wcreDp06	706	wcreDp06_01_tig00000005	2811	976
Dp	wcreDp06	1209	wcreDp06_02_tig00000003	2811	976
Dp	wcreDp06	1328	wcreDp06_04_tig00000001	2811	976
Dp	wcreDp06	853	wcreDp06_04_tig00000004	2811	976
Dp	wcreDp06	1856	wcreDp06_04_tig00000005	2811	976
Dp	wcreDp07	2147	wcreDp07_01_tig00000002	3166	1490
Dp	wcreDp07	2194	wcreDp07_01_tig00000003	3166	1490
Dp	wcreDp07	1899	wcreDp07_01_tig00000004	3166	1490
Dp	wcreDp07	1948	wcreDp07_01_tig00000005	3166	1490
Dp	wcreDp07	1885	wcreDp07_01_tig00000006	3166	1490
Dp	wcreDp07	1550	wcreDp07_01_tig00000007	3166	1490
Dp	wcreDp07	1319	wcreDp07_02_tig00000001	3166	1490
Dp	wcreDp07	2885	wcreDp07_02_tig00000002	3166	1490
Dp	wcreDp07	1738	wcreDp07_02_tig00000003	3166	1490
Dp	wcreDp07	2074	wcreDp07_02_tig00000004	3166	1490
Dp	wcreDp07	2756	wcreDp07_03_tig00000002	3166	1490
Dp	wcreDp07	1987	wcreDp07_03_tig00000003	3166	1490
Dp	wcreDp07	2517	wcreDp07_03_tig00000004	3166	1490
Hhim	wcreHhim02	5	wcreHhim02_02_tig00000001	1934	961
Hhim	wcreHhim02	878	wcreHhim02_04_tig00000002	1934	961
Hhim	wcreHhim02	259	wcreHhim02_04_tig00000003	1934	961
Hhim	wcreHhim02	620	wcreHhim02_04_tig00000004	1934	961
Hhim	wcreHhim03	2488	wcreHhim03_02_tig00000002	2847	1080
Hhim	wcreHhim03	279	wcreHhim03_02_tig00000003	2847	1080

Hhim	wcreHhim03	538	wcreHhim03_02_tig00000005	2847	1080
Hhim	wcreHhim03	1292	wcreHhim03_02_tig00000007	2847	1080
Hhim	wcreHhim03	3	wcreHhim03_03_tig00000002	2847	1080
Hhim	wcreHhim03	1481	wcreHhim03_03_tig00000005	2847	1080
Hhim	wcreHhim03	2275	wcreHhim03_03_tig00000008	2847	1080
Hhim	wcreHhim03	863	wcreHhim03_m1_tig00000001	2847	1080
Hhim	wcreHhim03	2474	wcreHhim03_m1_tig00000003	2847	1080
Hhim	wcreHhim03	2457	wcreHhim03_m1_tig00000004	2847	1080
Hhim	wcreHhim03	1863	wcreHhim03_m1_tig00000005	2847	1080
Hhim	wcreHhim03	728	wcreHhim03_m1_tig00000006	2847	1080
Hhim	wcreHhim03	309	wcreHhim03_m1_tig00000006	2847	1080
Hhim	wcreHhim04	1122	wcreHhim04_01_tig00000001	2703	1372
Hhim	wcreHhim04	25	wcreHhim04_01_tig00000001	2703	1372
Hhim	wcreHhim04	12	wcreHhim04_01_tig00000002	2703	1372
Hhim	wcreHhim04	25	wcreHhim04_01_tig00000002	2703	1372
Hhim	wcreHhim04	2004	wcreHhim04_01_tig00000003	2703	1372
Hhim	wcreHhim04	1584	wcreHhim04_01_tig00000004	2703	1372
Hhim	wcreHhim04	10	wcreHhim04_03_tig00000001	2703	1372
Hhim	wcreHhim04	25	wcreHhim04_03_tig00000001	2703	1372
Hhim	wcreHhim04	1923	wcreHhim04_03_tig00000002	2703	1372
Hhim	wcreHhim04	1201	wcreHhim04_05_tig00000001	2703	1372
Hhim	wcreHhim04	10	wcreHhim04_05_tig00000002	2703	1372
Hhim	wcreHhim04	2305	wcreHhim04_05_tig00000003	2703	1372
Hhim	wcreHhim04	1207	wcreHhim04_05_tig00000004	2703	1372
Hhim	wcreHhim07	3	wcreHhim07_03_tig00000001	1715	838
Hhim	wcreHhim07	6	wcreHhim07_03_tig00000001	1715	838
Hhim	wcreHhim07	691	wcreHhim07_03_tig00000002	1715	838
Hhim	wcreHhim07	604	wcreHhim07_03_tig00000003	1715	838
Hhim	wcreHhim07	194	wcreHhim07_03_tig00000004	1715	838
Hhim	wcreHhim07	5	wcreHhim07_03_tig00000005	1715	838
Hhim	wcreHhim07	310	wcreHhim07_03_tig00000005	1715	838
Hhim	wcreHhim07	294	wcreHhim07_04_tig00000001	1715	838
Hhim	wcreHhim07	3	wcreHhim07_04_tig00000003	1715	838
Hhim	wcreHhim10	515	wcreHhim10_01_tig00000001	2301	1170
Hhim	wcreHhim10	939	wcreHhim10_01_tig00000002	2301	1170
Hhim	wcreHhim10	1208	wcreHhim10_01_tig00000004	2301	1170
Hhim	wcreHhim10	165	wcreHhim10_01_tig00000004	2301	1170
Jc	wcreJc03	1357	wcreJc03_01_tig00000001	1663	582
Jc	wcreJc03	432	wcreJc03_01_tig00000002	1663	582
Jc	wcreJc03	742	wcreJc03_56_tig00000001	1663	582
Jc	wcreJc03	432	wcreJc03_56_tig00000002	1663	582
Jc	wcreJc05	1968	wcreJc05_17a_tig00000001	2509	953
Jc	wcreJc05	342	wcreJc05_17a_tig00000002	2509	953
Jc	wcreJc05	929	wcreJc05_17b_tig00000001	2509	953
Jc	wcreJc05	1173	wcreJc05_17b_tig00000002	2509	953

Jc	wcreJc05	179	wcreJc05_17b_tig00000002	2509	953
Jc	wcreJc05	1084	wcreJc05_17b_tig00000003	2509	953
Jc	wcreJc05	658	wcreJc05_17b_tig00000004	2509	953
Jc	wcreJc05	953	wcreJc05_20_tig00000001	2509	953
Jc	wcreJc05	552	wcreJc05_20_tig00000003	2509	953
Jc	wcreJc05	1168	wcreJc05_20_tig00000004	2509	953
Jc	wcreJc06	638	wcreJc06_24_tig00000002	2575	1160
Jc	wcreJc06	2245	wcreJc06_40_tig00000001	2575	1160
Jc	wcreJc06	613	wcreJc06_40_tig00000003	2575	1160
Jc	wcreJc06	319	wcreJc06_40_tig00000005	2575	1160
Jc	wcreJc07	851	wcreJc07_13_tig00000002	1499	283
Jc	wcreJc07	1169	wcreJc07_13_tig00000004	1499	283
Jc	wcreJc07	895	wcreJc07_13_tig00000005	1499	283
Jc	wcreJc07	2	wcreJc07_15_tig00000001	1499	283
Jc	wcreJc07	14	wcreJc07_15_tig00000001	1499	283
Jc	wcreJc07	1168	wcreJc07_15_tig00000002	1499	283
Jc	wcreJc07	1214	wcreJc07_15_tig00000003	1499	283
Jc	wcreJc07	878	wcreJc07_15_tig00000004	1499	283
Jc	wcreJc07	851	wcreJc07_15_tig00000005	1499	283
Jc	wcreJc07	595	wcreJc07_15_tig00000006	1499	283
Jc	wcreJc10	1528	wcreJc10_01_tig00000001	2550	1322
Jc	wcreJc10	1468	wcreJc10_01_tig00000002	2550	1322
Jc	wcreJc10	129	wcreJc10_01_tig00000003	2550	1322
Jc	wcreJc10	24	wcreJc10_03_tig00000001	2550	1322
Jc	wcreJc10	442	wcreJc10_03_tig00000002	2550	1322
Jc	wcreJc10	1627	wcreJc10_05_tig00000002	2550	1322
Jc	wcreJc10	416	wcreJc10_05_tig00000003	2550	1322
Vc	wcreVc02	5	wcreVc02_07_tig00000001	3164	1429
Vc	wcreVc02	957	wcreVc02_07_tig00000002	3164	1429
Vc	wcreVc02	5	wcreVc02_10_tig00000001	3164	1429
Vc	wcreVc02	782	wcreVc02_10_tig00000002	3164	1429
Vc	wcreVc03	3	wcreVc03_46_tig00000001	1346	395
Vc	wcreVc03	3	wcreVc03_62_tig00000001	1346	395
Vc	wcreVc04	1133	wcreVc04_15_tig00000002	1445	359
Vc	wcreVc05	5	wcreVc05_03_tig00000001	2668	727
Vc	wcreVc05	5	wcreVc05_03_tig00000002	2668	727
Vc	wcreVc05	460	wcreVc05_03_tig00000003	2668	727
Vc	wcreVc05	132	wcreVc05_03_tig00000004	2668	727
Vc	wcreVc05	469	wcreVc05_03_tig00000005	2668	727
Vc	wcreVc05	1265	wcreVc05_17_tig00000002	2668	727
Vc	wcreVc05	977	wcreVc05_17_tig00000003	2668	727
Vc	wcreVc05	5	wcreVc05_24_tig00000001	2668	727
Vc	wcreVc05	4	wcreVc05_24_tig00000002	2668	727
Vc	wcreVc05	702	wcreVc05_24_tig00000003	2668	727
Vc	wcreVc06	1211	wcreVc06_10_tig00000001	2819	872

Vc	wcreVc06	4	wcreVc06_10_tig00000002	2819	872
Vc	wcreVc06	3	wcreVc06_10_tig00000002	2819	872
Vc	wcreVc06	21	wcreVc06_10_tig00000003	2819	872
Vc	wcreVc06	795	wcreVc06_10_tig00000003	2819	872
Vc	wcreVc06	1485	wcreVc06_10_tig00000004	2819	872
Vc	wcreVc06	1250	wcreVc06_15_tig00000002	2819	872
Vc	wcreVc06	497	wcreVc06_15_tig00000003	2819	872
Vc	wcreVc06	1638	wcreVc06_15_tig00000004	2819	872
Vc	wcreVc06	2081	wcreVc06_16_tig00000001	2819	872
Vc	wcreVc06	2385	wcreVc06_16_tig00000002	2819	872
Vc	wcreVc06	1707	wcreVc06_16_tig00000004	2819	872
Vc	wcreVc06	1702	wcreVc06_16_tig00000005	2819	872
Vc	wcreVc06	882	wcreVc06_16_tig00000006	2819	872
Vc	wcreVc06	1546	wcreVc06_16_tig00000007	2819	872
Vc	wcreVc07	756	wcreVc07_01_tig00000001	1689	348
Vc	wcreVc07	756	wcreVc07_01_tig00000002	1689	348
Vc	wcreVc07	866	wcreVc07_06_tig00000001	1689	348
Vc	wcreVc07	964	wcreVc07_06_tig00000002	1689	348
Vc	wcreVc07	343	wcreVc07_06_tig00000004	1689	348
Vc	wcreVc07	780	wcreVc07_p2_Fw1_tig00000001	1689	348
Vc	wcreVc07	3	wcreVc07_p2_Hw1_tig00000001	1689	348
Vc	wcreVc07	335	wcreVc07_p2_Hw1_tig00000003	1689	348
Vc	wcreVc07	921	wcreVc07_p2_Hw1_tig00000004	1689	348
Vc	wcreVc07	342	wcreVc07_p2_Hw2_tig00000003	1689	348
Vc	wcreVc07	3	F0_Vc07_1_2_P1_tig00000001	1689	348
Vc	wcreVc07	978	F0_Vc07_1_2_P1_tig00000001	1689	348
Vc	wcreVc07	823	F0_Vc07_1_2_P1_tig00000002	1689	348
Vc	wcreVc07	580	F0_Vc07_1_2_P1_tig00000003	1689	348
Vc	wcreVc07	8	F0_Vc07_1_2_P2_tig00000001	1689	348
Vc	wcreVc07	860	F0_Vc07_1_2_P2_tig00000003	1689	348
Vc	wcreVc07	188	F0_Vc07_1_2_P2_tig00000004	1689	348
Vc	wcreVc07	646	F0_Vc07_1_2_P2_tig00000005	1689	348
Vc	wcreVc07	449	F0_Vc07_1_3_P5_tig00000001	1689	348
Vc	wcreVc07	744	F0_Vc07_1_3_P5_tig00000002	1689	348
Vc	wcreVc07	911	F0_Vc07_1_3_P5_tig00000003	1689	348
Vc	wcreVc07	337	F0_Vc07_1_3_P5_tig00000004	1689	348
Vc	wcreVc07	623	F0_Vc07_2_3_P3_tig00000001	1689	348
Vc	wcreVc07	428	F0_Vc07_2_3_P3_tig00000002	1689	348
Vc	wcreVc07	293	F0_Vc07_2_3_P3_tig00000003	1689	348
Vc	wcreVc07	953	F0_Vc07_2_3_P3_tig00000005	1689	348
Vc	wcreVc07	584	F0_Vc07_2_3_P4_tig00000001	1689	348
Vc	wcreVc07	952	F0_Vc07_2_3_P4_tig00000003	1689	348
Vc	wcreVc07	11	F1_Vc07_2_3_m1_tig00000001	1689	348
Vc	wcreVc07	978	F1_Vc07_2_3_m1_tig00000002	1689	348
Vc	wcreVc07	823	F1_Vc07_2_3_m1_tig00000004	1689	348

Vc	wcreVc07	598	F1_Vc07_2_3_m1_tig00000005	1689	348
Vc	wcreVc07	7	F0_Vc07_1_2_P2_tig00000004	1689	348
Vc	wcreVc07	10	F0_Vc07_1_2_P2_tig00000005	1689	348
Vc	wcreVc07	3	F0_Vc07_1_3_P5_tig00000001	1689	348
Vc	wcreVc07	3	F1_Vc07_2_3_m1_tig00000002	1689	348
Vc	wcreVc07	18	F1_Vc07_2_3_m1_tig00000005	1689	348
Vc	wcreVc09	1846	wcreVc09_36_tig00000001	2244	933
Vc	wcreVc09	5	wcreVc09_36_tig00000002	2244	933
Vc	wcreVc09	892	wcreVc09_36_tig00000003	2244	933
Vc	wcreVc09	40	wcreVc09_36_tig00000003	2244	933
Vc	wcreVc10	1913	wcreVc10_01_tig00000001	3072	1516
Vc	wcreVc10	1617	wcreVc10_01_tig00000002	3072	1516
Vc	wcreVc10	2443	wcreVc10_01_tig00000003	3072	1516
Vc	wcreVc11	492	wcreVc11_07_tig00000001	2841	1082
Vc	wcreVc11	31	wcreVc11_08_tig00000001	2841	1082

Distance from 3' oligo to most 3' gRNA cut site	Number of gRNAs	Maximum expected KO	ratio del size/ WT PCR size	substract WT PCR - Deletion size
82	3	266	0.002213614	1803
82	3	266	0.004427227	1799
82	3	266	0.556723852	801
82	3	266	0.699501937	543
82	3	266	0.614831212	696
82	3	266	0.003873824	1800
82	3	266	0.844493636	281
82	3	266	0.003873824	1800
82	3	266	0.003320421	1801
82	3	266	0.004427227	1799
82	3	266	0.004427227	1799
82	3	266	0.647482014	637
82	3	266	0.662423907	610
978	3	417	0.451315789	834
978	3	417	0.570394737	653
978	3	417	0.003289474	1515
978	3	417	0.003289474	1515
978	3	417	0.003289474	1515
978	3	417	0.542763158	695
978	3	417	0.621052632	576
978	3	417	0.735526316	402
978	3	417	0.310526316	1048
978	3	417	0.557894737	672
1148	2	113	0.463191587	1174
1148	2	113	0.002743484	2181
1148	2	113	9.14E-04	2185
1148	2	113	0.376771834	1363
1148	2	113	0.216278006	1714
1148	2	113	0.268404207	1600
1148	2	113	0.003200732	2180
1148	2	113	0.003200732	2180
1148	2	113	0.002286237	2182
1148	2	113	0.428898034	1249
1148	2	113	0.003200732	2180
1148	2	113	0.41563786	1278
1148	2	113	0.024691358	2133
1195	3	412	0.138795987	2575
1195	3	412	0.763210702	708
1195	3	412	0.756856187	727
1195	3	412	0.005351171	2974
1195	3	412	0.726086957	819

600	4	302	0.164968462	1721
600	4	302	0.001940805	2057
600	4	302	0.413391557	1209
600	4	302	0.405143134	1226
600	4	302	0.03930131	1980
600	4	302	0.420669578	1194
600	4	302	0.010189229	2040
1212	4	378	0.165073849	1922
1212	4	378	0.060382276	2163
1212	4	378	0.002606429	2296
1212	4	378	0.240660295	1748
1212	4	378	0.014769765	2268
1212	4	378	0.005647263	2289
1212	4	378	0.137706342	1985
1212	4	378	0.542571677	1053
1220	3	343	0.00266223	2997
1472	2	241	0.856389987	436
1034	3	238	0.202772964	1840
1034	3	238	0.248266898	1735
1034	3	238	0.10355286	2069
1034	3	238	0.491334489	1174
1034	3	238	0.348786828	1503
1034	3	238	0.002599653	2302
1034	3	238	0.751733102	573
1034	3	238	0.003032929	2301
1034	3	238	0.003032929	2301
1034	3	238	0.003032929	2301
1034	3	238	0.518630849	1111
1034	3	238	0.786828423	492
383	2	276	0.003097893	1609
383	2	276	0.238537794	1229
383	2	276	0.087980173	1472
383	2	276	0.885997522	184
383	2	276	0.65551425	556
1506	2	223	0.574510788	848
1506	2	223	0.802809834	393
1506	2	223	0.752132464	494
1506	2	223	0.464124436	1068
1506	2	223	0.480682388	1035
1506	2	223	0.586552935	824
1506	2	223	0.003512293	1986
1506	2	223	0.581535374	834
1506	2	223	0.803813347	391
1506	2	223	0.008529854	1976
1506	2	223	0.827897642	343

1506	2	223	0.679377822	639
1506	2	223	0.660311089	677
1506	2	223	0.82288008	353
1506	2	223	0.509282489	978
1506	2	223	0.466633216	1063
1506	2	223	0.005017561	1983
1198	2	559	0.318704284	1956
1036	4	869	0.301978592	2152
1036	4	869	0.345442751	2018
1036	4	869	0.617904638	1178
1036	4	869	0.795329225	631
1036	4	869	0.64385339	1098
950	4	483	0.780298121	339
950	4	483	0.650032404	540
950	4	483	0.712248866	444
950	4	483	0.779650032	340
950	4	483	0.35191186	1000
1405	3	411	0.795802206	574
1405	3	411	0.011383849	2779
1405	3	411	0.010672359	2781
1405	3	411	0.455709712	1530
1405	3	411	0.251156172	2105
1405	3	411	0.430096051	1602
1405	3	411	0.47242974	1483
1405	3	411	0.303450729	1958
1405	3	411	0.660263252	955
1323	4	334	0.678142767	1019
1323	4	334	0.692987997	972
1323	4	334	0.599810486	1267
1323	4	334	0.615287429	1218
1323	4	334	0.595388503	1281
1323	4	334	0.489576753	1616
1323	4	334	0.416614024	1847
1323	4	334	0.911244473	281
1323	4	334	0.548957675	1428
1323	4	334	0.655085281	1092
1323	4	334	0.870499052	410
1323	4	334	0.627605812	1179
1323	4	334	0.795009476	649
693	3	258	0.002585315	1929
693	3	258	0.453981386	1056
693	3	258	0.133919338	1675
693	3	258	0.320579111	1314
1215	3	533	0.873902353	359
1215	3	533	0.097997893	2568

1215	3	533	0.188970847	2309
1215	3	533	0.453811029	1555
1215	3	533	0.001053741	2844
1215	3	533	0.520196698	1366
1215	3	533	0.799086758	572
1215	3	533	0.303126098	1984
1215	3	533	0.868984896	373
1215	3	533	0.863013699	390
1215	3	533	0.654373024	984
1215	3	533	0.255707763	2119
1215	3	533	0.1085353	2538
898	3	414	0.41509434	1581
898	3	414	0.009248983	2678
898	3	414	0.004439512	2691
898	3	414	0.009248983	2678
898	3	414	0.741398446	699
898	3	414	0.586015538	1119
898	3	414	0.003699593	2693
898	3	414	0.009248983	2678
898	3	414	0.711431743	780
898	3	414	0.444321125	1502
898	3	414	0.003699593	2693
898	3	414	0.852756197	398
898	3	414	0.446540881	1496
536	3	321	0.001749271	1712
536	3	321	0.003498542	1709
536	3	321	0.402915452	1024
536	3	321	0.352186589	1111
536	3	321	0.113119534	1521
536	3	321	0.002915452	1710
536	3	321	0.180758017	1405
536	3	321	0.171428571	1421
536	3	321	0.001749271	1712
596	4	515	0.223815732	1786
596	4	515	0.408083442	1362
596	4	515	0.524989135	1093
596	4	515	0.071707953	2136
629	3	432	0.815995189	306
629	3	432	0.259771497	1231
629	3	432	0.4461816	921
629	3	432	0.259771497	1231
883	4	654	0.784376246	541
883	4	654	0.136309287	2167
883	4	654	0.370267039	1580
883	4	654	0.467516939	1336

883	4	654	0.071343165	2330
883	4	654	0.432044639	1425
883	4	654	0.262255879	1851
883	4	654	0.379832603	1556
883	4	654	0.220007971	1957
883	4	654	0.465524113	1341
884	4	512	0.24776699	1937
884	4	512	0.87184466	330
884	4	512	0.238058252	1962
884	4	512	0.123883495	2256
347	4	849	0.567711808	648
347	4	849	0.779853235	330
347	4	849	0.59706471	604
347	4	849	0.001334223	1497
347	4	849	0.00933956	1485
347	4	849	0.779186124	331
347	4	849	0.809873249	285
347	4	849	0.585723816	621
347	4	849	0.567711808	648
347	4	849	0.396931288	904
570	4	637	0.599215686	1022
570	4	637	0.575686275	1082
570	4	637	0.050588235	2421
570	4	637	0.009411765	2526
570	4	637	0.173333333	2108
570	4	637	0.638039216	923
570	4	637	0.163137255	2134
909	4	806	0.001580278	3159
909	4	806	0.302465234	2207
909	4	806	0.001580278	3159
909	4	806	0.247155499	2382
569	3	363	0.002228826	1343
569	3	363	0.002228826	1343
724	4	343	0.784083045	312
1452	3	469	0.001874063	2663
1452	3	469	0.001874063	2663
1452	3	469	0.172413793	2208
1452	3	469	0.049475262	2536
1452	3	469	0.175787106	2199
1452	3	469	0.474137931	1403
1452	3	469	0.366191904	1691
1452	3	469	0.001874063	2663
1452	3	469	0.00149925	2664
1452	3	469	0.263118441	1966
1436	4	491	0.429584959	1608

1436	4	491	0.001418943	2815
1436	4	491	0.001064207	2816
1436	4	491	0.00744945	2798
1436	4	491	0.282014899	2024
1436	4	491	0.526782547	1334
1436	4	491	0.443419652	1569
1436	4	491	0.176303654	2322
1436	4	491	0.581057112	1181
1436	4	491	0.738205037	738
1436	4	491	0.846044697	434
1436	4	491	0.605533877	1112
1436	4	491	0.603760199	1117
1436	4	491	0.312876907	1937
1436	4	491	0.548421426	1273
1072	3	249	0.447602131	933
1072	3	249	0.447602131	933
1072	3	249	0.512729426	823
1072	3	249	0.570751924	725
1072	3	249	0.203078745	1346
1072	3	249	0.461811723	909
1072	3	249	0.001776199	1686
1072	3	249	0.198342214	1354
1072	3	249	0.545293073	768
1072	3	249	0.202486679	1347
1072	3	249	0.001776199	1686
1072	3	249	0.579040853	711
1072	3	249	0.487270574	866
1072	3	249	0.343398461	1109
1072	3	249	0.00473653	1681
1072	3	249	0.509177028	829
1072	3	249	0.111308467	1501
1072	3	249	0.382474837	1043
1072	3	249	0.265837774	1240
1072	3	249	0.440497336	945
1072	3	249	0.53937241	778
1072	3	249	0.199526347	1352
1072	3	249	0.368857312	1066
1072	3	249	0.253404381	1261
1072	3	249	0.173475429	1396
1072	3	249	0.564239195	736
1072	3	249	0.345766726	1105
1072	3	249	0.563647128	737
1072	3	249	0.006512729	1678
1072	3	249	0.579040853	711
1072	3	249	0.487270574	866

1072	3	249	0.354055654	1091
1072	3	249	0.004144464	1682
1072	3	249	0.005920663	1679
1072	3	249	0.001776199	1686
1072	3	249	0.001776199	1686
1072	3	249	0.010657194	1671
960	4	332	0.822638146	398
960	4	332	0.002228164	2239
960	4	332	0.397504456	1352
960	4	332	0.017825312	2204
691	4	846	0.622721354	1159
691	4	846	0.526367188	1455
691	4	846	0.795247396	629
1476	3	264	0.173178458	2349
1476	3	264	0.010911651	2810

Materials Design Analysis Reporting (MDAR) Checklist for Authors

The MDAR framework establishes a minimum set of requirements in transparent reporting applicable to studies in the life sciences (see Statement of Task: doi:10.31222/osf.io/9sm4x.). The MDAR checklist is a tool for authors, editors and others seeking to adopt the MDAR framework for transparent reporting in manuscripts and other outputs. Please refer to the MDAR Elaboration Document for additional context for the MDAR framework.

Materials

Antibodies	Yes (indicate where provided: page no/section/legend)	n/a
For commercial reagents, provide supplier name, catalogue number and RRID, if available.		X

Cell materials	Yes (indicate where provided: page no/section/legend)	n/a
Cell lines: Provide species information, strain. Provide accession number in repository **OR** supplier name, catalog number, clone number, **OR** RRID		X
Primary cultures: Provide species, strain, sex of origin, genetic modification status.		

Experimental animals	Yes (indicate where provided: page no/section/legend)	n/a
Laboratory animals: Provide species, strain, sex, age, genetic modification status. Provide accession number in repository **OR** supplier name, catalog number, clone number, **OR** RRID		X
Animal observed in or captured from the field: Provide species, sex and age where possible		X
Model organisms: Provide Accession number in repository (where relevant) **OR** RRID		X

Plants and microbes	Yes (indicate where provided: page no/section/legend)	n/a
Plants: provide species and strain, unique accession number if available, and source (including location for collected wild specimens)		X
Microbes: provide species and strain, unique accession number if available, and source		X

Human research participants	Yes (indicate where provided: page no/section/legend)	n/a
Identify authority granting ethics approval (IRB or equivalent committee(s), provide reference number for approval.		X
Provide statement confirming informed consent obtained from study participants.		X
Report on age and sex for all study participants.		X

Design

Study protocol	Yes (indicate where provided: page no/section/legend)	n/a
For clinical trials, provide the trial registration number **OR** cite DOI in manuscript.		X

Laboratory protocol	Yes (indicate where provided: page no/section/legend)	n/a
Provide DOI or other citation details if detailed step-by-step protocols are available.	ATAC-seq: Buenrostro et al. 2015:10.1002/0471142727.mb2129s109 CRISPR: Zhang & Reed 2017: 10.1007/978-981-10-4956-9_8 Hi-C: Rao et a., 2014: 10.1016/j.cell.2014.11.021	

Experimental study design (statistics details)	Yes (indicate where provided: page no/section/legend)	n/a
State whether and how the following have been done**, or** if they were not carried out.		
Sample size determination	Sample size was not pre-determined	
Randomisation	Samples were not randomized	
Blinding	No blinding was done	
Inclusion/exclusion criteria	No samples were excluded	

Sample definition and in-laboratory replication	Yes (indicate where provided: page no/section/legend)	n/a
State number of times the experiment was replicated in laboratory	ATAC-seq had three biological replicates per each tissue	
Define whether data describe technical or biological replicates	All data describes biological replicates	

Ethics	Yes (indicate where provided: page no/section/legend)	n/a
Studies involving human participants: State details of authority granting ethics approval (IRB or equivalent committee(s), provide reference number for approval.		X
Studies involving experimental animals: State details of authority granting ethics approval (IRB or equivalent committee(s), provide reference number for approval.		X
Studies involving specimen and field samples: State if relevant permits obtained, provide details of authority approving study; if none were required, explain why.		X

Dual Use Research of Concern (DURC)	Yes (indicate where provided: page no/section/legend)	n/a
If study is subject to dual use research of concern, state the authority granting approval and reference number for the regulatory approval		X

Analysis

Attrition	Yes (indicate where provided: page no/section/legend)	n/a
State if sample or data point from the analysis is excluded, and whether the criteria for exclusion were determined and specified in advance.		X

Statistics	Yes (indicate where provided: page no/section/legend)	n/a
Describe statistical tests used and justify choice of tests.	Wald test p-value was used to compare read counts in peak call annotations.	

Data Availability	Yes (indicate where provided: page no/section/legend)	n/a
State whether newly created datasets are available, including protocols for access or restriction on access.	All sequencing data is available in NCBI. Butterfly wing data is in Dryad.	
If data are publicly available, provide accession number in repository or DOI or URL.	https://www.ncbi.nlm.nih.gov/bioproject/695303 https://doi.org/10.5061/dryad.8cz8w9gpr	
If publicly available data are reused, provide accession number in repository or DOI or URL, where possible.		X

Code Availability	Yes (indicate where provided: page no/section/legend)	n/a
For all newly generated code and software essential for replicating the main findings of the study:		
State whether the code or software is available.	All code used is available	
If code is publicly available, provide accession number in repository, or DOI or URL.	https://doi.org/10.5061/dryad.8cz8w9gpr	

Reporting

Adherence to community standards	Yes (indicate where provided: page no/section/legend)	n/a
MDAR framework recommends adoption of discipline-specific guidelines, established and endorsed through community initiatives. Journals have their own policy about requiring specific guidelines and recommendations to complement MDAR.		
State if relevant guidelines (eg., ICMJE, MIBBI, ARRIVE) have been followed, and whether a checklist (eg., CONSORT, PRISMA, ARRIVE) is provided with the manuscript.		X